MAY 2015

Ph.D in CIVIL ENGINEERING

ADNAN ABDUL WAHHAB ISMAEL

UNIVERSITY OF GAZİANTEP

GRADUATE SCHOOL OF

NATURAL & APPLIED SCIENCES

STUDY OF LOCAL SCOUR AROUND UNCONVENTIONAL BRIDGE PIERS

Ph.D THESIS

IN

CIVIL ENGINEERING

BY

ADNAN ABDUL WAHHAB ISMAEL

Study of Local Scour Around Unconventional Bridge Piers

Ph.D Thesis

in

Civil Engineering

University of Gaziantep

Supervisor
Prof. Dr. Mustafa GÜNAL
Co-Supervisor
Assist. Prof. Dr. Hamid H. Hussein

by

Adnan Abdul Wahhab ISMAEL

May 2015

REPUBLIC OF TURKEY
UNIVERSITY OF GAZİANTEP
GRADUATE SCHOOL OF NATURAL & APPLIED SCIENCES
CIVIL ENGINEERING DEPARTMENT

Name of the thesis: Study of Local Scour around Unconventional Bridge Piers.

Name of the student: Adnan Abdul Wahaab ISMAEL

Exam date: 22.05.2015

Approval of the Graduate School of Natural and Applied Sciences

Prof. Dr. Metin BEDİR

Director

I certify that this thesis satisfies all the requirements as a thesis for the degree of Doctor of Philosophy.

Prof. Dr. Mustafa GÜNAL

Head of Department

This is to certify that we have read this thesis and that in our consensus opinion it is fully adequate, in scope and quality, as a thesis for the degree of Doctor of Philosophy.

Assist. Prof. Dr. Hamid H. Hussein

Co-Supervisor

Prof. Dr. Mustafa GÜNAL

Supervisor

Examining Committee Members:	Signature
Prof. Dr. Yalçın YÜKSEL	.....
Prof. Dr. Esin ÇEVİK	.....
Prof. Dr. Mustafa GÜNAL	.....
Assoc. Prof. Dr. Aytaç GÜVEN	.....
Assist. Prof. Dr. Mazen KAVVAS	.....

I hereby declare that all information in this document has been obtained and presented in accordance with academic rules and ethical conduct. I also declare that, as required by these rules and conduct, I have fully cited and referenced all material and results that are not original to this work.

Adnan Abdul Wahhab ISMAEL

ABSTRACT
STUDY OF LOCAL SCOUR AROUND UNCONVENTIONAL BRIDGE PIERS

ISMAEL, Adnan Abdul Wahhab
Ph.D. in Civil Engineering
Supervisor: Prof. Prof. Dr. Mustafa GÜNAL
Co-Supervisor: Assist. Prof. Dr. Hamid H. Hussein

May 2015
132 pages

Local scour around bridge pier is the leading cause of bridge failure, effecting significantly on the total construction and maintenance costs. Therefore, scouring around uniform pier with cylindrical shape is commonly used in the field. The shape of bridge piers has important effect on the local scour. A literature review showed that there is still a lack of experimental studies on the effects of non-uniform pier, especially under live-bed scour. The present study experimentally investigated the effect of bridge pier shape on scouring process. Three different shapes of bridge piers (10-4, 10-6 and 10-8 cm) were tested using with three discharges (38, 48 and 58 l/s) for duration of 3 hours under live-bed condition. The present experimental studies consist of two different orientations of bridge piers according to flow direction. These orientations are named as "upstream-facing round nosed pier (US-FRNP)" and "downstream-facing round nosed pier (DS-FRNP)" according to flow direction. The experimental results of oriented US-FRNP and DS-FRNP models are compared with round-nosed pier (10-10 cm) and circular pier (10 cm diameter) models. The results of comparison between the performances of bridge piers under different flow conditions reveal that downstream facing round-nosed bridge pier (DS-FRNP) is an effective countermeasure to reduce the depth of scour. An empirical relationship was also developed on the basis of obtained experimental results.

In this study, the three-dimensional flow field inside scour hole is also experimentally investigated. The velocity field measurements were obtained using an Acoustic Doppler Velocimeter (ADV). Vector plots of the flow field in the upstream and downstream plane of bridge piers reveal that the existence of downward flow and subsequently vortex formed at the toe of the pier named horseshoe vortex and the wake vortex in the downstream. Scouring effect of downflow and horseshoe vortex was decreased by changing the orientation of bridge pier. The bed-shear stresses are also calculated from Reynolds stresses and Turbulent Kinetic Energy method.

Key Words: Bridge pier, pier orientation, scour, scour depth, local scour.

ÖZET

Konvansıyonel olmayan köprü ayakları etrafındaki yerel oyulmanın araştırılması

ISMAEL, Adnan Abdul Wahhab

Doktora Tezi, İnşaat Mühendisliği Bölümü

Tez Yöneticisi: Prof. Dr. Mustata GÜNAL

Yardımcı Tez Yöneticisi: Yrd. Doç. Hamid H. HUSSEIN

Mayıs 2015

132 sayfa

Köprü ayağı etrafında oluşan ve köprünün zarar görmesine neden olan yerel oyulma, köprülerin yeniden yapım ve onarım maliyetlerini arttıran nedenlerin ilk sıralarında yer almaktadır. Bu nedenle, çalışmalar genellikle dairesel kesitli köprü ayağı etrafında oluşan yerel oyulma alanında olmuştur. Köprü ayağı şeklinin yerel oyulmanın yapısı üzerinde önemli etkisi vardır. Literatürde, özellikle, hareketli taban üzerinde düzgün olmayan köprü ayağı kullanılarak yapılan deneysel çalışmalar yeterli değildir. Bu çalışma, köprü ayağı şeklinin yerel oyulmanın oluşumu üzerindeki etkisini araştırmaktadır. Hareketli taban şartlarında ve üç farklı debi kullanılarak 3 saatlik oyulma deneyleri üç farklı köprü ayak modeli (10-4, 10-6 ve 10-8 cm) kullanılarak deneyler yapılmıştır. Bu deneysel çalışmada köprü ayağı akım yönüne göre iki farklı şekilde konumlandırılmıştır. Bu konumlar akım yönüne göre; "membaya bakan yuvarlak burunlu köprü ayağı (US-FRNP)" ve "mansaba bakan yuvarlak burunlu köprü ayağı (DS-FRNP)" olarak isimlendirilmiştir. Farklı konumlandırılmış US-FRNP ve DS-FRNP ayak modelleri ile yapılan deneylerden elde edilen sonuçlar yuvarlak burunlu (10-10 cm) ve dairesel kesitli (10 cm çaplı) modellerle karşılaştırılmıştır. Farklı akım şartlarında yapılan deneylerden elde edilen sonuçlar, mansaba bakan yuvarlak burunlu köprü ayağı modelinin (DS-FRNP) oyulma derinliğini azaltma yönündeki performansının etkili olduğunu ortaya çıkarmıştır. Deneylerden elde edilen sonuçlar kullanılarak bir empirik bağıntı da ayrıca elde edilmiştir.

Bu çalışmada, oyulma çukuru içerisindeki akım yapısı üç-boyutlu olarak incelenmiştir. Hız ölçümleri Akustik Dopler Anemometre (ADV) kullanılarak elde edilmiştir. Köprü ayağının memba ve mansabında elde edilen hız ölçümleri kullanılarak oluşturulan vektör grafikleri, köprü ayağının topuk tarafında tabana doğru bir akım olduğunu ve bu akımın sonucunda da at başı döngülerin oluştuğunu göstermiştir. Tabana doğru olan akımın ve sonucunda oluşan at başı döngülerin oyma etkisinin köprü ayağı konumunun değiştirilmesi ile azalmıştır. Reynolds gerilmesi ve Türbülans Kinetik Enerji metodu kullanılarak taban kayma gerilmeleri de hesaplanmıştır.

Anahtar Kelimeler: Köprü ayağı, köprü ayağı konumu, oyulma, oyulma derinliği, yerel oyulma.

ACKNOWLEDGMENTS

The author wishes to express his deepest gratitude to his supervisor Professor Dr. Mustafa GÜNAL for his valuable guidance and support throughout the conduction of experiments and preparation of this thesis.

Also special thanks to my co-supervisor Assistant Professor Dr. Hamid Hussein for his guidance and support during the study.

I am also grateful to my friends for their help during different phases of this study.

Finally, words cannot express my appreciation for my wife for her support and encouragement during the study.

TABLE OF CONTENTS

LIST OF TABLES

Page

LIST OF FIGURES

Page

LIST OF SYMBOLS

b	Pier width (m)
u	Flow velocity (m/s)
ρ_s	Density of particle size (kg/m^3)
ρ	Density of fluid (kg/m^3)
h	Flow depth (m)
g	Gravitational acceleration (m/s^2)
d_{50}	Median particle size (mm)
ks	Shape factor= $D_{u/s}/ D_{d/s}$
$D_{u/s}$	Upstream diameter of pier (m)
$D_{d/s}$	Downstream diameter of pier (m)
D	Pier diameter (m)
Fr	Froude number = $[v / (gh)^{0.5}]$
FD_{50}	Densimetric Froude number
R	Correlation coefficient
d_{16}	Grain size for which 16% by weight of the sediment is finer
d_{84}	Grain size for which 84% by weight of the sediment is finer
∂g	$= (d_{84}/d_{16})^{0.5}$ Geometric standard deviation of the grain size distribution

CHAPTER 1

INTRODUCTION

1.1 General

Scour holes created by the flow of water past bridge piers are a major cause of failure of bridge pier foundation (Chiew 1984). Scouring is a major process that greatly affects the health of modern infrastructure. In America, it has been estimated that 60% of bridges fail due to processes involving river hydraulics, including pier scour (Melville and Coleman, 2000). In New Zealand it has been approximated that one bridge fails per year due to scouring (Melville and Coleman, 2000).

There have been a lot of floods, which lead to bridge failures in Turkey during last decades. Some of these floods occurred in Trabzon (1990), Malatya (1991), Bartın (1998), Hatay (2001), and Mersin (2001) (Yanmaz, 2002). The prediction of scour depth during the design is more important because in case of under prediction of scour depths it leads to bridge failures and may be loss of life; while in case of overestimation of scour depths it leads to spending millions of dollars on a bridge.

Most scour prediction formulae, such as the Colorado State University (CSU) equation [currently used in the U.S. Federal Highway Administration (FHWA) Hydraulic Engineering Circular Number 18 (HEC-18)], and those published by Sheppard et al. (2004), Melville (2000), and Breusers (1977) are empirical and based on laboratory-scale data. Many of these equations yield similar results for laboratory-scale structures, but differ significantly in their predictions for prototype scale structures. The over prediction of many of these equations for large structures in fine sands is well

documented and is referred to as the "Wide Pier" problem. Sheppard (2004) believes this problem results from the exclusion of the pier width to sediment diameter ratio in many of these equations as well as to the wrong functional dependence of this parameter in those equations that do include it. He presents a possible explanation for why equilibrium scour depth depends on this ratio as well as why this dependence diminishes with increased values of this parameter. The limited field data that exist support his conclusions. Additionally, the field data confirm the functional relationship of this parameter in his equations, thus eliminating the "wide pier problem."

For engineering purposes, sediment scour at bridge sites is normally divided into four categories: 1) general scour, 2) aggradation and degradation scour, 3) contraction scour and 4) local scour.

Local scour is further divided into pier and abutment scour. General scour refers to mechanisms such as river meanders, tidal inlet instability, etc.

Aggradation and degradation scour refer to the raising or lowering of the streambed due to changes taking place up and/or downstream of the bridge (i.e., an overall lowering or rising of the stream bed).

Contraction scour results from a reduction in the channel cross-section at the bridge site. This reduction is usually attributed to the encroachment by the bridge abutments and/or the presence of large bridge piers (large relative to the channel cross-section). Local abutment scour results from the obstruction to the flow at the bridge abutments at the edges of the waterway.

Local scour is likewise the result of a flow obstruction, but one located within the flow field.

Local scour is divided into two different scour categories that depend on the flow and sediment conditions upstream of the structure. **Clear-water scour** refers to the local scour that takes place under the conditions where sediment is not in motion on a flat-bed upstream of the structure**.** If sediment upstream of the structure is in motion, then the local scour is called **live-bed scour**.

In this thesis, a new bridge pier shape will be determined through experimental investigations. The new bridge pier shape or shapes will be economic and reduce local scour upstream and downstream of the pier. Therefore, a detailed experimental study will be carried out to determine the effect bridge pier shape on scouring around the bridge piers.

1.2 Research Objective

The main objectives of the thesis are as follows:

1. Experimental investigation of unconventional bridge pier shapes to mitigate and reduce the depth and size of local scour around bridge piers.
2. Investigates the performance of different upstream and downstream round nose diameter with respect to local scour under live bed condition and compare the experimental results with the most practically used circular piers.
3. Reducing the depth and size of local scour around bridge piers, by using different upstream and downstream round nosed diameters.
4. Analyze the evolution of turbulent flow characteristics (flow velocity, turbulent intensities, turbulent kinetic energy and bed shear stress within the scour hole).

1.3 Layout of Thesis

This thesis is composed of five chapters. Brief descriptions of each chapter are given as:

Chapter 1 Introduction:

Introducing a brief history of scour around bridge pier, in addition explain the research objective and the layout of the thesis.

Chapter 2 Literature Review:

This chapter covered previous work that deals with, local scour around bridge piers, predicted maximum scour depth, parameters effecting on local scour and countermeasures of local scour.

Chapter 3 Experimental Setup and Methodology:

This chapter gives a description of the experimental apparatus, models and procedures.

Chapter 4 Results and Discussion:

This chapter gives results and discussions of results, analysis of flow field and turbulent field around upstream and downstream-facing round nosed pier.

Chapter 5 Conclusions and Recommendations:

Presents the principle conclusions drawn from the results of the study and recommendations for future works.

CHAPTER 2

LITERATURE REVIEW

2.1 Introduction

Numerous studies in a literature have been introduced on the local scour of cohesion less bed sediment around a bridge pier. This chapter attempts to present state of understanding of local scour in cohesion-les soil, the local scouring mechanism and countermeasures for decreasing local scour at bridge pier.

2.2 Types of scour and mechanism of local scour

Scour is defined as lowering of the level of the riverbed by water erosion induce exposing of bridge pier foundation. The amount of this reduction below the natural level is called depth of scour. The types of scour can be divided into three types' general scour, contraction scour and local scour as shown in Figure 2.1.

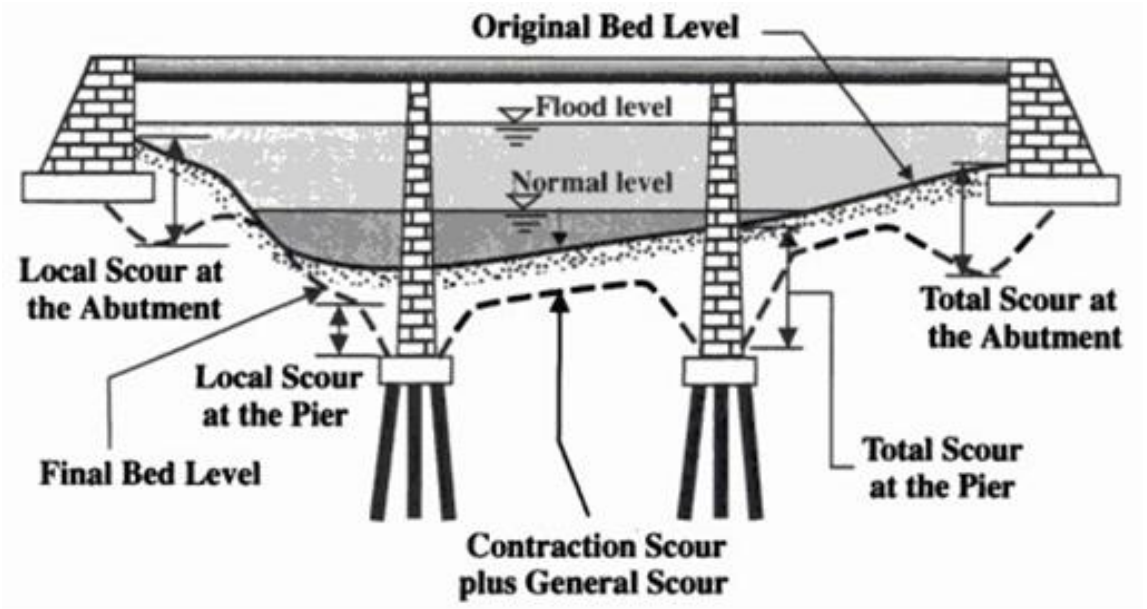

Figure 2.1 Types of scouring at a bridge crossing

General scour contains the removal of material from the bed and banks through all or most of the width of a channel. This type of scour may be natural or man prompted causes and needs both sediment and geomorphologic analysis.

2.2.2 Contraction scour

Contraction scour results from the acceleration of the flow due to either a natural or bridge contraction. With a reduction in flow area there is an increase in average velocity and bed shear stress. Because of the growth in velocity and shear stress, more bed material is transported through the constricted reach than the reaches have no contraction.

2.2.3 Local scour

The elementary mechanism causing local scour at bridge piers and abutments is the creation of vortices at their base. The vortex eliminates bed material from the base of the obstruction. As the sediment carrying amount, which is leaving from the scour hole is higher than that coming into, a scour hole develops. As the depth of the scour growths, the strength of the vortices is decreased. On the other hand, there are vertical vortices downstream of the structure called wake vortices. The strength of wake vortices weakens quickly as the distance downstream of the structure rises. Generally, depths of local scour are much larger than general or contraction scour depths, often by a factor of ten (Federal Highway Administration, 2001).

2.3 Local Scour Process and Flow Field around Piers

The flow field at a bridge pier is a complex three dimensional turbulent phenomenon resulting from hard flow-pier-sediment interaction. The basic mechanism inducing local scour at piers is the increased turbulence and created secondary flow in form of vortices and downflow close to a pier (Shen et al. 1969, Melville 1975, Breusers and Raudkivi

1991, Hoffmans and Verheij 1997, Muzzammil et al. 2004). Flowing towards the pier, the flow velocity becomes to zero on the upstream front of the pier, called stagnation point. This causes an increase of the pressure at the pier. As the flow velocity diminishes from the surface to the bed, the pressure on the pier side falls consequently. The downward pressure gradient forces the flow down the pier aspect. The resulting downflow hits the bed and produces a hole at the pier base. The downflow rolls_up again as it continues to make a hole and by interaction with the coming flow forms a complex vortex system, named horseshoe vortex. This improves as an effect of flow separation at the upstream face of the scour hole. The horseshoe vortex is very effective in carrying sediment particles out from the pier. As the scour depth growths, the strength of the horseshoe vortex decreases, leading to a reduction of the scouring rate. At the downstream face of the pier a wake vortex system is formed due to the separation of the flow on the pier sides. Both the horseshoe and the wake vortices erode sediment from the base region around the pier. The wake vortex strength reduces with the distance and as a result the eroded sediment deposits downstream the pier. Figure 2.2 shows local scour processes at a cylindrical pier.

2.3.1Clear and live bed scour

The first major division is between clear-water scour and live-bed scour. The critical issue here is whether or not the mean velocity (u m/s) of the flow upstream of the bridge is less than or larger than the scour-critical velocity (u_c m/s) needed to move the bed material. If $u < u_c$ then the bed material upstream of the bridge is at rest: this is referred to as the clear water condition because the approach flow is clear and does not contain sediment. This means that any bed material that is removed from a local scour hole is not replaced by sediment being transported by the approach flow. The maximum local scour depth is achieved when the size of the scour hole results in a local reduction in

velocity and the flow can no longer take away bed material from the scoured area. Live-bed scour occurs where u> u_c and the bed material upstream of the crossing is moving. This means that the approach flow continuously transports sediment into a local scour hole. By itself, a live bed in a uniform channel will not cause a scour hole; for this to be created some additional increase in velocity is needed, such as that caused by a contraction (natural or artificial, such as a bridge) or a local obstruction (e.g. a bridge pier).

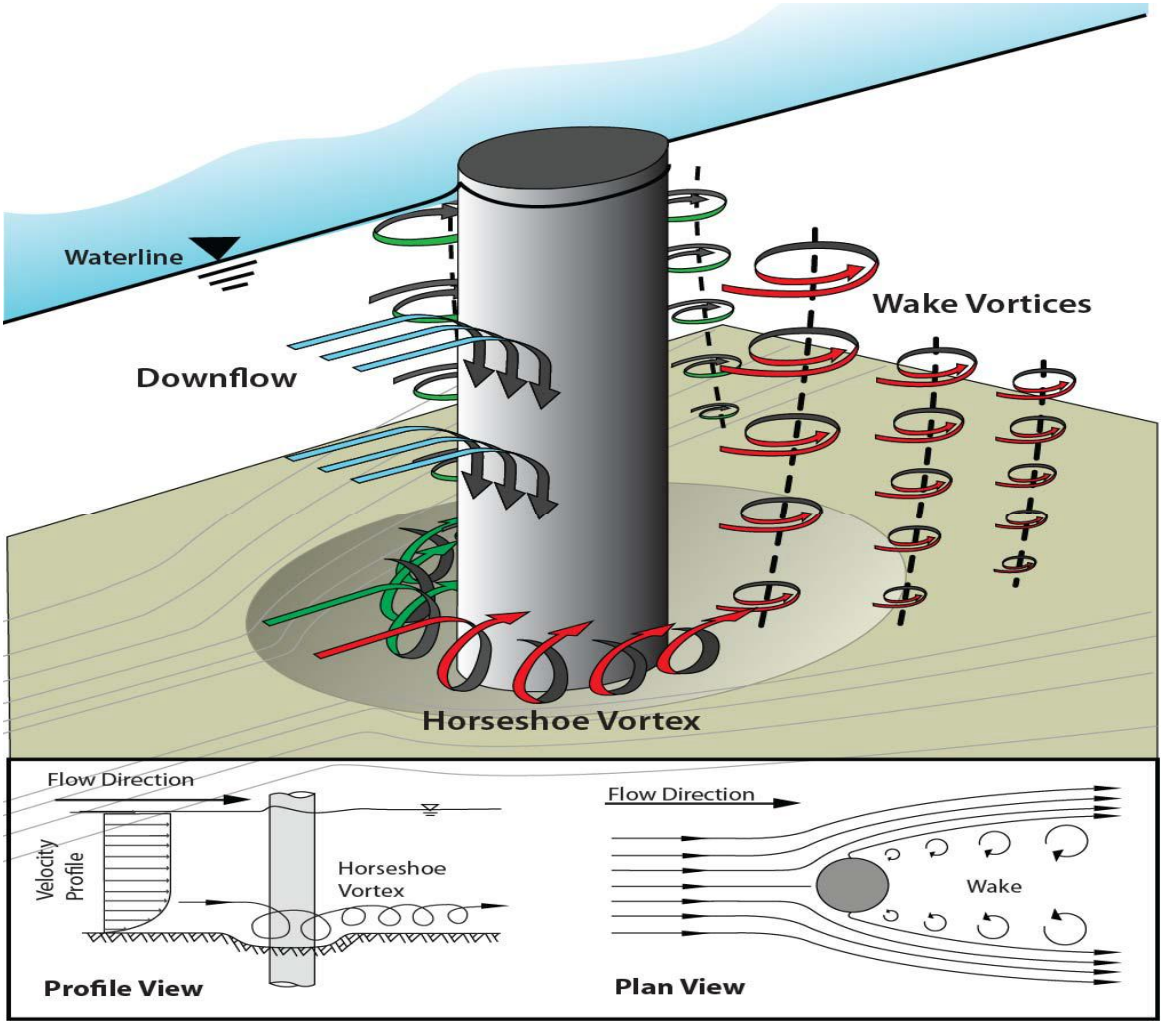

Figure 2.2 Schematic drawing of local scour processes at a cylindrical pier

.

The equilibrium scour depth is achieved when material is transported into the scour hole at the same rate at which it is transported out. The clear-water and live-bed conditions are significant because to some degree the growth of the scour hole will depend upon whether or not the bed material is already in motion.

2.4 Physical modeling of local scour around bridge pier

Experimental techniques and modeling in scour study is the best way to understand how the scour around bridge pier or abutment happened. Laboratory studies are needs to more adequate in work and give us a data that we need to compared with numerical data and developed it by an equation to predict a worse case. There are many researchers which are depending on laboratory data, to described behavioral patterns around bridge piers scours. Some of them summarized the important work on local scour around bridge piers like Dargahi (1982*)* and Breusers et al. (1977). Hosny (1995) studied the effect of cohesive soils on local scour around cylindrical pier by using remolded clays in his experiments and found that the equilibrium scour Depth in non-cohesive soils greater than in cohesive soils. He prepared an equation to estimate maximum scour depth in cohesive soil in terms of the flow Froude number, compaction, initial water content and cylinder diameter.

Yanmaz, A. M., and Altinbilek, H. D. (1991) was carried out in clear water scour case he used square and circular shape of piles, for circular shape the diameter was, 5.7cm, 6.7cm and 4.7 cm, using sand with size d_{50}= 0.84 mm and 1.07mm.

Graf et al. (2001) studied on cylindrical bridge pier sample to investigate the flow patterns in plan of upstream and downstream by using Acoustic-Doppler Velocity Profiler (ADVP). They found that the turbulent kinetic energy was very great at the

foot of the cylindrical bridge pier on the upstream side but compared to the approach flow the shear stress was reduced in the scour hole.

Mia, M and Nago (2003) study by experimental work to predict the local scour depth with time. He used a cylindrical pier under clear-water flows placed in uniform beds. By depends on sediment transport equation the pier scour depth was calculated. When the bed-shear stress tends to critical bed-shear stress the local scour depth reached to the Equilibrium. Therefore, at the circular bridge pier the changes to bed-shear stress should be included in the sediment transport theory.

Later, Unger and Hager (2007) examined the features of downflow and horseshoe vortex at the vertical plane at the face of a wall-side attached half cylinder by utilizing the PIV. Two sediment sizes were used, a uniform sand with d50 = 1.14 mm and s = 1.18 as well as a non-uniform sand mixture with d50 = 5.00 mm and s = 2.29. The found data Supplied an experimental data bases for numerical simulation.

Ming Zhao Liang Cheng (2010) studied local scours around a submerged vertical circular cylinder experimentally in steady currents and numerically. The experiments were conducted for two diameters of cylindrical pier the experiments conducted in water channel 4m wide, 45 m long, 2.5 m deep, the flume supply with pump 1 m^3/s capacity. The section of the test was 4 m long, 4 m wide 0.25 m deep median size of the sand was d_{50}=0.4 mm. Transient scour depth at the stagnation point (upstream edge) of the cylinder was measured using the so-called conductivity scour probes. Seabed topography around each cylinder pier was measured by using laser profiler. The effect of the height-to-diameter ratio on the scour depth was investigated in this study. The experimental results show that the scour depth at the stagnation point is independent on cylinder height-to-diameter ratio when the latter is smaller than two. The increase rate

of equilibrium scour depth with cylinder height increases with an increase in Shields parameter.

Jau-Yau Lu and other (2011) works on cylindrical piers with unexposed foundation to estimate the temporal development of scour depth. A cylindrical pier with a foundation is considered as non-uniform pier. The concept of primary vortex and the principle of volumetric rate of sediment transport are used to develop a methodology to characterize the rate of evolution of the scour hole at non-uniform cylindrical piers. The scouring process includes three zones; Zone one having the scouring phenomenon similar to that of a uniform pier, Zone two in which the scour depth remains unchanged with its value equal to the depth of the top level of foundation below the initial bed level while the dimensions of the scour hole increase, and in Zone 3 the geometry pier foundation influences the scouring process. A concept of superposition using an effective pier diameter is proposed to simulate the scouring process in Zone 3. In addition, the laboratory experiments were conducted to utilize the laboratory results were used uniform sand with d_{50}= 0.52 mm having geometrical standard deviation of less than 1.4. The laboratory experiments were carried out in a 17 m long rectangular flume having a cross section of 0.6 m wide and 0.6 m deep at the Department of Civil Engineering, National Chung Hsing University, Taichung, Taiwan. The pier models made of plexiglass were embedded vertically in the middle of the sand recess of 7.5 m long, 0.6 m wide, and 0.25 m. The simulated results obtained from the proposed model are in good agreement with the present experimental results and also other experimental data. Also, the effect of unsteadiness of flow is incorporated in the model and the results of the model are compared with the experimental data. The model agrees satisfactorily with the experimental data.

Ozlap, C., M. (2013).Investigated experimentally the effect of inclination of two bridge pier groups. The experiments have been conducted with 3 inclination angels. The researcher observed that the amount of local scour reduces substantially by the effect of inclination in the group piers. The data was analyzed and an empirical scour depth equation is developed.

Kuila, A. (2013) carried out experiments to study the horseshoe vortex flow field at three cylindrical piers. The piers where two of them are arranged inline along the direction of flow and the other one is placed eccentrically in between them. All the experiments were conducted under clear water condition; with discharge 25 l/s. ADV was used to measure the velocity field. The time averaged velocity vectors were plotted. The vorticity and circulation of horseshoe vortex is determined. The results show that the circulation obtained for the eccentric pier is more than that of the inline piers and the circulation of horseshoe vortex for the inline rear pier was higher than for the inline front pier. Vector plots of the flow fields reveal the vorticity and circulation characteristics of the horseshoe vortex flow associated with an up flow at equilibrium scour hole condition.

2.5 Factors affecting local scour

2.5.1 Flow intensity effect

Flow intensity *(*$u / u_{c)}$, defined as the ratio of the mean approach flow velocity to the critical velocity (threshold velocity for the motion of the sediment in the approaching flow), is used extensively as indicator of scour conditions (Raudkivi and Ettema 1983, Breusers and Raudkivi 1991, Hoffmans and Verheij 1997). For uniform sediment material, clear water scour occurs for flow intensity up to unity, for which there is no sediment supply from the upstream to the scour hole. Live bed scour occurs when flow u_a controls scour conditions in addition to the flow intensity (Melville and Sutherland 1988). For non-

uniform sediment material, clear water scour conditions exist when u/u_c **<**1 and live-bed scour occurs when (u/u_c) **>**1. For clear-water scour conditions, the equilibrium scour depth in uniform sediment increases almost linearly with the flow velocity to a maximum at the critical velocity which is called as threshold peak, see Figure 2.3. As the mean flow velocity exceeds the critical velocity, the average scour depth first reductions and then increases again to a second peak which is called the live-bed peak. This second peak happens at the transition flat-bed conditions and does not exceed the threshold peak. Other investigators noted that the live-bed peak may exceed the threshold peak at higher velocities.

2.5.2 Effect of flow shallowness

The flow depth to pier width ratio *h/D* is known as flow shallowness and represents the influence of flow depth on local scour. Many researchers have been investigated the effect of flow depth on the local scour depth at piers, such as Laursen and Toch (1956), Breusers et al.(1977), Ettema (1980), and Chiew (1984). They concluded that the scour depth growths with the flow depth up to a limiting value for the flow shallowness ratio.

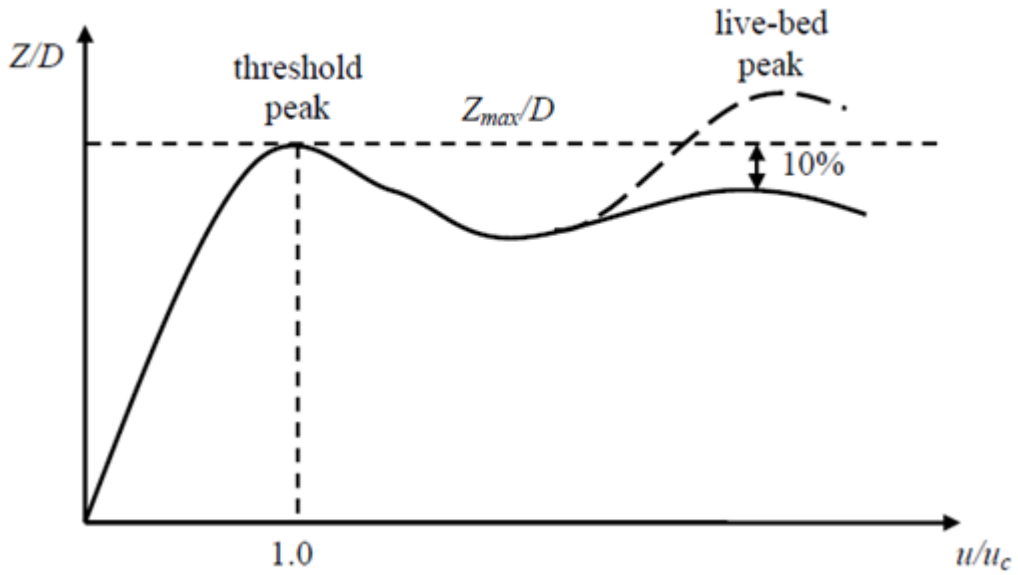

Figure 2.3 Local pier scour depth versus flow intensity (Modified after Breusers and Raudkivi 1991)

This value is about 2.6 according to Melville and Sutherland (1988). Beyond this value, the local scour depth becomes independent of the flow depth. Figure 2.4 shows the relative local scour depth versus flow shallowness. Flow depth has little effect on scour depth for H/D > 1-3 Bonasoundas (1973). Melville and Coleman (2000) present a useful classification of scour processes at bridge piers depending on the flow shallowness as shown in Table 2.1. The interference between the two rollers which are the horseshoe vortex at the base of the pier and the surface bow wave help to understand the effect of flow depth. For narrow pier class or deep flow, there is no interference between the two rollers and the scour depth depends only on the pier width. While at wide piers, the interference between the bow wave and the horseshoe vortex which rotates in opposite direction reduces the capability of the horseshoe vortex to entrain sediment from the scour hole. That results in a decrease of the scour depth with a decrease in the flow depth. For intermediate width class, the scour depth depends on both parameters flow depth and pier width.

Table 2.1 Classification of local scour processes at bridge piers

Class	D/h	Local scour dependence
Narrow pier	$D/h < 0.7$	$z \alpha D$
Intermediate pier width	$0.7 < D/h < 5.0$	$z \alpha \overline{hD}$
Wide pier	$D/h > 5.0$	$z \alpha h$

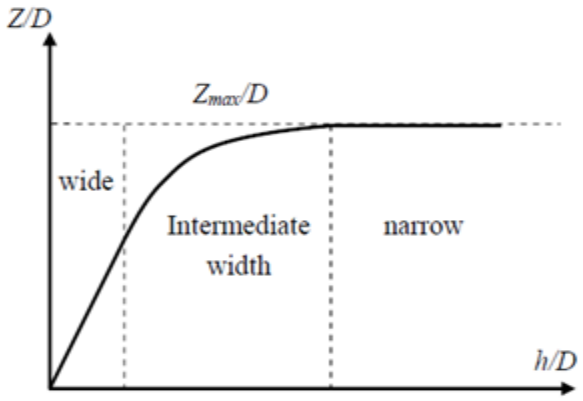

Figure 2.4 Local pier scour depth versus flow shallowness (Melville and Coleman 2000)

2.5.3 Sediment size, coarseness and gradation effect

Sediment size in sand size range has little effect on scour depth but will affect the time required to reach the equilibrium (Hoffmans and Verheij 1997). Raudkivi and Ettema (1977a, b) investigated experimentally the influence of sand size on the scour depth at circular pier. They concluded that a flat bed, i.e. clear water scour, cannot be maintained in the laboratory near the threshold conditions when the grain size d50 <0.70mm. The ripples are expected to develop when the flow velocity exceeds 60% of the threshold velocity. Breusers and Raudkivi (1991) give the same conclusion for ripples formation with an exception: clear water scour conditions can be maintained when the geometric standard deviation of the sand is between 1.30 and 1.50.

The effect of sediment gradation on local scour was investigated by many researchers, such as Ettema (1980), Chiew (1984), Dey (1995) and Molinas (2003). The general conclusion was that both the scour rate and the scour depth decrease as the geometric standard deviation increases. Dey et al. (1995) divided the sediment material into uniform sediment (σg < 1.4) and non-uniform sediment (σg >1.40).

2.5.4 Relative Sediment Coarseness

The ratio of the pier width to the mean grain size of the sediment material is defined as relative sediment coarseness D/d_{50}. Figure 2.5 shows the scour depth versus the sediment coarseness ratio. As shown, the scour depth increases with sediment coarseness up to a maximum at D/d_{50} = 25 - 50, and apparently becomes independent when D/d_{50} ratio exceeds 50 (Raudkivi 1986, Breusers and Raudkivi 1991, Melville and Sutherland 1998).

Ettema (1980) found that the effect of sediment coarseness ratio was significant up to

D/d_{50} = 20 – 25, and for higher values of sediment coarseness, the scour depth became independent of D/d_{50}, see Figure 2.5. With decreasing values of D/d_{50}, the sediment becomes increasingly coarser compared to the scale of the local flow within the scour hole, and a significant proportion of the energy of the down flow is dissipated at the base of the scour hole. However, Sheppard et al. (1995) and (2004) investigated local scour at a circular pier in a large flume and concluded that the sediment coarseness ratio with very large values may decrease the scour depth. Recently, Lee and Strum (2009) studied the effect of sediment size on local scour depending on laboratory and field data. Their outcomes revealed that after the scour depth reached a peak value at D/d_{50} = 25, it decreased again as the sediment coarseness increased.

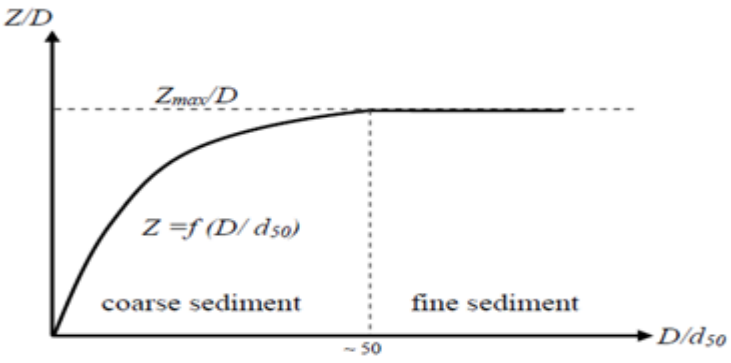

Figure 2.5 Local pier scour depth versus sediment coarseness (Melville and Coleman 2000)

2.5.5 Time Effect

Development of local pier scour is dependent on time and scour conditions. Under Clearwater conditions, scour depth develops gradually in time following a first order exponential relation towards the equilibrium clear-water scour depth. For live-bed conditions, scour depth growths quickly with the time reaching a maximum value in short duration. Then scour depth fluctuates over time around a mean value called equilibrium live-bed scour depth (Raudkivi 1976, Melville and Chiew 1999). The equilibrium scour depth under live-bed is about 10% less than under clear-water conditions (Graf, 1996). Figure 2.6 illustrates the time development of scour depth. For clear-water conditions, the known relations for predicting the equilibrium scour depth were developed through laboratory models. The time required to achieve the equilibrium depends on the scale of these experiments. This is a very important point because the results obtained after short run time may give scour depths smaller than the equilibrium scour depth. The data obtained in small-scale laboratory experiments after short run time of 10 to 12 hours can lead to scour depths less than 50% of the equilibrium depth of scour (Melville and Chiew 1999). Therefore, it is necessary to run experiments for several days. For live-bed conditions, the equilibrium scour depth (clear-water) is appropriate. During flood events, live-bed scour occurs during the flood duration. The hydrograph and duration of the flood help to determine if the equilibrium Live-bed scour will develop. During the duration of recession flow, clear water conditions may prevail and induce additional scour (Breusers et al., 1977).

2.5.6 Effect of Pier Shape and orientation

The amount of scour is also affected by the pier shape, size as well as orientation (Roads, 2013). For example, one would predict that an elliptical pier may produce less scour than a square pier due to its shape.

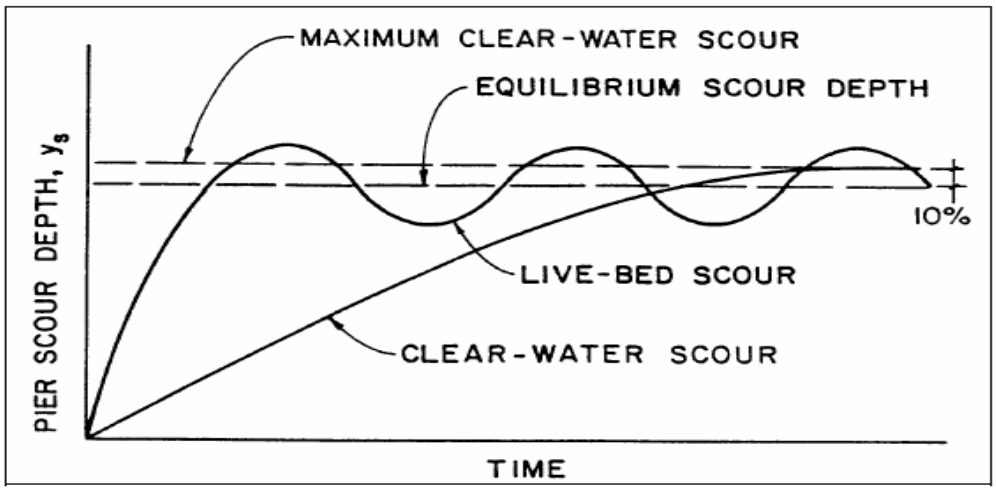

Figure 2.6 Scour depths as a function of time (Breusers and Raudkivi 1991)

Various experiments have been performed to examine closely the effect of pier shape on scour. Figure 2.7 summarizes the results of one such study (Mostafa 1994, cited in Melville and Coleman 2000).

Shape	l/b	Projected width of pier (mm)	$d_{s(noncircular)}/d_{s(circular)}$
A	4	140	1.50
B	4		1.33
C	1		1.29
D	200		1.28
E	1		1.28
F	1		1.07
G	1		1.00

Figure 2.7 the shapes A to G on the scour depth relative to a circular pier (Melville, 2000)

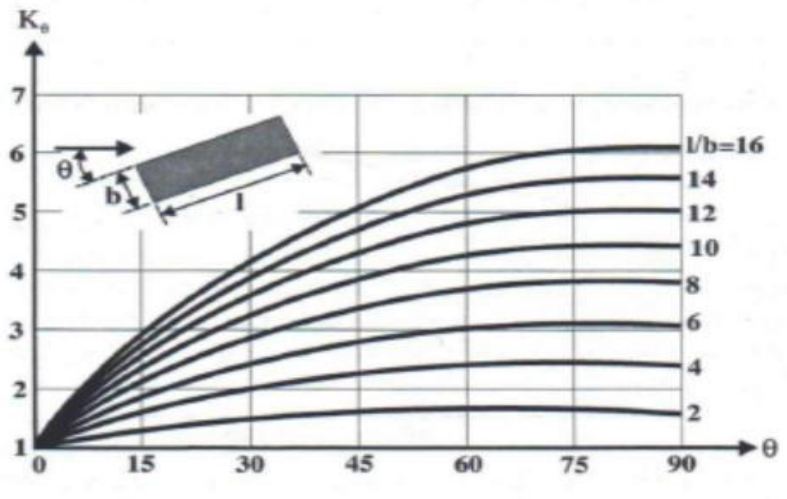

Figure 2.8 the effect of pier orientation on the scour depth. (Melville, 2000)

With the exception of circular piers, the angle at which the water hits the pier is an important factor in the depth of local scour as shown in Figure 2.8. The Kθ axis represents the factor by which the scour depth is expected to increase as found in experiments by Ettema (Ettema et al. 1998).

2.6 Scour prediction equation

There are more than 35 equation have been written for estimating the local scour at bridge pier according to McIntosh (1989). Most of local scour equations are based on research in laboratory flumes with non-cohesive, uniform bed material and limited verification of results with field data (McIntosh, 1989). The equations are classified according to a local scour type if its live-bed scour or clear water scour and there are many method to develop local scour equations by curveting or another method. Some of these equations are developed using regression method to compute maximum scour depths and the computing this results from predicted equations may be useful for design purposes because the results from this equations may give the designer more predict for risks and then to put a suitable factor of safety against local scour.

1-Breusers equation

Breusers (1965) developed an equation for local scour depth at piers for tidal flow Breusers concluded, that maximum depth of the scour was 1.4 times the pier diameter.

$$d_s = 1.4b \quad (2.1)$$

Where, b= pier diameter (m)

2-Laursen equation

Laursen and Toch (1956) developed equations by depend on experimental work in Iowa institute of hydraulic research, Laursen and Toch equations assumes that flow depth is the most important factor in determining scour depth, but Shen (1966) developed an equation assumed that velocity is important by including Froude number. The below equations (Laursen and Toch) are for square-nosed piers (Dr Les Hamill, (1999) Bridge hydraulic).

Live bed-scour:

$$d_{sp} = 1.5\ {b_p}^{0.7} Y^{0.3} \quad (2.2)$$

Clear-water scour:

$$d_{sp} = 1.35\ {b_p}^{0.7} Y^{0.3} \quad (2.3)$$

Where, d_{sp} is the pier scour depth (m), b_p is width of the pier (m), Y is the depth of approach flow (m).

Shen II equation;

$$d_{sp} = 3.4\ {b_p}^{0.67} F^{0.67} Y^{0.33} \quad (2.4)$$

Where: F is the Froude number of the approach flow.

3-Larras equation

Larras (1963) he depends on field investigation to get the required data in several French rivers and scale-model investigation to developed Larras equation:

$$y_s = 1.42\ K_{S2} b^{0.75} \quad (2.5)$$

Where K_{S2} is a coefficient based on the shape of the pier nose (1.0 for cylindrical piers and 1.4 for rectangular piers).Where y_s and b in ft.

Larras measured scour depth after a flood had passed, there for the equation depends on pier width and shape only (Shen and others, 1969).

Local scouring has been studied fairly extensively which has resulted in a wide range of equations. An example of this is the equation developed by Richardson and Davis this is used in HEC-18 (Melville & Coleman, 2000). According to this equation, the scour depth depends on the width of the pier, the velocity, the shape of the pier, the approach angle of water onto the pier, armoring by bed material as well as the width of the pier.

$$d_s/\text{b}=2.0\ k_s k_\theta k_3 k_4 \left(\frac{y}{b}\right)^{0.35} F_r^{\ 0.43} \quad (2.6)$$

Where, k_s is factor for the shape of the pier, k_θ is factor for the angle of approach, k_3 is factor for the mode of sediment transport, k_4 is factor for armoring by bed material, b is width of the pier, d_s is scour depth, F_r is Froude number, y is water depth before the constriction.

2.7 Development of maximum scour depth with time

Chabert and Engeldinger (1956) designated the behavior shape of scour at a cylindrical pier according to the difference of scour depth with time. In clear-water scour, equilibrium scour depth is transfer asymptotically with time, while in live-bed scour the

scour develops quickly and then fluctuates in with respect to the passage of bed forms. According to Shen et al. (1969), the equilibrium scour depth in live-bed scour is less than in clear-water scour by 10% as shown in Figure 2.6.

Table 2.3. Summary of predicted equilibrium scour depth equations

Researcher	Equations	Description
Breusers (1965)	$d_s = 1.4b$	d_s is maximum scour depth b is pier diameter
Laursen and Toch (1956)	$d_{sp} = 1.5\ {b_p}^{0.7} Y^{0.3}$	d_{sp} is the pier scour depth (m), b_p is width of the pier (m),Y is the depth of approach flow, for live bed scour
Laursen and Toch (1956)	$d_{sp} = 1.35\ {b_p}^{0.7} Y^{0.3}$	For clear-water scour
Shen II	$d_{sp} = 3.4\ {b_p}^{0.67} F^{0.67} Y^{0.33}$	F is the Froude number of the approach flow
Larras (1963)	$y_s = 1.42\ K_{S2} b^{0.75}$	K_{S2} is a coefficient based on the shape of the pier nose
HEC-18 equation	$\frac{y_S}{y_o} = 2\ K_1 K_2 K_3 \left(\frac{b}{y_o}\right)^{0.65} {F_O}^{0.43}$	F is a Froude number K_1 K_2 K_3 is coefficient
Melville and Sutherland (1988)	$d_S = K_1 K_d K_y K_\propto K_s b$	
Raudkivi and Ettema(1983)	$y = 2.3bK\sigma$	where $K = f(\sigma_g) = 1$ for uniform sediment,σ_g= geometric standard deviation of the grain size distribution
Shen et al. (1969)	$y_{se} = 0.000223{R_b}^{0.619}$	where R_b = pier Reynolds number

2.7.1 Equilibrium scours depth and some definitions of time to equilibrium

Equilibrium scour depth is said to happen when the scour depth becomes stable appreciably with time. Equilibrium between the erosive ability of the flow and the resistance to movement of the bed materials is gradually reached through erosion of the flow boundary. The concept of an equilibrium scour condition is widely reported in the literature. Franzetti et al. (1982) made reference to the work of both Baker and Qadar in which the existence of an equilibrium scour condition was confirmed. In this context, Franzetti et al. refer to equilibrium as the state of scour development where no further change occurs with time. The occurrence of a non-equilibrium condition, however, has also been reported by many researchers. Because an equilibrium clear-water scour condition is advanced asymptotically with time, Melville and Chiew (1999) observed that it can take an infinite amount of time for the equilibrium scour hole to grow. They observed that an deceptive equilibrium scour hole may carry on to deepen at a relatively slow rate long after equilibrium conditions were thought to exist. For an equilibrium scour condition to be achieved in small-scale laboratory experiments of clear-water scour, tests must be run for several days (Melville and Coleman, 2000). Melville and Coleman also pointed out that experiments carried out for a shorter period of time, say 10 to 12 hours, can result in a scour depth less than one-half of the equilibrium scour depth. The definition of time to scour equilibrium adopted for a given test is more significant in the results obtained and also in the conclusions reached (Franzetti et al. 1982). They also observed that, if care is not taken, the definition of time to equilibrium scour depth can affect the results such that the same experiment carried out under the same experimental conditions but for a different timeframe can yield a different conclusion. Several researchers have come up with different definitions of time to equilibrium scour depth (e.g. Heidarpour et al. 2003; Zarrati et al. 2004; Mia and Nago

2003; Sheppard et al. 2004). Because it takes a very long time for an equilibrium condition to be attained, it is time demanding to carry out experiments of such long duration. In view of this, the maximum time of the experiments performed by Bozkus and Osman (2004) was limited to two hours. Although the maximum duration of equilibrium scour depth was not achieved within two hours, they observed that the rate of growth in the depth of the scour hole was substantially reduced after two hours. Ettema (1980) defined the time to equilibrium scour as the time at which no more than 1 mm of incremental scour was realized within a timeframe of four hours. Sheppard et al. (2004) and Melville and Chiew (1999) stopped their experiments when the change in the scour depth did not exceed 5% of the pier diameter during a 24-hour period. A uniform period of 24 hours was used for all of the tests carried out by Lauchlan (1999). Jones and Sheppard (2000) noted that the duration for many of the experiments reported in the literature was insufficient for the scour depth to have reached an equilibrium condition and, as such, much of the data reported therein may not be useful. They also found that the lack of complete reporting of experimental conditions rendered some data unusable. It may be concluded, therefore, that the whole concept of an experimental equilibrium scour condition warrants further investigation.

2.8 Flow Field around a Scour Hole

The flow field in the vicinity of a blunt-nosed vertical obstruction is complicated and dominated by a system of vortices. Much research has attempted to ascertain a complete understanding of the mechanisms which lead to the system of vortices. Some of the more prominent contributions made by various investigators are discussed below.

Shen et al. (1966a) performed an extensive analysis of the mechanisms which lead to pier scour at a blunt-nosed pier. They concluded that an adverse pressure gradient is created at the pier which in turn effects a three-dimensional separation of the boundary

layer. A stagnation point occurs at approximately three-quarters the depth of the pier, above which the water has zero velocity. Below the stagnation point, a strong downward flow is produced. The downflow is thought to have a velocity equal in magnitude to the approach velocity. Once the downflow impacts the channel bed, it rolls back onto itself, forming a vortex. The vortex is forced in an upstream direction due to the momentum of the downflow, and is eventually turned around to the normal direction of flow once the momentum of the normal flow is sufficiently strong to overcome the downflow momentum Figure 2.9. The vortex then sheds from either side of the pier to form the horseshoe vortex system.

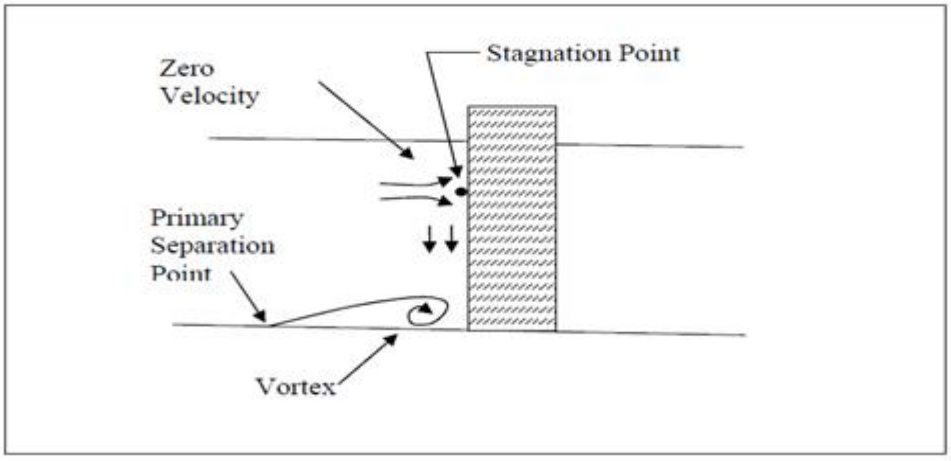

Figure 2.9 Representation of the mechanisms responsible for the development of a scour hole

Shen et al. (1966a) also analyzed the mechanics of the vortex and concluded that it is the pier acting as an obstruction which concentrates the vorticity already present in the flow. Upon presenting an extensive mathematical Zero Velocity Stagnation Point Primary Separation Point Vortex analysis, they stated that the horseshoe vortex can be considered to possess a core which rotates as a rigid body. Additionally, they showed that the strength of the vortex core is proportional to the pier Reynolds number. Finally, through experimental analysis, Shen et al. (1966a) confirmed that the primary vortex is

un-steady and moves up the scoured slope while its rotational velocity increases, and eventually sheds downstream.

Shen et al. (1969) suggested that for the purpose of experimental investigation the width of an experimental flume should be at least eight times the pier size for clear water scour condition, so that blockage effect are minimized.

Melville and Raudkivi (1977) presented results of the flow field, turbulence intensity distributions and boundary shear stresses in the scour zone of a circular pier under clear water conditions. They used a hydrogen bubble technique to trace the flow patterns in the scour hole. They observed the formation of the horseshoe vortex system due to the downflow reflecting off the pier, as well as an increase in vortex size as the scour hole grows deeper. Estimates of mean bed shear stresses were made at 2 mm from the bottom using Newton's equation for viscosity. Melville and Raudkivi state that maximum shear stress occurs at the sides of the pier, which also coincides with the location where scour commences. Because of the difference in location of maximum shear and that of maximum scour depth, they concluded that scour must be caused by the downflow impacting on the bed, thereby dislodging the particles which eventually are carried downstream by the horseshoe vortex.

Rajaratnam (1980) studied the effects of vertical jets on an erodible non-cohesive bed. He found that the vertical jet creates a scour hole which is highly dependent on the velocity of the flow as it impinges on the bed.

Baker (1980) used dye visualization to show that the vortex circulation at the base of a pier remains constant even as the vortex grows in size while settling into the scour hole. Therefore, as the vortex grows, its tangential velocity decreases and thus the shear beneath the vortex also decrease.

Breusers et al. (1977) reported that Vautier (1972) measured flow features around vertical piers in two separate flumes of different widths, with the same approach flow conditions. They found that the pier nose vortex shedding frequencies were between 0.25 and 0.50 cycles per second, with no important difference in either the autocorrelation function or the spectral density function for flow velocity measurements.

Raudkivi (1986) used laboratory analysis to show that a downflow exists on the upstream face of a pier. The downflow is generated by a decreasing pressure gradient from the water surface to the channel bottom. He showed that the downflow has a velocity distribution with a maximum value occurring at 0.02 to 0.05 cylinder diameters upstream of the cylinder, being closer to the cylinder nearer to the channel bed. The maximum velocity of the downflow reaches about 80 percent of the mean approach flow velocity. The horseshoe vortex develops as a result of the downflow impacting on the channel bottom and Raudkivi believed it to be a result of scour, not the cause of it. Raudkivi stated that the downflow is the main scouring agent and acts as a vertical jet which loosens and dislodges sediment particles.

Grecco (1990) observed that a horseshoe vortex system undergoes the following stages as the pier Reynolds number increases: steady single and multiple vortex regimes, simple oscillation, irregular unsteady motion, transition and turbulence. The critical Reynolds number from transition to turbulence is 4750. Eckerle and Awad (1991) defined a dimensionless parameter $(Re_D)^{1/3}(D/\delta)$, where Re_D = Reynolds number, D =depth of flow, and δ = boundary layer thickness, for a turbulent boundary layer flow. When this parameter is less than 1000, one horseshoe vortex system exists in the plane of symmetry; when this parameter is greater than 1000, no vortex is present.

Wen et al. (1993) made comparisons between the vortex systems that form on a rigid bed at the intersection of the bed and cylinder, and at the intersection of the cylinder and bed in a scour hole. They found that at the flat bed (before scour would commence), the vortex system consists of multiple strong primary (clockwise) vortices as well as weak secondary (counter-clockwise) vortices. The vortices oscillate upstream then back downstream before shedding around the pier. The frequency of shedding becomes unstable as the Reynolds number is increased. The vortex system within a scour hole generally consists of one vortex which is comparable to the size of the scour hole. The vortex rotates very slowly, and hence produces a weaker bed shear stress than in the flat bottom situation. The position of the vortex changes little, but oscillates slightly for higher Reynolds numbers.

Dey et al. (1995) developed a series of equations for velocity profile predictions in the x, y, and z directions in the upstream, downstream, and in the scour hole. The circulating and oscillating nature of the flow within the scour hole made measurements difficult, thereby questioning the applicability of the equations in this vicinity. Additionally, Dey et al. remarked that because of the downflow at the front face of the pier impacting the bed, the no-slip condition cannot be applied, resulting in the disappearance of a boundary layer.

Ahmed and Rajaratnam (1998) analyzed the effects of bottom bed material on the resulting flow field in the area of cylindrical piers. Three bed conditions were analyzed: smooth, rough (rigid), and mobile. They found that for all bed conditions, the effect of the pier on the approaching velocity distribution can be felt for approximately 2.5 pier diameters in the upstream direction. The velocity decreases gradually as the cylinder is approached. Near the bed, the velocity diminished steadily to a point of negativity,

which is due to the formation of the vortex system at the base of the pier. The pressure rises gradually as the pier is approached. However, the point at which the pressure begins to rise varies according to the approach flow velocity, proposing that the existence of the pier is felt more upstream during flows with higher velocities. Also, larger piers produced higher pressure values at the face of the pier. Ahmed and Rajaratnam also found that the downflow produced by the presence of the pier exhibits a uniform velocity distribution. The maximum downflow velocity was measured to be as much as 95 percent of the maximum approach flow velocity once the scour hole was formed. This result was also discovered by Ettema (1980). The maximum downflow velocity before the initiation of a scour hole reached about 35 percent of the approach flow velocity.

Ali and Karim (2002) reported on the principal features of the flow field which lead to pier scour. In summary, the flow slows as it approaches the cylinder, coming to rest at the face of the pier. The associated stagnation pressures are highest near the surface, where the deceleration is greatest, and decrease downwards. In response to the downwards pressure gradient at the pier face, the flow reaches a maximum just below the bed level. Ali and Karim claim that it is this downflow impacting on the bed which is the main scouring agent. The downflow acts like a vertical jet eroding a trench in front of the pier; the eroded material then is transported downstream by the development of the horseshoe vortex. The combination of the downflow and the horseshoe vortex provides the dominant scour mechanism. They also noted that the scour hole development begins at the sides of the pier with the two holes quickly transmitting upstream around the perimeter of the cylinder to meet on the centerline. Dargahi (1990) noted that the initiation of scour at the sides of the pier is due to the increased velocities of the flow at the sides of the pier, but that maximum scour is a

result of the downflow and horseshoe vortex which form at the upstream face of the pier.

Kuila, A. (2013) carried out experiments to study the horseshoe vortex flow field at three cylindrical piers. The piers where two of them are arranged inline along the direction of flow and the other one is placed eccentrically in between them. All the experiments were conducted under clear water condition; with discharge 25 l/s. ADV was used to measure the velocity field. The time averaged velocity vectors were plotted. The vorticity and circulation of horseshoe vortex is determined. The results show that the circulation obtained for the eccentric pier is more than that of the inline piers and the circulation of horseshoe vortex for the inline rear pier was higher than for the inline front pier. Vector plots of the flow fields reveal the vorticity and circulation characteristics of the horseshoe vortex flow associated with an up flow at equilibrium scour hole condition.

Scour hole characteristics around a single vertical pier in clearwater have been investigated by Dash, Ghosh and Mazumdar (2012), they were concluded that the scour hole dimension effected by densimetric Froude number (F_{D50}) and flow depth (h). Empirical relationships were developed on the basis of obtained results.

Many studies investigating experimentally and numerically the flow field around the bridge piers have been carried out, such as Dargahi (1987), Muzzammil and Gangadhariah (2003), Unger and Hager (2007), Dey and Raikar (2007), Kirkil et al. (2008), Link et al. (2008a), and Gobert et al. (2010). Flow field has been investigated with different experimental techniques, e.g. hydrogen-bubble flow visualization technique, Acoustic Doppler Velocimeter (ADV), Acoustic Doppler Velocity Profilers

(ADVP), and Particle Image Velocimeter (PIV) and numerical techniques in both plane and scoured beds under clear-water and live-bed conditions at circular piers.

Graf and Istiarto (2002) experimentally investigated the flow field in a scour hole by an Acoustic Doppler Velocity Profiler (ADVP). At the upstream side of the cylinder, the following results were observed: (1) approaching the cylinder, the (longitudinal) u-component of velocity diminishes over the entire depth, and begins to show negative values close to the bed; (2) in the approach region, the (vertical) w-component of velocity remains negligible, but produces significantly and reaches a value equal to roughly 60 percent of the approach flow mean velocity; and (3) the (lateral) v-component of velocity remains negligible but has some small values close to the bed, indicating three-dimensional flow. In regard to the vorticity of the flow field, they observed: (1) a positive vorticity is strong at the brink of the scour hole, leading to a weak counter-clockwise vortex; (2) directly upstream of the cylinder a strong clockwise vortex is developed; and (3) in the remaining part of the scour hole, the vorticity is weak and is of the same order as the approach flow vorticity. Shear stress measurements also were calculated based on the velocity profile and corresponding Reynolds stresses. The resulting values in the scour hole were less than the critical values of shear stress presented by Shields (1966), implying no sediment movement. Turbulence intensities were observed to be very strong at the foot of the cylinder on the upstream side.

Dargahi 1990 experimentally investigated the scour around a circular cylinder with clear water condition , the researcher found that the first scour appear in the wake area of the cylinder and the main scouring is the result of down flow and horseshoe vortex at the upstream face of the bridge pier.

2.9 Countermeasure techniques for reducing scour depth

The purpose of this section of the literature review is to briefly shed light on the various methods available for preventing local scour at a bridge pier. Lagasse et al. (2001) defined countermeasures as measures incorporated into a highway-stream crossing system to monitor, control, inhibit, change, delay, or minimize stream instability and bridge scour problems. They further stated that an action plan for monitoring structures during or after flood events can also be considered a countermeasure. Mitigation measures for local scour at bridge piers can be grouped into armoring techniques and flow alteration devices (Johnson et al. 2001 and Melville and Hadfield 1999).

2.9.1 Armoring techniques

Piers are protected to withstand shear stresses during high flow events while the flow altering device aims to disrupt the flow field around the pier and thereby decrease the erosive strength of the down-flow and horseshoe vortex systems by way of breaking up vortices and reducing the velocity in the vicinity of the piers (Lauchlan 1999). Armoring technique for piers and abutments include riprap, precast concrete units, grout-filled bags, foundation extensions, concrete aprons, and gabions. Armoring devices protect the river bed within the vicinity of the pier against erosive forces. When installed to prevent local scour around a pier, riprap prevents the down-flow and horseshoe vortex systems created by the presence of the pier from removing sediment from the pier face. The use of riprap to deal with pier scour problems is very common in civil engineering practice (Lauchlan 1999).

Akib et al. (2014) they examine the use of collars and geobags for reducing local scour around bridge piles. The efficiency of collars and geobags was studied experimentally. The data from the experiments were compared with data from earlier studies on the use of single piles with a collar and with a geobags. The results showed that using a

combination of a steel collar and a geobags yields the most significant scour reduction for the front and rear piles, respectively.

2.9.2 Flow Altering Devices

Using flow altering devices, the shear stresses on the riverbed, in the vicinity of pier, are reduced by altering the flow pattern around a pier which in turn reduces the scour depth at the pier. Attempts have been made by several investigators to reduce the depth of scour around a pier using flow altering devices (Chiew 1992 Gupta and Gangadhariah 1992, Chiew 1992, Vittal *et. al.* 1994, Melville and Hadfield 1999, Kumar *et. al.* 1999, Muzzammil et al. 2004, Zarrati *et. al.* 2004, 2006, Tafarojnoruz et. al. 2012 Chen et al. 2012).

Tafarojnoruz et, al. 2012 they evaluated experimentally different types of flow- altering countermeasures contrary to pier scour under clear water conditions with flow strength below the threshold of sediment movement; they concluded that a single flow – alteration countermeasures may consider an insufficient protection. In addition the performance of any flow altering countermeasures should be assessed under live-bed condition.

Use of a hooked collar for reducing local scour around a bridge pier was examined by Chen et al. (2012).The efficiency of collars was studied through experiments and compared with an unprotected pier. Acoustic Doppler Velocimeter was used to measure velocity field. Results showed that a pier with a hooked-collar has effectiveness for reducing scour more than unprotected pier. With hooked collar installed at the bed level, there was no sign of scouring and horseshoe vortex at the upstream face of the pier. In addition, the down flow and turbulent kinetic energy were reduced under the effects of the hooked collar.

Grimaldi et al. (2009) investigated the behavior of a slot as countermeasure against local scouring through a circular bridge pier. The results showed that the slot reduces the local scour at pier. The maximum reduction of the scour depth was about 30% in the best configurations.

A slot is an opening in the pier, which allows part of the flow to go through the pier itself; therefore, it acts by reducing the strength of the downflow and, consequently, of the horseshoe vortex as shown in Figure 2.30.

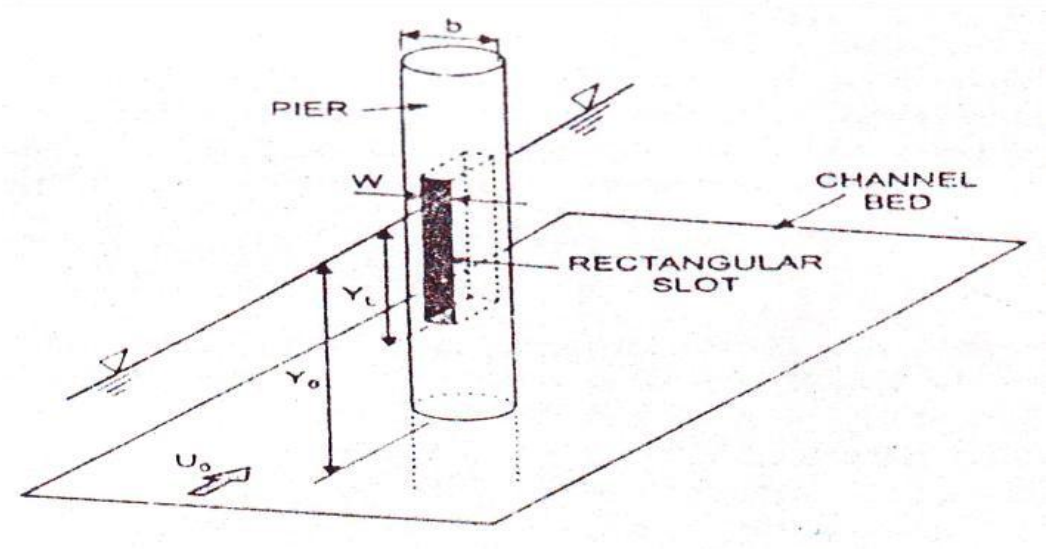

Figure 2.30 Slot through a pier

There are limitations on the use of a slot through pier. The danger of choking of the slot space due to debris and floating materials is very high. They also reduce the strength of pier structure. Hence, they cannot be considered as good scour protection device (Beg, M. and Beg, S. 2013).

2.10 Characteristics of Horseshoe Vortex within Scour Holes

A large number of investigations were carried out and focused on prediction of the maximum scour depth, (Breusers and Raudkivi 1991, Sumer and Fredsøe 1992, Dey 1997, Hoffmans and Verheij 1997, Melville and Coleman 2000, Barbhuiya and Dey

2004). The understanding of local scour mechanism from the viewpoint of the flow and turbulence characteristics of the horseshoe vortex during the development of scour hole is still lacking. Complete understanding of the turbulent flow fields aids prediction of scour magnitude accurately. Several studies that focused on the turbulent flow fields within a scour hole at piers reported by Melville and Raudkivi 1977, Dey et al. 1995, Ahmed and Rajaratnam 1998 Graf and Istiarto 2002, Dey et al. (2007).

Melville and Raudkivi (1977) were measured the turbulent flow field within a scour hole at a circular pier with the aid of the hot-film anemometer. He measured the flow field in the upstream axis of symmetry and the near-bed turbulence intensity for the case of a flat bed, intermediate, and equilibrium scour hole. He also estimated the bed-shear stresses from the measured near-bed velocities.

Graf and Istiarto (2002) detected velocities, turbulence intensities, Reynolds stresses, and bed-shear stresses in different azimuthal planes within the equilibrium scour hole at a circular pier aided by the Acoustic Doppler Velocity Profiler (ADVP).

Dey and Raikar (2007) presented spatial features of horseshoe vortex in rising scour holes in different planes around a circular and square pier applying an ADV. The contours of the time-averaged velocities, turbulence intensities and Reynolds stresses at different azimuthal planes 0°, 45° and 90° were presented. It was observed that the flow and turbulence intensities in the horseshoe vortex flow in a developing scour hole are reasonably similar. Their results added useful knowledge on time variation of the flow field during scour in a non-cohesive soil.

Das et al. (2013) present an experimental investigation on the characteristics of horseshoe vortex system within the equilibrium scour hole at circular and square pier measured by an Acoustic Doppler Velocimeter (ADV). In order to have a comparative

study, the ADV measurements within an equilibrium scour hole at a square pier (side facing the approaching flow) of sides equaling the width of the circular pier were also taken. The contours and distributions of the time-averaged velocities, turbulence intensities, turbulent kinetic energy and Reynolds stresses at different azimuthal (0°, 45° and 90°) planes are presented. The circulation of the horseshoe vortex is determined by using Stokes theorem and Forward difference technique. Bed-shear stresses are also determined from the Reynolds stress distributions.

2.11 Numerical Model Simulations

With advancements in computer technology, detailed mathematical simulation of the flow field in the vicinity of vertical obstructions has become feasible. Numerical approximations of the Navier-Stokes equations based on finite difference, finite element, or finite volume solutions have been incorporated into computer algorithms and used to analyze the mechanics of the scour problem. Estimations of bottom shear stress, turbulence intensities, and the formation of the vortex systems have been a primary area of focus. The use of these programs has allowed researchers to analyze the effects of subtle adjustments to flow variables, which could not be accomplished easily during laboratory experiments.

Olsen and Melaaen (1993) used a three-dimensional numerical model to simulate the development of a scour hole. The simulation was based on the results of a physical model. The scour hole was only partially developed. The model was completed through 10 iterations of the changing bathymetry of the scour hole. Although they received encouraging results, Olsen and Melaaen warned that because the numeric model cannot simulate the transient nature of the oscillating vortices in front of the pier, it may prove faulty for maximum scour depth predictions.

Mendoza-Cabrales (1993) used the k-ε turbulence closure model to ascertain the bottom shear stress distribution on a rigid bed in front of a circular cylinder. His geometric data and flow variables were identical to those used by Melville and Raudkivi (1977) for a laboratory flume experiment. His results showed large discrepancies from values measured by Melville and Raudkivi. Mendoza-Cabrales concluded that the k-ε turbulence closure model is inadequate for determining the flow field and associated shear stresses in front of cylindrical objects due to: (1) the inability of the model to handle anisotropic turbulence of three-dimensional curved flows, (2) the lack in representing the negative contributions to the generation of the kinetic energy of turbulence, (3) the inability to express the dependency of each component of the Reynolds-stress tensor on one component of the mean strain rate tensor, and (4) the inability to account for Reynolds-stress relaxation.

In an attempt to produce better results than Mendoza-Cabrales (1993), Richardson and Panchang (1998) used the Computational Fluid Dynamics model FLOW-3D to simulate the flow field around a circular pier, based on the experiments of Melville and Raudkivi (1977). The FLOW-3D model is based on the solution of the transient three-dimensional Navier Stokes equations by the volume-of-fluid method. In addition, the model can handle turbulence closure through a number of accepted schemes, including: Prandtl's mixing length theory, eddy viscosity model, two equation k-ε models, and the renormalized group (RNG) theory. The results of the simulation showed that with proper calibration of input variables, a flow field similar to the one reported by Melville and Raudkivi (1977) can be obtained. Shear stress distributions, however, were said to vary drastically but were not reported. No explanation was given for the discrepancy. Richardson and Panchang (1998) further showed that by tracking a single fluid particle at the bottom of a scour hole, predictions could be made as to a maximum depth of

scour by noticing when the particle becomes trapped in the scour hole. They warned that this may not be a viable method for predicting a maximum scour depth, unless an accurate representation of geometric data can be simulated.

Ali and Karim (2002) used the FLUENT CFD computer program to model the flow structure at a cylindrical pier. Bed shear stresses also were predicted using the model. Various simulations were performed, representing different time steps at the development of a scour hole. The geometric and flow conditions were based on experimental data provided by Yanmaz and Altinbilek (1991). Analysis of the results showed favorable comparison to the experimental results of the flow field. However, there was only a fair agreement between the bed shear stresses predicted by FLUENT and those calculated from the experimental velocities. This is most likely due to the fact that FLUENT gives on-bed predictions for shear stress, whereas the ones reported by Yanmaz and Altinbilek (1991) were at a distance of 8 mm above the bed. While the results obtained by Ali and Karim are acceptable, they state that using a numerical model such as FLUENT CFD cannot produce truly accurate results due to its inability to model certain phenomenon such as turbulent bursts or the oscillating nature of the horseshoe vortex.

Few studies show a few numerically models simulated the problem of three-dimensional flow around bridge piers on flat- bed or with scour model. Tseng et al. (2000), Roulund et al. (2005), Nagata et al. (2005), Said et al. (2008), and (Mammar and Soudani. (2012).

Said et al. (2008) simulated the flow in the wake region of a single cylinder and two tandem cylinders on flat bed, using Reynolds stress turbulence model. Nagata et al. (2005) performed a model based on the Reynolds Averaged Navier Stokes equations, together the k-epsilon turbulence model for bed deformation around bridge pier.

Roulund et al. (2005) calculated the flow and scouring around a cylindrical pile, using a model that uses the rigid- bed. Tseng et al. (2000) simulated numerically the three dimensional turbulent flow fields around circular and square piers. The results showed that the downflow strength and the domain of the high bed shear stress were greater in the case of square pier.

Flow patterns around a T-shape spur dike and support structure have been simulated by Vaghefi et al. (2015). They using Flow-3D model, the numerical and experimental data are compared in longitudinal section to verify numerical model. The results show very good correspondence between numerical and laboratory data. The support structure has been installed upstream the T-shape spur dike to alteration flow patterns and hydraulic parameters such as power of secondary flow, and separation zone in all sections. The power of secondary flow around main spur dike decreases by 40-120% and the length of separation zone increases from 0.8 to 2.5 times bigger than the length of T-shape spur dike.

Tuna and Emiroglu (2013) analyze the effect of step geometry on the dynamics of local scour processes in the context of scour that takes place downstream from a stepped chute. Three different step heights have been used to study the scour process for various chute angles, stilling basin sill heights, tailwater depth and flow rate conditions. The results show that the equilibrium depth of scour is highly dependent on the step geometry. In addition, the equilibrium depth of scour decreases while the step height increases. Also, the equilibrium depth of scour also increases with an increase in a discharge and chute angle.

Afzal M, S. (2013) performed two turbulence models ($k-\omega \; and \; k-\epsilon$) to simulate a complex sediment transport using CFD around abutment and pier. The numerical results

have been validated with physical experiment. Comparison in performance of ($k-\omega\ and\ k-\epsilon$) turbulence models is done for abutment and pier scour under constant discharge. The result reveals that the performance of the $k-\omega$ model is similar to the $k-\epsilon$ in the pier scour case.

Fevzi Onen (2014) predicts the local scour at a side-weir known as a lateral intake structure, which is widely used in irrigation. The study presents artificial neural network (ANN) and gene expression programming (GEP) models, which is an algorithm based on a genetic algorithms and genetic programming, for prediction of the clear-water scour depth at side-weir. The GEP-based formulation and ANN approach are compared with laboratory results, multiple linear/nonlinear regression (MLR/MNLR). The performance of GEP is found in slightly more influential than ANN approach and MNLR for predicting the clear water scour depth at side-weir.

CHPTER 3

EXPERIMENTAL SETUP AND METHODOLOGY

3.1 Introduction

The following sections include the developed experimental installation, measuring techniques, and experimental procedures. All the experiments were carried out in Hydraulic Laboratory at the University of Gaziantep.

3.2 Flume

The experiments were conducted in a recirculating flume, 12 m long, 0.8 m wide and 0.9 m deep as shown in Figure 3.1 with glass sides and steel bottom. The test section was made with a ramp which is located at the beginning and the end of the section. The test section is 3 m long and 0.2 m depth as shown in Figure 3.1.

Flume discharge was measured by a magnetic flow meter installed in the pipe system before the inlet of channel as illustrated in Figure 3.2. The scour hole and the elevation of the bed were measured by laser meter as shown in Figure 3.3. The calibration of magnetic flow meter and laser meter were made by the fabrication for the. Therefore, there is no need to make a calibration for the two instruments. The instrument mounted on a manually moving carriage sliding on rails on the top of the flume wall. Initial bed elevations were taken randomly to check the leveling of the test section by using laser meter.

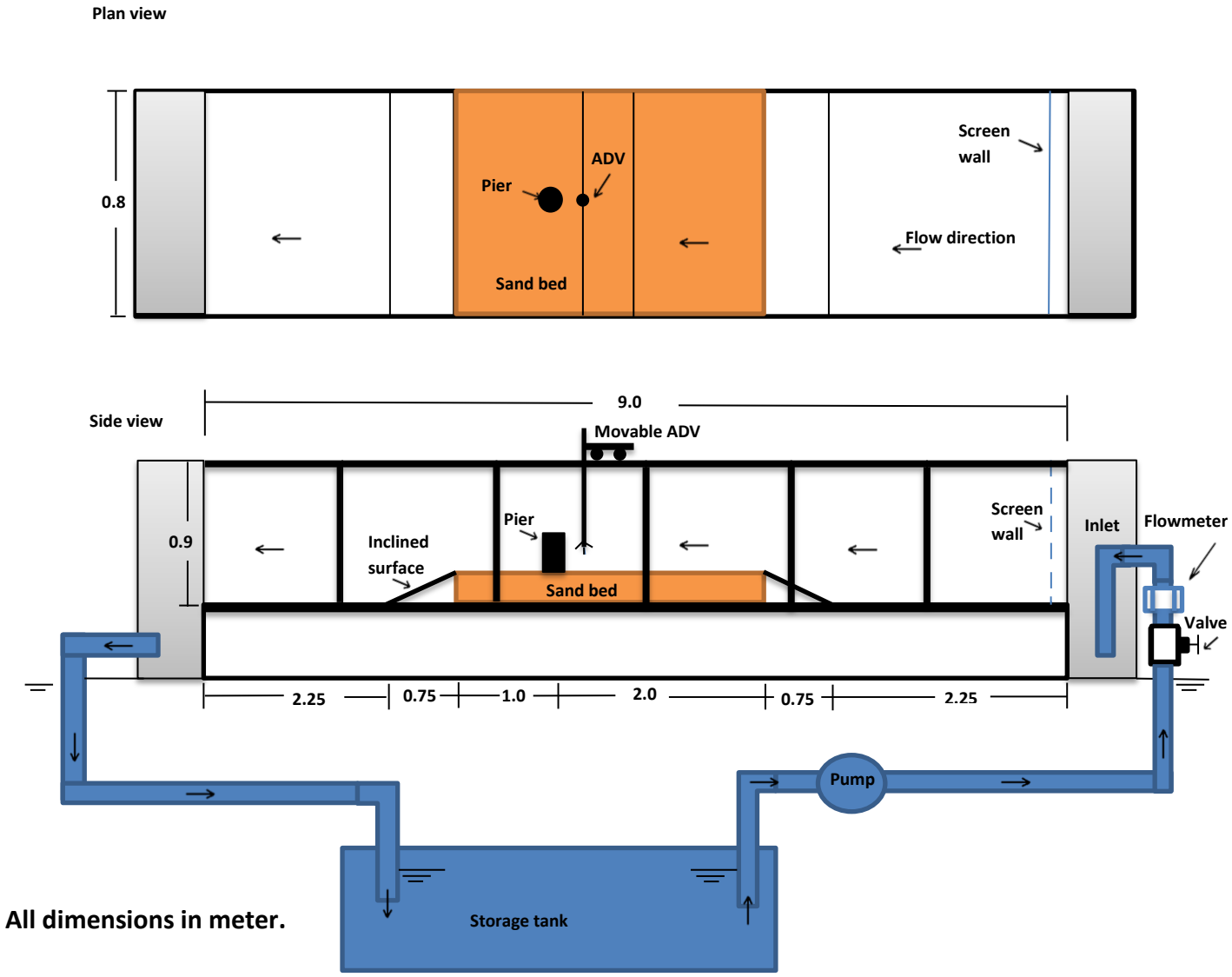

Figure 3.1 Schematic layout of the flume

Figure 3.2. Magnetic flow meter installed in the pipe system

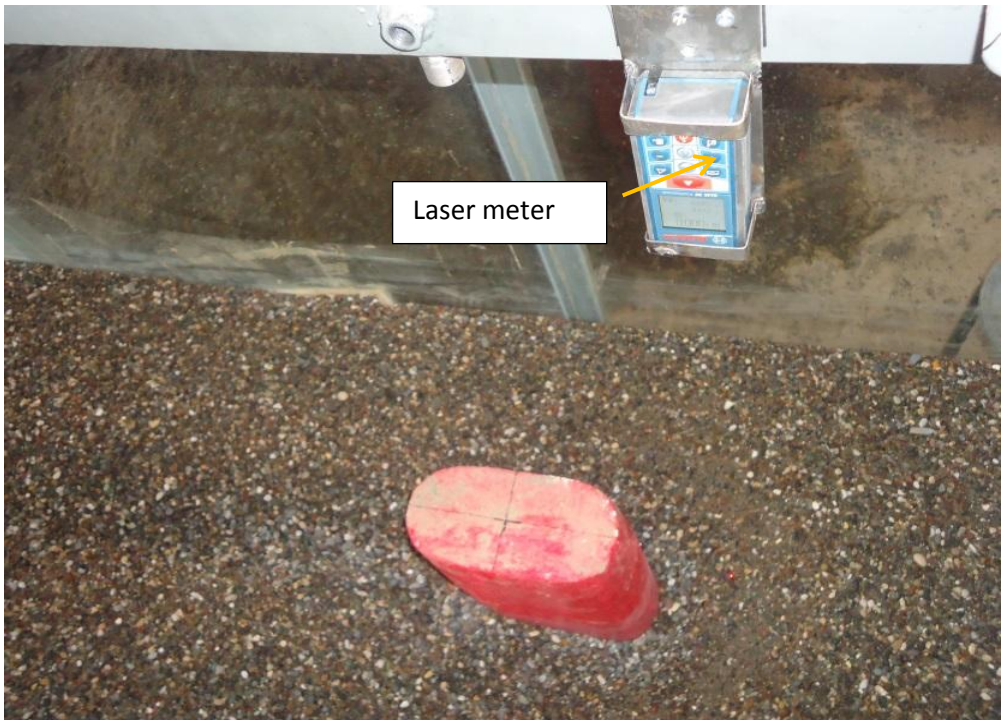

Figure 3.3 Laser meter installed in the channel

3.3 Pier Shape

Four different piers were used in the scouring tests, (1) round nosed pier (10-10) cm, (2) upstream-facing round nosed pier with three different diameters ((10-8), (10-6) and (10-4) cm) (3) upstream-facing aerofoil shaped pier and (4) circular pier (10) cm. Piers were manufactured from thermo-stone and painted to decrease the surface roughness of these piers. Figure 3.4 shows photographs and dimensions of tested bridge piers. In each case, the pier was placed on the centerline of the flume and at a certain longitudinal location, keeping the coordinates of the pier centerline constant for all the conducted experiments. This was important for inter-comparison of measured contour profiles.

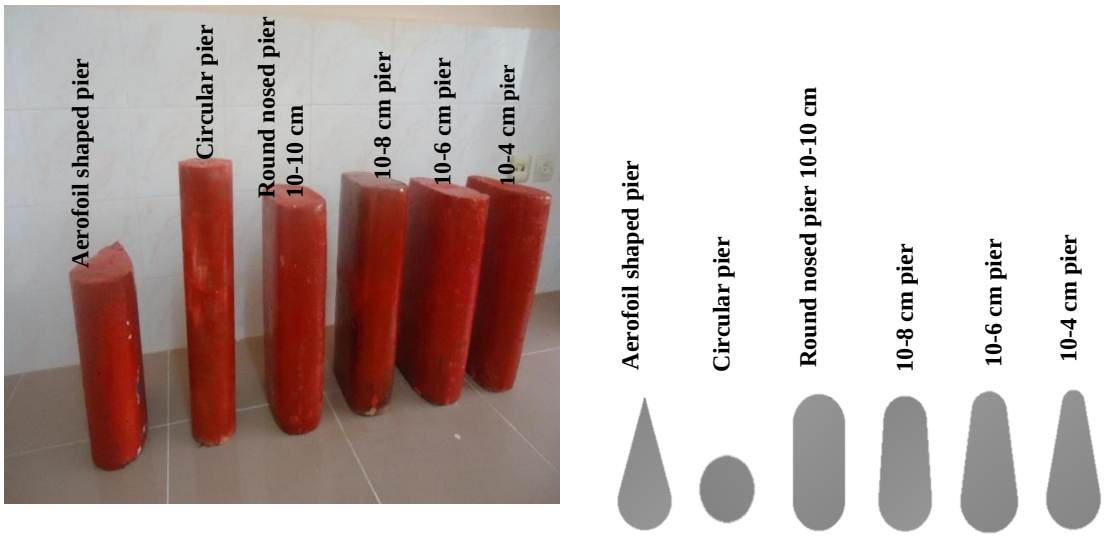

Figure 3.4 Photographs and dimensions of tested bridge piers.

3.4 Flow Velocity Field

An Acoustic Doppler Velocimeter ADV, developed by SonTek (5cm down-looking and sampling rate up to 50 Hz) was mounted together with a vertical positioning on carriage in order to measure the three dimensional velocity components as well as the turbulence intensities. This instrument carriage was mounted on rails on the top of the flume sides allowing the movement of ADV in both longitudinal and transverse direction of the flume. Scales were fitted in the flume wherever necessary to provide a reference datum. The ADV probe and its operating mechanism are shown in Figure 3.5.

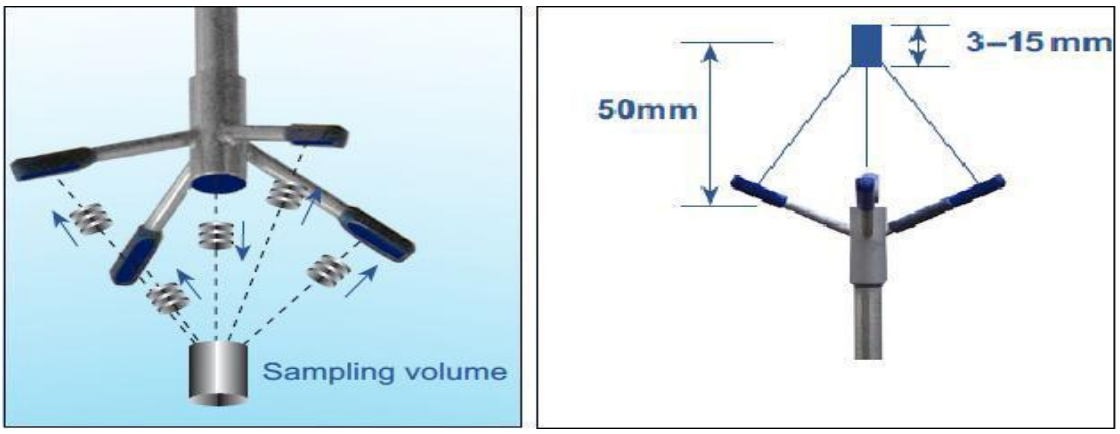

Figure 3.5 Nortek ADV probe with transducer, receiver, and sampling volume (Reproduced with permission from Nortek-US).

The Cartesian coordinates system (x, y, z) were utilized to represent the flow velocity field as shown in Figure 3.6. Here, the time-averaged velocity components in (x, y, z) were represented by (*u, v, w)* and their fluctuations were (*u*', *v', w'*) respectively. The lowest possible point of ADV reading was 1 cm above the bed. Velocity components and turbulence intensities were plotted in *xz* planes using EXCEL and SURFER 11 programs.

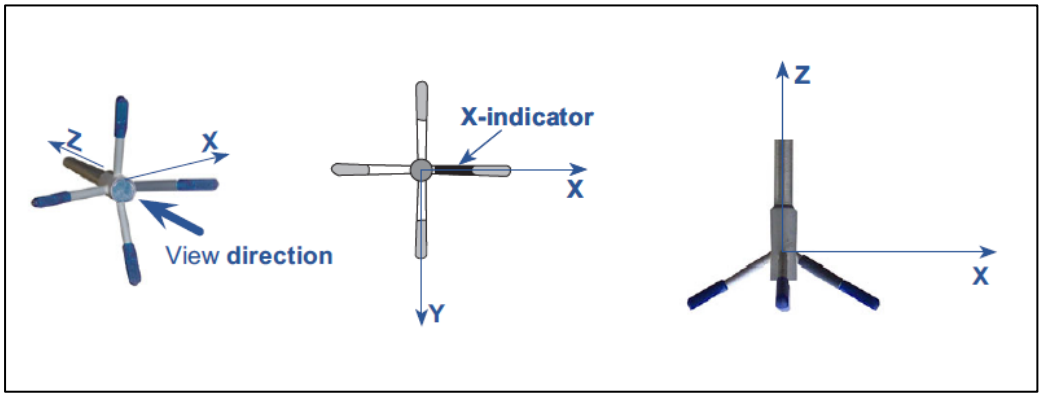

Figure 3.6 Defining the XYZ coordinates.

3.4.1 Acoustic Doppler Velocimeter Measurements

During each experiment, the velocity is periodically monitored using ADV. Stream velocity is measured upstream of the pier using the ADV in the center of the flume. The

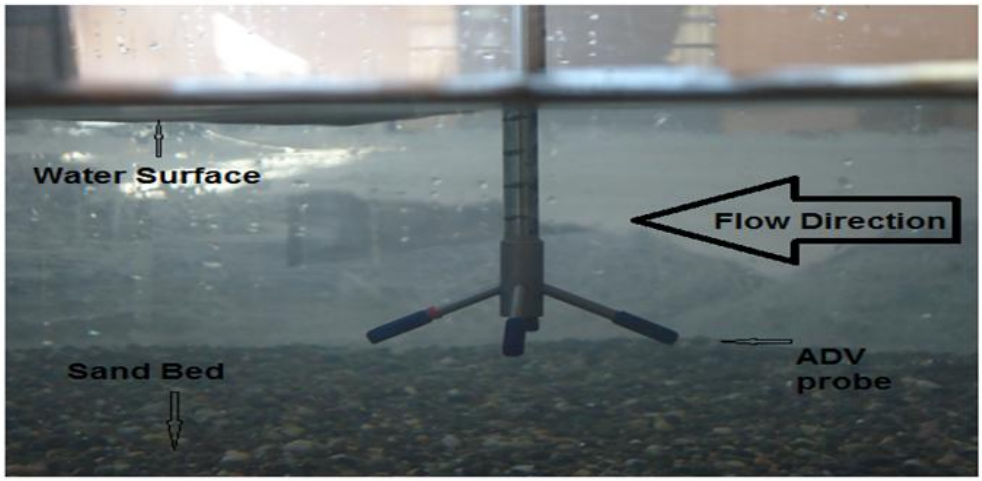

Figure 3.7 Typical ADV Setup

typical ADV setup is shown in Figure 3.7. The ADV probe was then positioned above the scour hole and velocities were recorded for a period of 180 seconds. The sample period of 180 seconds was chosen to ensure that sufficient flow variations were captured.

3.4.2 Velocity Measurement Coordinates

Velocities were measured over half the width of the flume due to the symmetrical shape of the pier and the centered alignment of the pier within the flume. Velocities were recorded in interval from X= -28 cm to X= 24 cm for each Y coordinate from Y=0 cm (center line of channel) to Y=10 cm for upstream-facing aerofoil-shaped pier as in Figure 3.8. The Z coordinates at the bed level is zero.

Velocities were recorded for the downstream-facing aerofoil and circular piers using a similar methodology as was done for the upstream-facing pier.

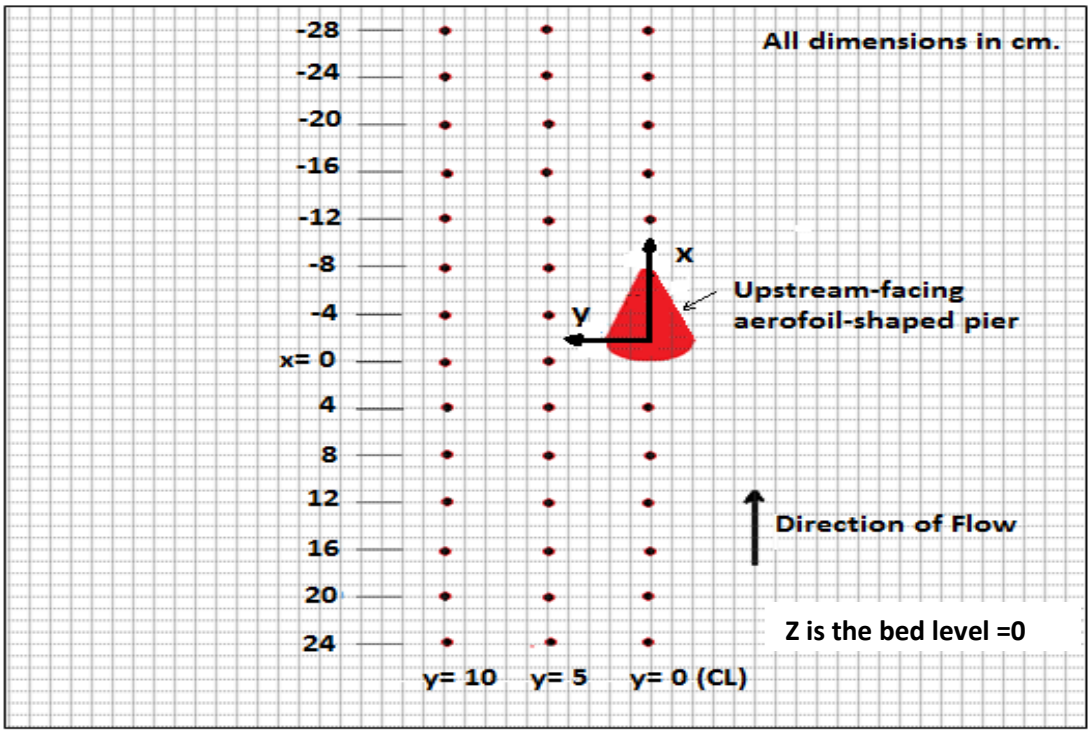

Figure 3.8 Velocity measurement coordinates

3.5 Sand bed

A series of tests were carried out to characterize the sand bed material present in the flume used for the study. The soil tests carried out included a mechanical sieve analysis and a specific gravity test. The results of the tests showed that the bed material consists of cohesion-less sand with a median particle size d_{50} of 1.45 mm and a specific gravity of 2.65. The geometric standard deviation of the sand size σ_g is 3.16, which implies that the sand is of non-uniform size distribution. The σ_g is defined as, $\sigma_g = (d_{84}/d_{16})^{0..5}$. The plot of the grain size distribution (sieve analysis) test is depicted in Figure 3.9. The pier diameter was also carefully chosen so that there was negligible effect of sediment size on the depth of scour. It is known that the bed material grain size does not affect the depth of scour if the pier width to grain size ratio exceeds a value of about 50 (Ettema,1980). For this study, the ratios are about 50-68 for all the piers used in the study, which satisfies the criterion of Ettema.

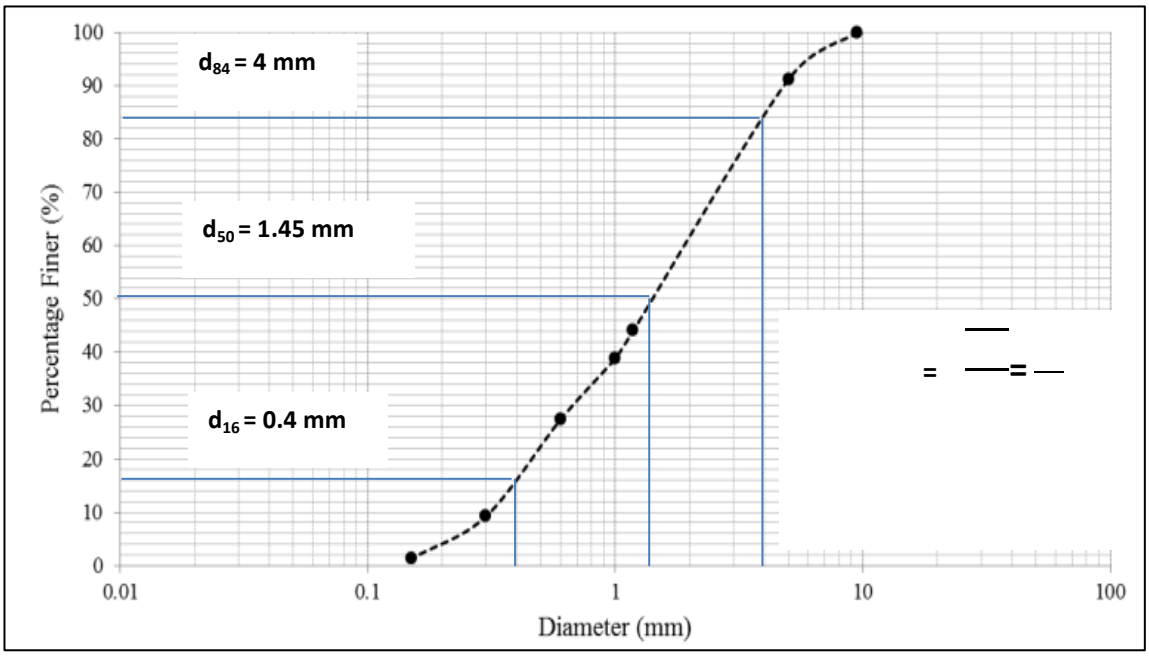

Figure 3.9 Grain size distributions

3.6 Test Program

The test program was developed to deal with the evaluation of the efficiency of using unconventional bridge piers to reduce local scour around pier. In addition, the current study is to provide a new method to reduce scour depth in front of bridge pier. The idea of this method is dependent on the change the orientation of bridge pier so that it faces downstream rather than upstream according to the direction of flow (named after here as downstream-facing round nosed pier.

The test program was divided into seven series of tests, with each test series representing a complete set of tests. The seven series of tests are referred to as series 1, series 2, series 3, series 4, series 5, and series 6 and series 7. The experiments were performed under live-bed conditions at three different flow intensities (**V/Vc**) of 1.17, 1.11 and 1.03.

A summary of the basic test and flow conditions are shown in Table 3.1. The series of tests (Series 1, 2 and 3) were designed to investigate the effect of pier shapes (unconventional bridge pier) on local scour. The used shapes were circular, round nosed pier and upstream-facing round nosed pier (10-8, 10-6 and 10-4) cm with different discharges under live-bed scour conditions. The series of tests (Series 4, 5 and 6) were conducted to study the effect of changing the orientation of bridge pier according to flow direction as a mitigation technique against pier scour. The orientation of bridge pier models was changed named here as downstream-facing round nosed pier (8-10, 6-10 and 4-10), were experimented under the same conditions of the first three series (1, 2 and 3). Finally, the series seven was performed to evaluate the effect of upstream-facing aerofoil shaped pier and downstream-facing aerofoil shaped pier on scour.

Results from Series 1, 2 and 3 tests were analyzed together with the results gained from Series 4, 5 and 6. Empirical relationship was developed on the basis of experimental

results. The longitudinal and transverse scour profiles through the center of the pier were also plotted using software called Surfer version 11 and the results were discussed. Surfer version 11 is a full-function 3-D surface modeling/mapping program and contouring package. Surfer is capable of quickly and easily converting XYZ data into contour, surface, wireframe, vector, image and shaded relief plots. The Surfer tool was employed to convert the scour hole topographical data into a contour map as well as into a three-dimensional profile of the scour hole region. Surfer is also capable of calculating the volume of the contour hole using inbuilt trapezoidal and Simpson rules. It can also calculate the surface area of the scour hole.

Table 3.1. Summary of test conditions for Series 1, 2, 3, 4, 5, 6 and 7 tests.

Test	Run No.	Pier name and diameter	Flow depth (cm)	Mean velocity (m/sec)	Discharge (m^3/sec.)	Froude Number
Series 1	A1	Circular pier (10)	12.5	0.58	0.058	0.523
	A2	RNP (10-10)	12.5	0.58	0.058	0.523
	A3	US-FRNP (10-8)	12.5	0.58	0.058	0.523
	A4	US-FRNP (10-6)	12.5	0.58	0.058	0.523
	A5	US-FRNP (10-4)	12.5	0.58	0.058	0.523
Series 2	B1	Circular pier (10)	11	0.54	0.048	0.525
	B2	RNP (10-10)	11	0.54	0.048	0.525
	B3	US-FRNP (10-8)	11	0.54	0.048	0.525
	B4	US-FRNP (10-6)	11	0.54	0.048	0.525
	B5	US-FRNP (10-4)	11	0.54	0.048	0.525
Series 3	C1	Circular pier (10)	9.7	0.49	0.038	0.51
	C2	RNP (10-10)	9.7	0.49	0.038	0.51
	C3	US-FRNP (10-8)	9.7	0.49	0.038	0.51
	C4	US-FRNP (10-6)	9.7	0.49	0.038	0.51
	C5	US-FRNP (10-4)	9.7	0.49	0.038	0.51
Series 4	D1	DS-FRNP (8-10)	12.5	0.58	0.058	0.523
	D2	DS-FRNP (6-10)	12.5	0.58	0.058	0.523
	D3	DSFRNP (4-10)	12.5	0.58	0.058	0.523
Series 5	E1	DS-FRNP (8-10)	11	0.54	0.048	0.525
	E2	DS-FRNP (6-10)	11	0.54	0.048	0.525
	E3	DS-FRNP (4-10)	11	0.54	0.048	0.525
Series 6	F1	DS-FRNP (8-10)	9.7	0.49	0.038	0.51
	F2	DS-FRNP (6-10)	9.7	0.49	0.038	0.51
	F3	DS-FRNP (4-10)	9.7	0.49	0.038	0.51
Series 7	G1	US-FASP (10)	12.5	0.58	0.058	0.523
	G2	DS-FASP(10)	12.5	0.58	0.058	0.523

* RNP = ROUND NOSED PIER.
* US-FRNP= UPSTREAM-FACING ROUND NOSED PIER.
* DS-FRNP = DOWNSTREAM-FACING ROUND NOSED PIER.
* US-FASP = UPSTREAM-FACING AEROFOIL-SHAPED PIER.
* DS-FASP = DOWNSTREAM-FACING AEROFOIL-SHAPED PIER

3.7 Froude Scaling

Froude numbers are used to determine dynamic similarity between flows. Where a geometric scale is applied to scale the flow depth and height, the Froude number is used to scale flows due to the importance of gravity on free-surface flow. It is used to compare the resistance of pier within the fluid between the realistic and scale model experiments.

Froude scaling uses the ratio of inertia forces to gravity forces to scale between models used in this research.

$$\frac{\boldsymbol{Innertia\ force}}{\boldsymbol{Gravity\ force}} = \frac{\boldsymbol{F_i}}{\boldsymbol{F_g}} \boldsymbol{\alpha} \frac{\boldsymbol{\rho V^2 L^2}}{\boldsymbol{\rho g L^3}} = \frac{\boldsymbol{V^2}}{\boldsymbol{gL}} \qquad (\mathbf{3.1})$$

Where $\boldsymbol{F_i}$ is force of inertia, $\boldsymbol{F_g}$ is gravity force, L is length, V is general velocity, $\boldsymbol{g}$ is gravity.

Using Equation (3.1) to scale from prototype to scale model,

$(\boldsymbol{F_r})_m = (\boldsymbol{F_r})_p$ $\qquad (\mathbf{3.2})$

$$(\boldsymbol{V/\sqrt{gL}})\boldsymbol{m} = (\boldsymbol{V/\sqrt{gL}})\boldsymbol{p} \qquad (3.3)$$

$$\frac{\boldsymbol{V_m}}{\boldsymbol{V_p}} = \frac{\overline{\mathbf{L_m}}}{\mathbf{L_p}} \qquad (3.4)$$

$$\frac{\boldsymbol{Q_m}}{\boldsymbol{Q_p}} = \frac{\boldsymbol{A_m V_m}}{\boldsymbol{A_p V_p}} = \frac{\boldsymbol{L_m}^2}{\boldsymbol{L_p}^2} \quad \frac{\overline{\boldsymbol{L_m}}}{\boldsymbol{L_p}} = \frac{\boldsymbol{L_m}^{2.5}}{\boldsymbol{L_p}^{2.5}} \qquad (\mathbf{3.5})$$

$$\boldsymbol{Q_m = Q_p\ L_R}^{2.5}$$

$\boldsymbol{Q_p\ River}$= 150 m^3/sec

$\boldsymbol{Q_m\ pump}$= 0.05 m^3/sec

0.05=150 $\boldsymbol{L_R}^{2.5}$

$$\boldsymbol{L_R = 0.0406}$$

$$\boldsymbol{D_{50\,m} = D_{50\,p}\ L_R}$$

1.45 = $\boldsymbol{D_{50\,p}}$ * 0.0406

$$\boldsymbol{D_{50\,p} = 35.7\ mm}$$

$\boldsymbol{D_{50\,p}}$ of the layer surface of river bed = 35.66 mm (Othman et al. 2012)

$\boldsymbol{35.66\ mm}$ ≅ 35.7 mm

Therefore, there is no scale effect.

Implication of Scale

The scale effect in laboratory pier scour experiments and the difficulty of obtaining a sufficiently complete set of field data have implications for further research on pier scour. Because of the typical dimensions of laboratory flumes as well as the lower limit of cohesion-less sediment size, it is difficult to satisfy the similitude requirements relating scour in the flume to scour in the river. This difficulty limits the use of laboratory flumes in developing accurate predictors of scour depths at full-scale piers. It is also affects laboratory experiments on local scour at other structures, such as abutments.

The D_{50} of bed surface of Tigris River as illustrated in Table 3.2 have been investigated by many researchers (Nedico 1976, Najib 1980, Khaleel 1986, Al-Taiee& Othman 1993 and Othman 2009) . The discharge of the river was 150 m^3/sec (Mohammad 2005).
In the present study the discharge of the pump Q_{model}= 0.05 m^3/sec, $Q_{prototype}$=150 m^3/sec and the length ratio L_R= 0.0406. According to Othman et al. 20102, d_{50} prototype= 35.66 mm. The $d_{50\ model}$= 35.7mm, which is approximately equal to sediment particle of the prototype, and no scale effect.

Table 3.2 Values of D_{16}, D50 and D_{84} for bed surface layer of Tigris River

	Nedico 1976	Najib 1980	Khaleel 1986	Al-Taiee& Othman 1993	Othman 2009
$D_{84\ (mm)}$	71	49	58	56	43
$D_{50\ (mm)}$	40	22	38	37	32
$D_{16\ (mm)}$	25	10	27	27	15

3.7 Experimental Procedure

1. The pier was installed in the flume at the desired location.

2. Before each run, the bed was carefully leveled throughout its length especially in the test section in the vicinity of the pier using a trowel with screed. This trowel with screed is of the same width as the flume and can be dragged along the flume rails. Some measurements to check the leveling of the bed were taken randomly using the laser meter.

3. To start the test, the flume was very slowly filled with water to the required water depth, taking care for escaping of the air bubbles from the bed and no sediment movement is allowed.

4. The pump was then turned on until the desired flow rate had been achieved.

5. The temporal variation of scour was monitored. The scour depth was measured under an intense light. The progress of scour depth was observed 3 hours.

6. At the end of each test, the pump was shut down and the water was slowly drained without disturbing the scour topography. The test section was then allowed to dry.

7. Photos of the scour topography around the pier were taken, and the final maximum scour depth was recorded using the laser meter. The contour profile of the scour hole, in the plane of symmetry of the pier and parallel to the flow direction, was taken with the laser meter supported by the mobile carriage of the flume.

8. After the test section was dried, the bed was frozen by pouring glue material (varnish)

9. Measurement of the flow velocity field around bridge pier was made by using ADV.

10. The above procedures were repeated for each test run.

CHAPTER 4

RESULT AND DISCUSSION

4.1 Introduction

Results obtained from all conducted scour experiments are presented. The experiments were conducted using unconventional bridge piers (upstream and downstream- facing round nosed) beside to circular pier and round-nosed pier. The results include the temporal evolution of scour; dimensions of the scour holes for each run of experiments were measured. The top width of scour in the transverse direction, distance from upstream face to front outer edge of hole, and depth at upstream face of the bridge piers were measured. In addition, the turbulent flow field around upstream and downstream-facing round nosed piers were presented and discussed in order to provide an insight on a complex flow field.

4.2 Scouring around Upstream and Downstream-Facing Round-Nosed, Round-Nosed and Circular Piers

Reduction of scour around bridge piers has been studied by many researchers (Abed and Gasser (1993), Dey and Raikar (2007), Ashtiani and Kordkandi (2012) and Roulund et al. (2005)) experimentally and numerically. Existing literature revealed that the shape of the obstruction to the flow can strongly affect the flow pattern around it and the strength of the down-flow, horseshoe vortex and the wake vortex are greater in the case of square piers compared to circular piers. Few studies have been reported on the local scour around non- circular piers such as round-nosed piers. The round-nosed pier reduces the bed shear stress value more than a circular does Guemou et al. 2013. In these experiments upstream-facing round-nosed (10-4,10-6 and 10-8 cm) and

downstream-facing round-nosed (4-10, 6-10 and 8-10 cm) , round-nosed (10-10 cm) and circular piers are used with three approaching flow intensities 38, 48 and 58 L/s. all the tests are carried out under live-bed condition at (v/v_c) of 1.03, 1.11 and 1.17 with flow depth 9.7, 11 and 12.5 cm, the sand used in the current study had a median grain size d_{50} of 1.45 mm and geometric standard deviation σ_g of 3.16.

The maximum time of the experiments performed by Bozkus and Osman (2004) was limited to two hours. Although the maximum duration of equilibrium scour depth was not achieved within two hours, they observed that the rate of growth in the depth of the scour hole was substantially reduced after two hours. When scour hole enlarges with respect to time, horseshoe vortices lose their strength and rate of scouring decreases. As it is predictable, scour holes around each pier are developed asymptotically in time and over 80% of the scour hole formation takes place in 2 hours (Ozalp 2013).

Yanmaz et al. (1991) have shown that most of the scour occurs during the first 3 or 4 hour of test duration. Mia and Nago (2003) the experiment is assumed to reach equilibrium when the development of scour in one hour is less than 1 mm, the experiment can be stopped. Based on these investigations the experiment duration was selected 3 hours except runs A2, A4 and A5 were conducted under duration of 6 hours to reach equilibrium scour depth as illustrated in Figure 4.1.

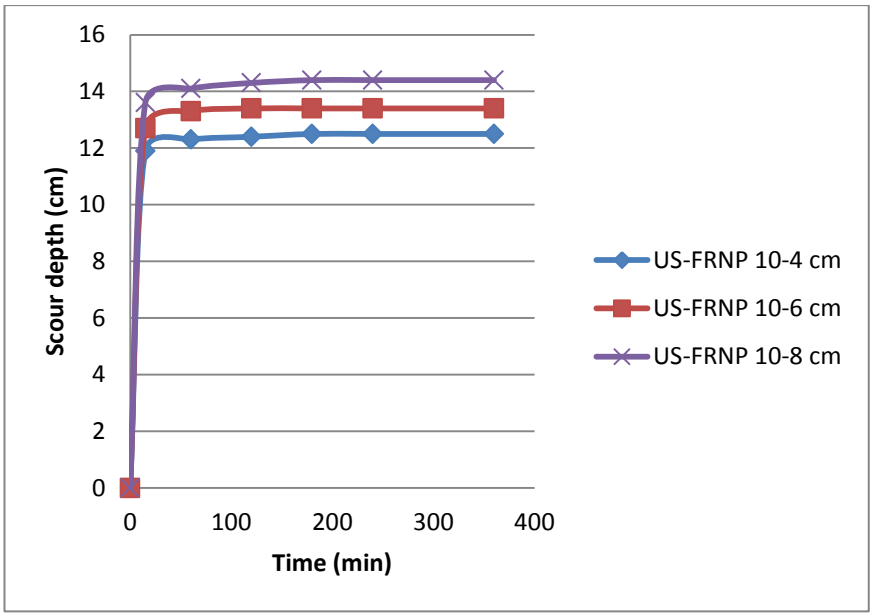

Figure 4.1 Scour Hole Development measured at the Upstream Face of bridge piers with Q= 58 l/s

4.2.1 Effect of Pier Shape on Local Scour

The effect of pier shape on developing scour hole geometry was investigated using upstream-facing round-nosed and round-nosed piers, in addition to the circular pier. The results of elapsed time taken from the start of each experiment for the scour hole and the dimensions of scour hole were measured and compared to each other's.

4.2.1.1 Scouring around Series1, 2 and 3

Time evolution of scour hole around Series 1 (A1-A5), Series 2 (B1-B5) and Series 3(C1-C5) in a sand bed is presented. Live-bed scour experiment were performed with v/v_c= 1.17, 1.11 and 1.03, flow depth (12.5, 11 and 9.7) cm and discharges (58, 48 and 38) (l/s). The test was performed for 3 hours. Figure 4.2 shows the final scour hole. It is seen that scour hole is symmetric around the longitudinal axis of the pier.

Figure 4.2 Scoured bed around A1, A2 and A5, Q= 58 l/s

Figure 4.3 shows the rate of scour upstream plane of A2, A3, A4 and A5 compared with A1. It observed that the shapes of upstream-facing round nosed pier US-FRNP have a better efficiency at reducing the rate of scour than the other piers installed on the same level and reduce the scour around the bridge piers. In addition, it is observed that scour formation is very rapid in the first five minutes.

Figures 4.4 and 4.5 show the time evolution of scour upstream plane of (B2-B5) and (C2-C5). US-FRNP minimize the rate of scour and then the local scour, besides at lower value of discharge the scour decreased and the scour depth increases when the

approaching discharge increases. The reason is that the kinetic energy of the flow increases and destructive effect of the flow increases.

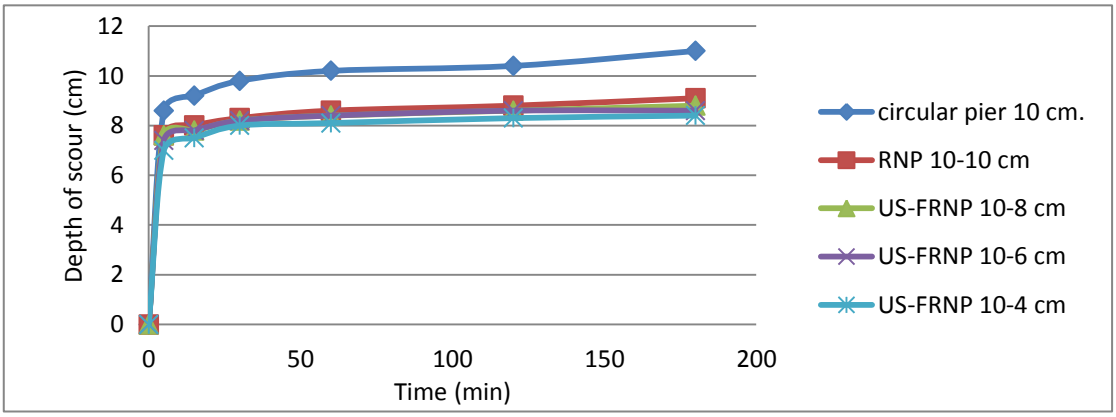

Figure 4.3 Scour Hole Development measured at the Upstream Face of bridge piers with Q= 58 l/s

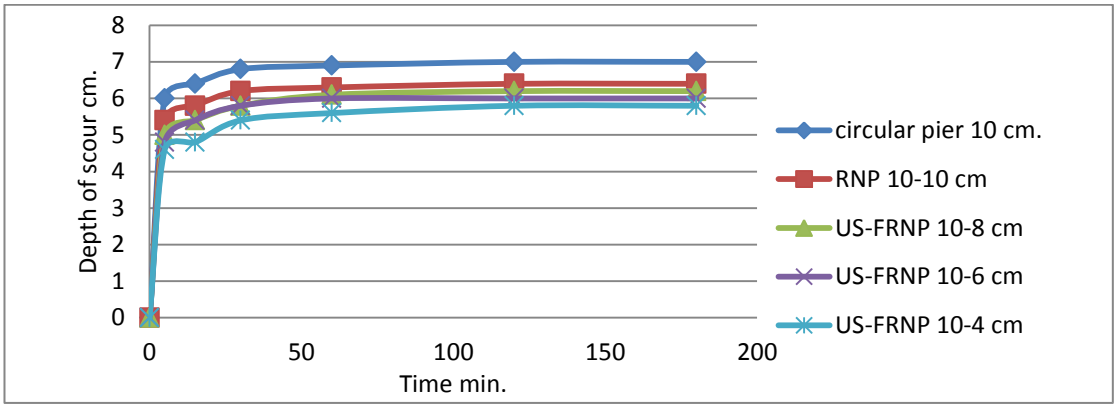

Figure 4.4 Scour Hole Development measured at the Upstream Face of bridge piers with Q= 48 l/s

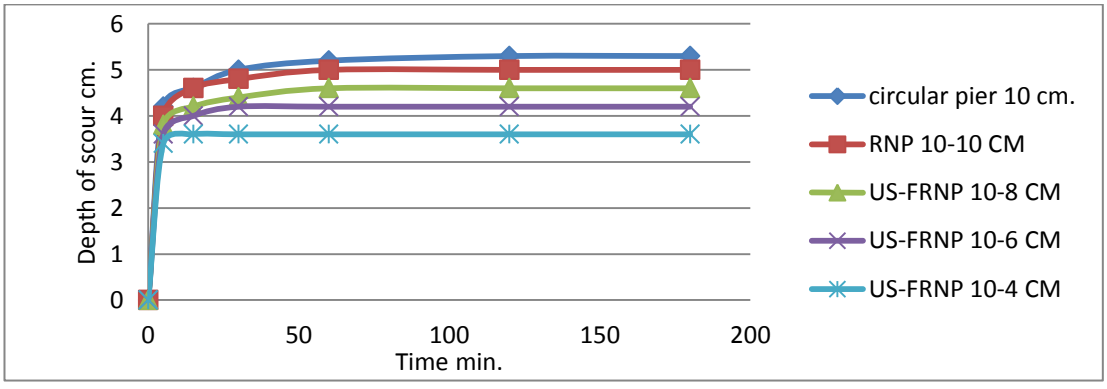

Figure 4.5 Scour Hole Development measured at the Upstream Face of bridge piers with Q= 38 l/s

4.2.1.2 Scour Hole Dimensions

Dimensions of the scour holes for each run of experiments were measured. The top width of scour in the transverse direction, distance from upstream face to front outer edge of hole, and depth at upstream face were compared for each of the bridge piers as shown in Figure 4.6, the same method were followed to measure the dimensions of scour holes for bridge piers as shown in Tables 4.1.

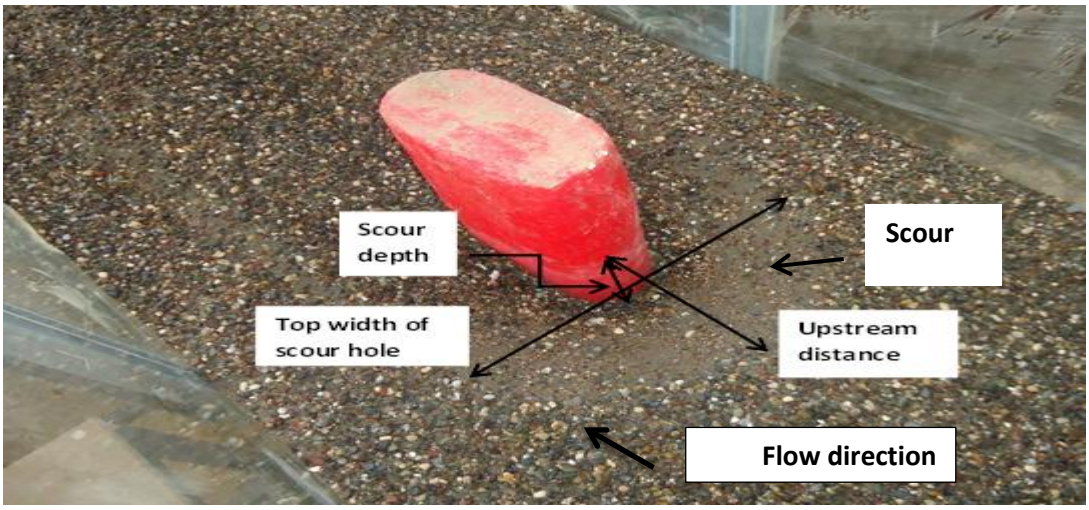

Figure 4.6 Location of scour hole dimensions around bridge pier

It is known that when, σg > 1.3 the sediment is considered non-uniform and armoring occurs on the channel bed and in the scour hole (Melville and Raudkivi 1997) as shown in Figure 4.7.

Figure 4.7 Armoring the channel bed and in the scour hole

Table 4.1 Dimensions of scour holes for bridge piers

Dimensions of the scour holes	US-FRNP 10-4 cm.	US-FRNP 10-6 cm.	US-FRNP 10-8 cm.	RNP 10-10 cm.	Circular Pier 10 cm.
Q=0.058 m^3/sec					
Top Scour Hole Width (m)	0.36	0.40	0.44	0.44	0.50
Distance from Upstream face to front outer edge of hole (m)	0.16	0.16	0.16	0.16	0.18
Depth at Upstream face (m)	0.084	0.086	0.088	0.091	0.11
Q= 0.048 m^3/sec					
Top Scour Hole Width (m)	0.32	0.36	0.36	0.36	0.4
Distance from Upstream face to front outer edge of hole (m)	0.11	0.12	0.12	0.12	0.12
Depth at Upstream face (m)	0.058	0.06	0.062	0.064	0.07
Q=0.038 m^3/sec					
Top Scour Hole Width (m)	0.24	0.28	0.28	0.28	0.28
Distance from Upstream face to front outer edge of hole (m)	0.07	0.08	0.08	0.08	0.08
Depth at Upstream face (m)	0.036	0.042	0.046	0.05	0.053

4.2.1.2.1 Longitudinal scour profile for Series 1, 2 and 3

The percentage reduction in distance from the upstream face of the pier to the upstream front outer edge of the hole as compared with the circular pier with US-FRNP 10-4 cm was 11%, 15% and 22% for flow intensities (v/v_c) 1.17, 1.11 and 1.03 respectively

are shown in Figures (4.8, 4.9 and 4.10). It is observed that the sediment deposition is occurred at the rear of US-FRNP.

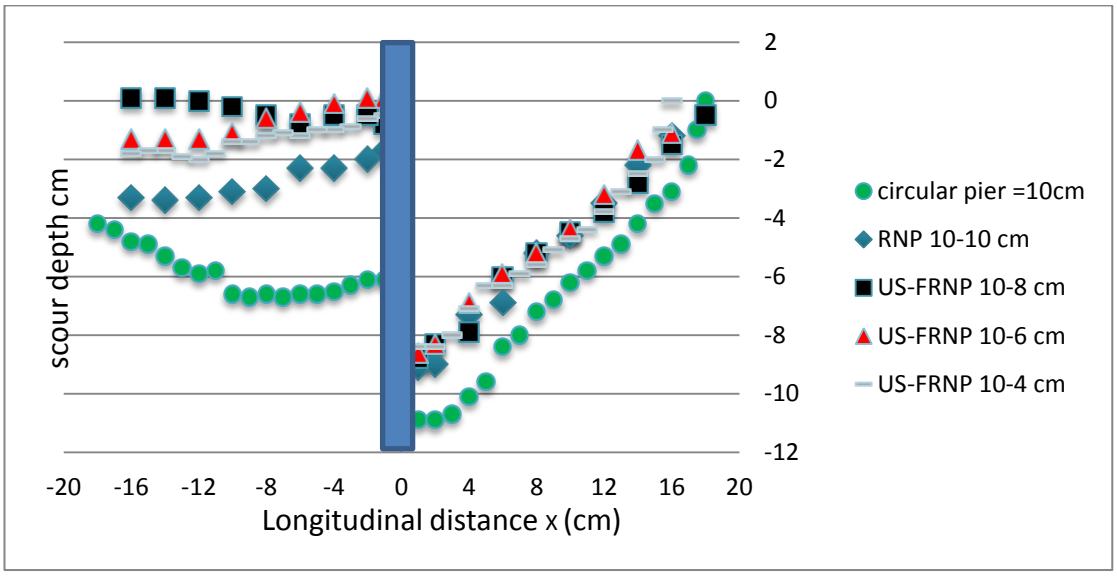

Figure 4.8 Longitudinal scours holes of runs (A1-A5)

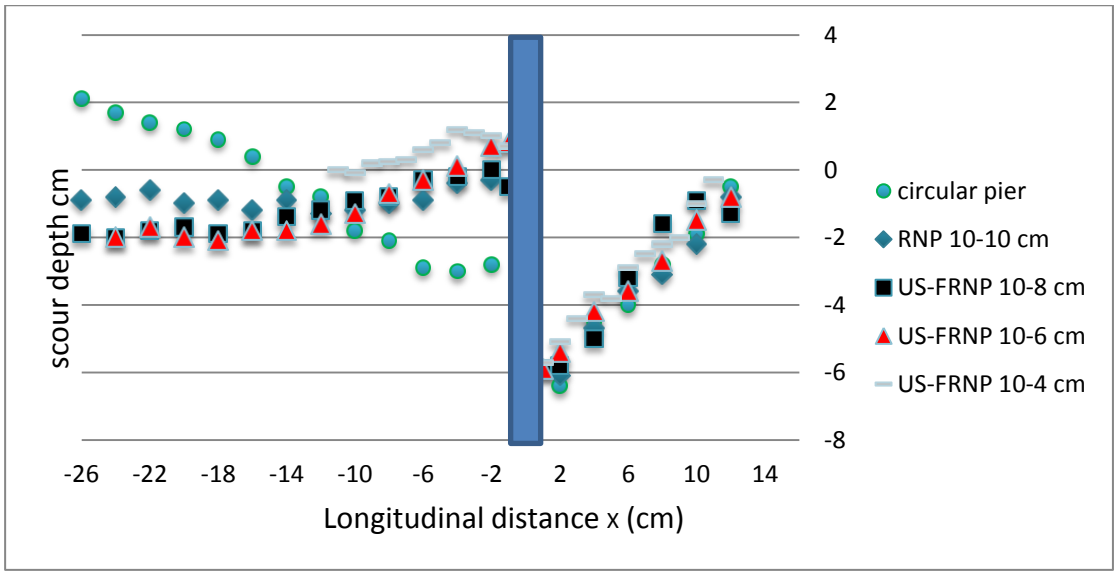

Figure 4.9 Longitudinal scours holes of runs (B1-B5)

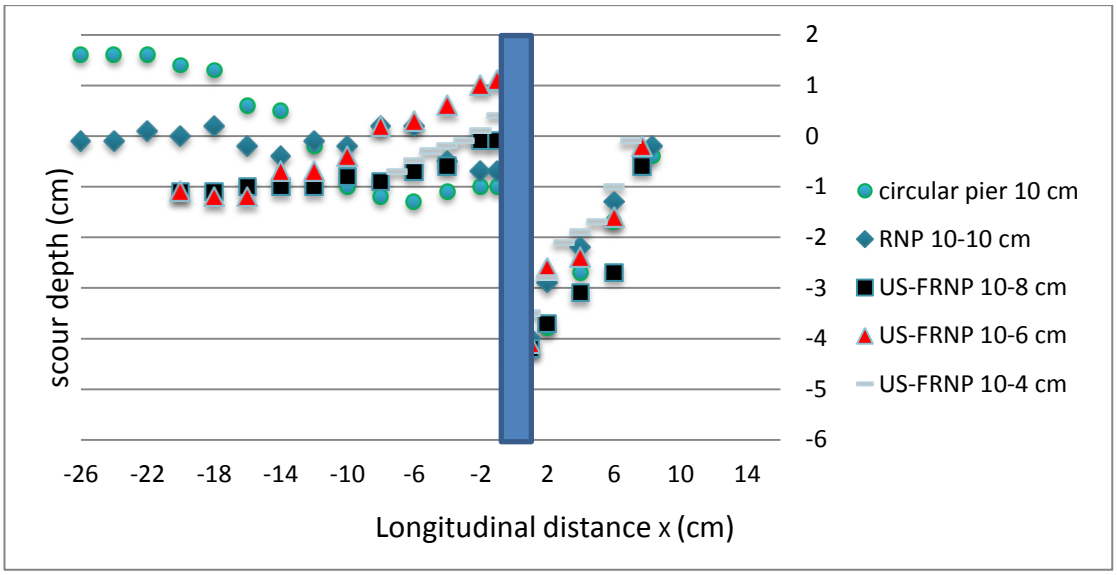

Figure 4.10 Longitudinal scours holes of runs (C1-C5)

4.2.1.2.2 Transvers section of scour hole for Series 1, 2 and 3

Figures (4.11-4.13) demonstrates the top scour holes of circular, RNP, US-FRNP bridge piers under discharge 38, 48 and 58 l/s. The top scour hole width of US-FRNP 10-4 cm was less than the others due to the effect of bridge shape on the scour. The same results show that the top scour width in A5 greater than B5 and C5, that means the top scour depth increases with increasing discharge.

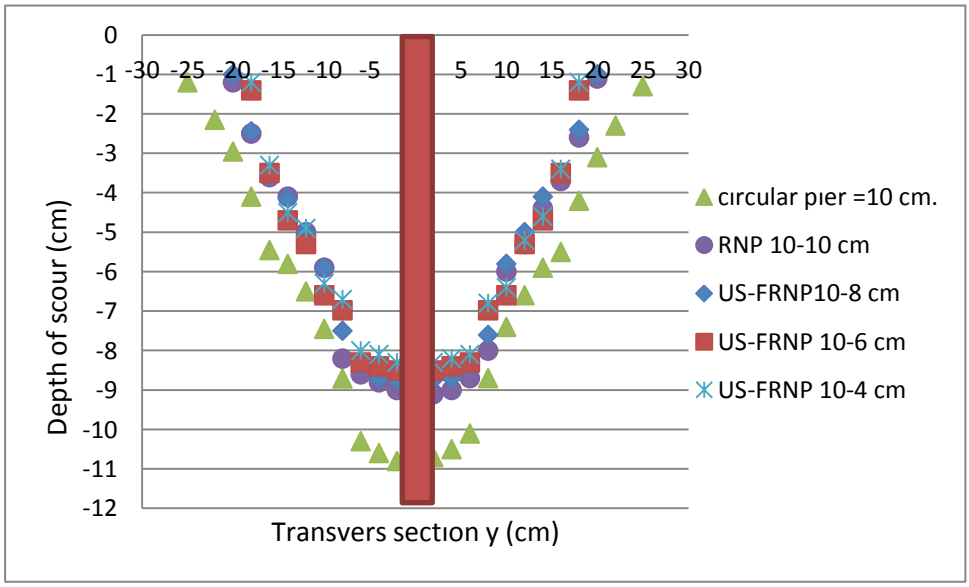

Figure 4.11 Transverse scour holes of (A1-A5)

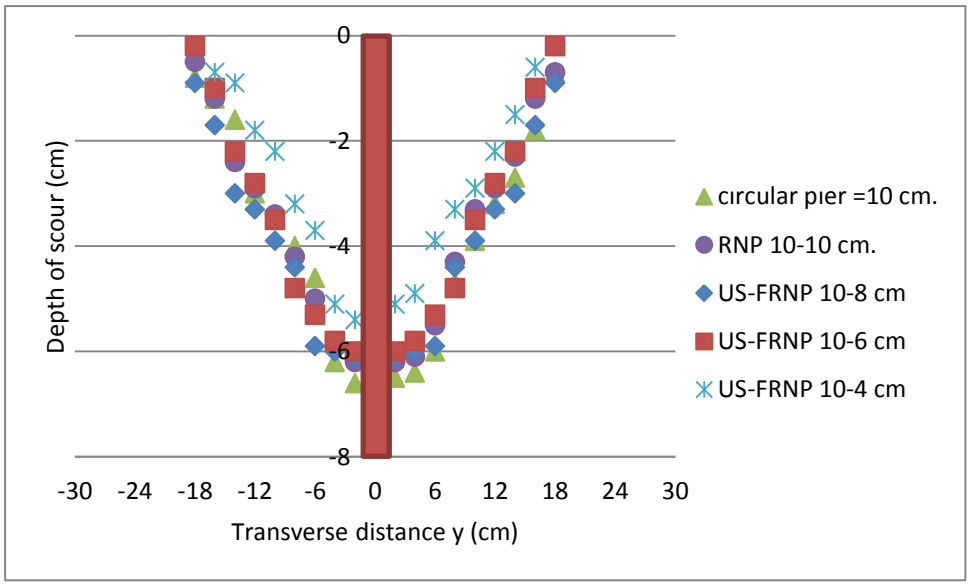

Figure 4.12 Transverse scour holes of (B1-B5)

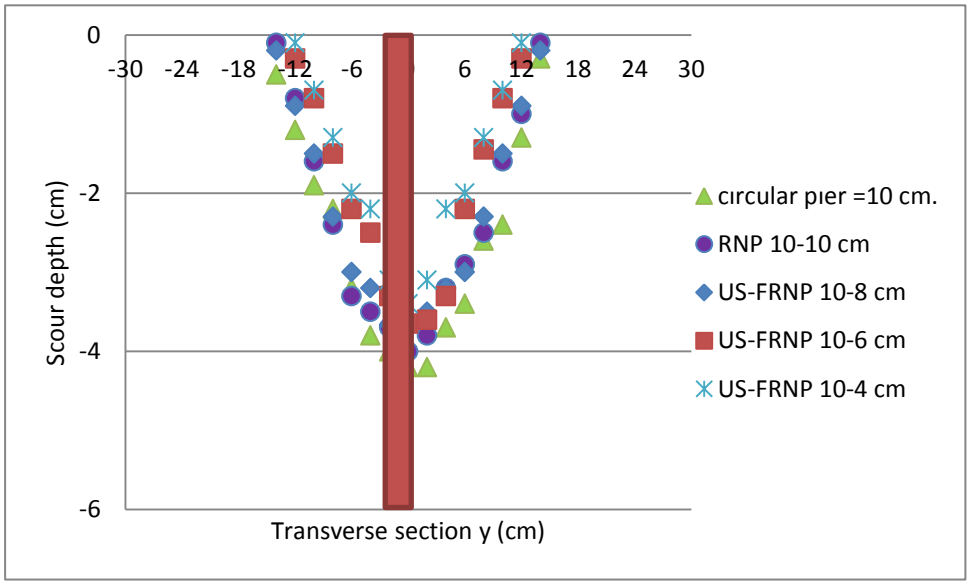

Figure 4.13 Transverse scour holes of (C1-C5)

4.3 Change the Orientation of Round Nosed Pier (RNP)

The current study is to provide a new method to reduce scour depth in front of bridge pier. The idea of this method is dependent on the change the orientation of upstream-facing round nosed pier so that it faces downstream rather than upstream according to the direction of flow (named after here as downstream-facing round nosed pier). The downflow deflected away from the front of the downstream-facing round nosed pier and the vortex becomes small and does not affect the pier. The orientation of three bridge piers were changed according to flow direction and compared with upstream-facing round nosed and circular piers to show the effect of changing the orientation of the pier on the local scour as illustrated in Figure 4.14.

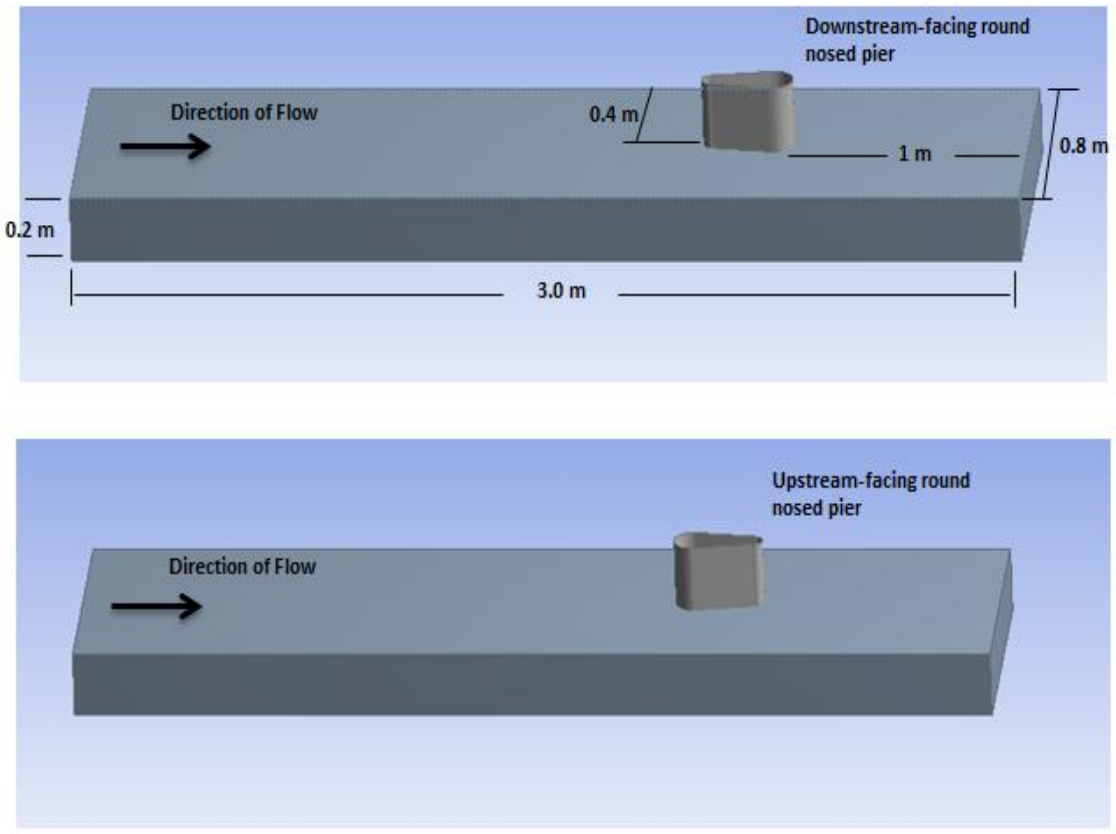

Figure 4.14 Location of upstream and downstream round nosed bridge pier to the flow direction

The study investigates the performance of different upstream and downstream round nose diameter with respect to local scour and compare the experimental results with the most practically used circular piers. The present experimental study shows that round nosed bridge pier performance improved by locating it as downstream facing to the flow. We hope that the results of the present study will be benefitted by the designers and engineers.

The present study is perhaps the first experimental work to place bridge pier in opposite direction according to flow direction under live-bed condition.

4.3.1 Scouring around Series 4, 5 and 6

From the Figures (4.15, 4.16 and 4.17) the time evolution of Series 4 (D1-D3), Series 5 (E1-E3) and Series 6 (F1-F3) as compared with circular pier. It is observed that the downstream-facing round nosed pier (DS-FRNP) (8-10, 6-10 and 4-10 cm) decrease the scour hole as compared with circular pier, the percentage of reduction was 27%, 36% and 54% respectively for Series 4, 28%, 34% and 60% respectively for Series 5 and finally, 32% , 52% and 74% respectively for Series 6.

In addition to a reduction of the scour depth, the rate of scouring is also reduced considerably as in Figures (4.15, 4.16 and 4.17). Reduction in the rate of scouring can reduce the risk of pier failure when the duration of floods is short Melville and Chiew (1999). It is clear that the DS-FRNP 4-10 cm was efficient in reducing the scour and the rate of scour as compared with the others.

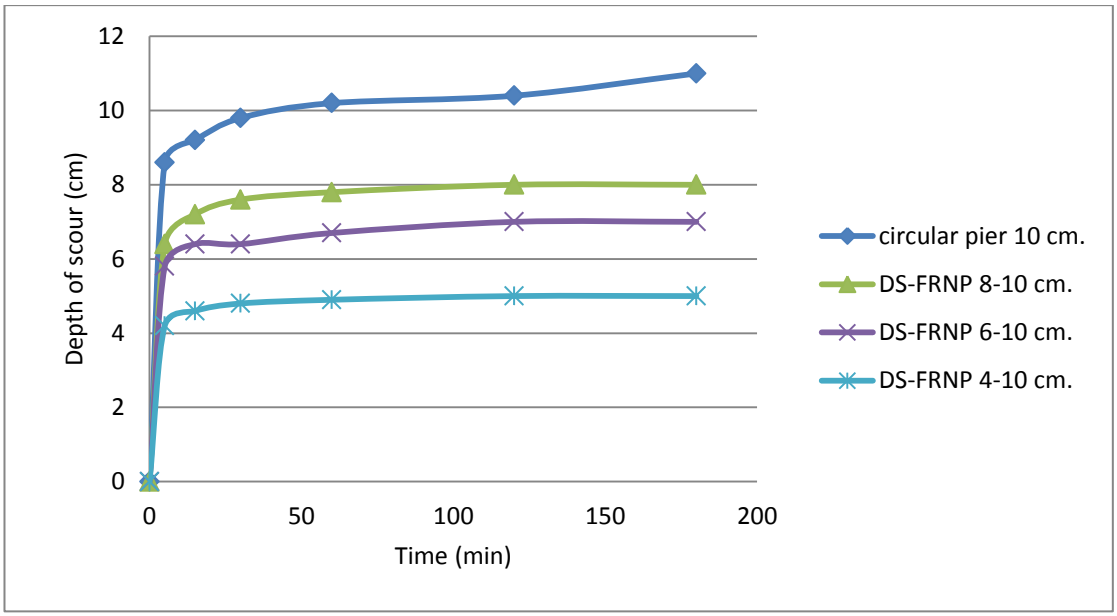

Figure 4.15 Scour Hole Development measured at the base of bridge piers with Q= 58 L/s

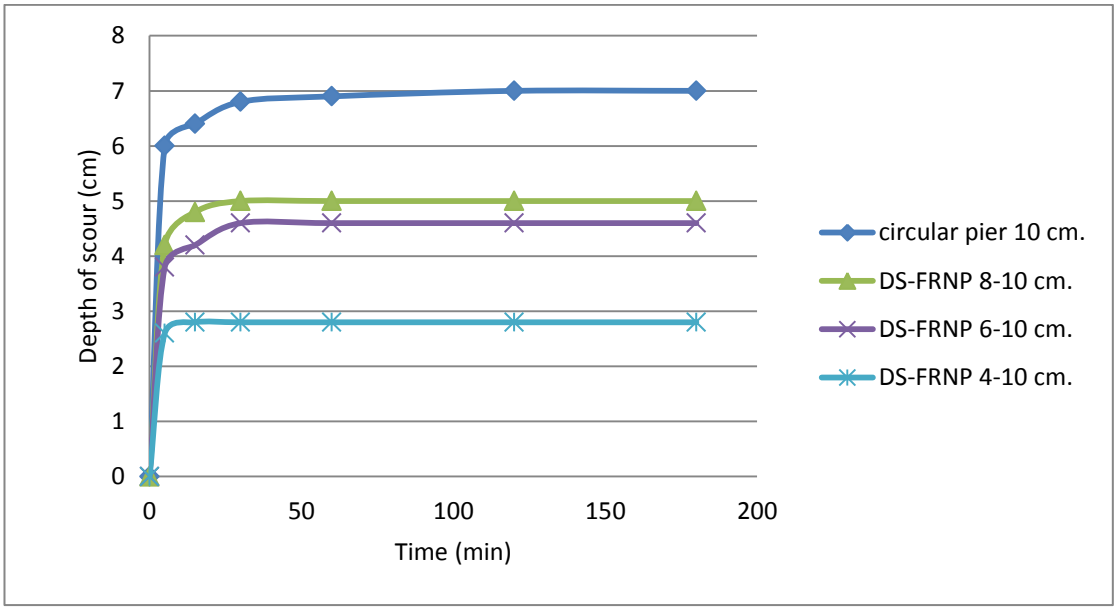

Figure 4.16 Scour hole development measured at the base of bridge piers with Q= 48 L/s

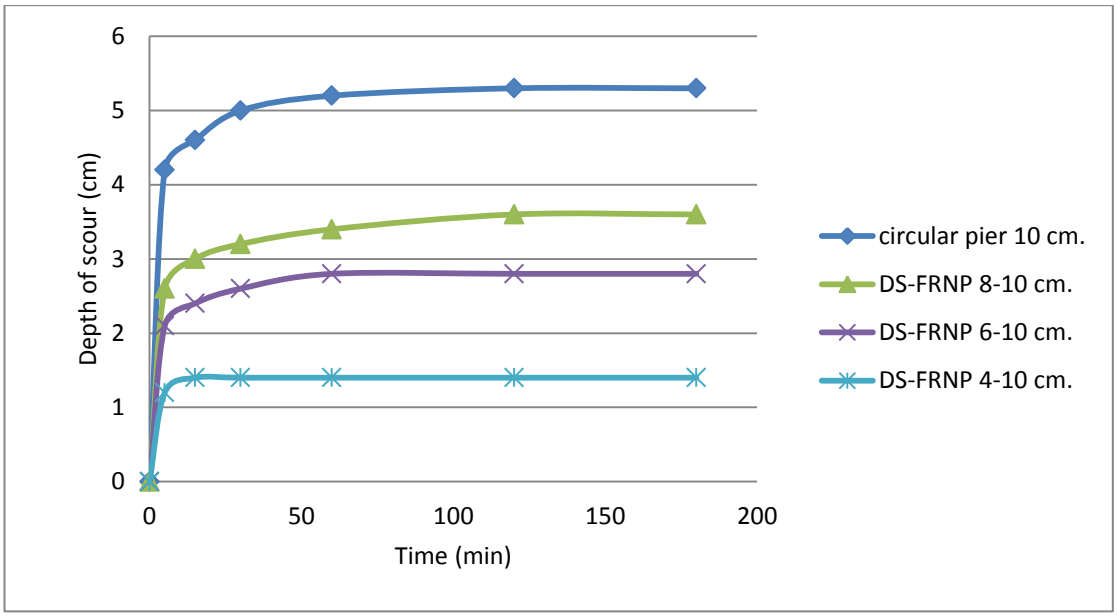

Figure 4.17 Scour hole development measured at the base of bridge piers with Q= 38 L/s

4.3.1.1 Scour Hole Dimensions

Dimensions of the scour holes for each run of Downstream-Facing Round Nosed Pier (DS-FRNP) experiments were measured. The top width of scour in the transverse direction, distance from upstream face to front outer edge of hole, and depth at upstream face were compared for each of the bridge piers as shown in Table 4.2.

Table 4.2 Dimensions of the scour holes

Dimensions of the scour holes	DS-FRNP 4-10 cm.	DS-FRNP 6-10 cm.	DS-FRNP 8-10 cm.
Q=0.058 m^3/sec			
Top Scour Hole Width	0.30	0.30	0.40
Distance from Upstream face to front outer edge of hole	0.07	0.07	0.16
Depth at Upstream face (m)	0.05	0.07	0.08
Q= 0.048 m^3/sec			
Top Scour Hole Width (m)	0.28	0.28	0.36
Distance from Upstream face to front outer edge of hole (m)	0.07	0.07	0.12
Depth at Upstream face	0.028	0.046	0.05
Q=0.038 m^3/sec			
Top Scour Hole Width	0.16	0.16	0.28
Distance from Upstream face to front outer edge of hole	0.03	0.05	0.05
Depth at Upstream face	0.014	0.028	0.036

4.4 Dimensional Analysis

Dimensional analysis was used to define the dimensionless parameters based on the selection of all variables governing the maximum scour depth at upstream of the bridge pier.

ds= $f_1(u, v, \rho, \rho_s, h, g, d_{50}, d_{u.s}, d_{d.s})$ (4.1)

In which, u is the flow velocity, v is the kinematic viscosity, ρ_s is the density of particle size, ρ is the density of fluid, h is the flow depth, g is the gravitational acceleration,

d_{50} is the median particle size and $d_{u.s}$ is the upstream pier diameter and $d_{d.s}$ is the downstream pier diameter as shown in Figure 4.18.

Dimensionless parameters are found by Buckingham π-theorem and the repeated parameters are selected as ρ, V and D, indicating fluid, flow and geometric characteristics. Rearranging the dimensionless parameters gives the following relationship:

$$ds/ d_{u.s} = f_2(F_r, R_e, \frac{\rho_s - \rho}{\rho}, \frac{h}{d_{50}}, \frac{d_{u.s}}{d_{50}}, \frac{d_{u.s}}{d_{d.s}}) \qquad (4.2)$$

For the conditions in this study, the general statement can be simplified by the two following assumptions:

The effect of Reynolds number is ignored for fully turbulent flow. Thus the term R_e is dropped. Densities of the fluid and sediment are constant throughout the study. In this way, relative density term ($\frac{\rho_s - \rho}{\rho}$) is dismissed.

$$ds/ d_{u.s} = f_2(F_r, \frac{h}{d_{50}}, \frac{d_{u.s}}{d_{50}}, \frac{d_{u.s}}{d_{d.s}}) \qquad (4.3)$$

ds is maximum depth of scour , Fr is Froude number range and $\frac{d_{u.s}}{d_{d.s}} = k_s$, k_s is the shape factor and is equal to (1.25,1.67 and 2.5) , $\frac{h}{d_{50}}$, $\frac{d_{u.s}}{d_{50}}$ are listed in Table 4.3.

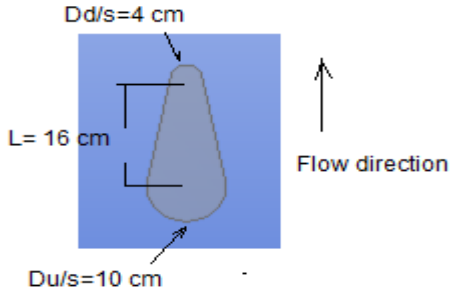

Figure 4.18 Dimension of upstream-facing round nosed pier

Table 4.3 Experimental data.

u (m/s)	h (m)	$d_{u.s}/d_{50}$	h/d_{50}	Fr
0.58	0.125	55.17	86.2	0.523
0.54	0.11	41.37	75.8	0.525
0.49	0.097	27.58	66.2	0.51

4.5 Prediction of Scour Depth

Using step-wise regression, Eq. (4.4) was developed to correlate the relative maximum scour depth to the Froude number, Fr, and the pier shape factor, ks

$$ds \quad d_{u.s} = 2.11 - 636.5 \ \frac{h}{d_{50}} \quad \overline{Fr} + 1.31 * lnks * \ log(\frac{d_{u.s}}{d_{50}}) * logFr \qquad (4.4)$$

The correlation coefficient (R) estimate for Eq. (4.4) is 94%. Figure 4.19 presents the predicted values of $ds/d_{u.s}$ using Eq. (4.4) versus the measured ones while Figure 4.20 shows the distribution of the residuals around the line of zero error. Both figures indicate that Eq. (4.4) represented the measured data very well and hence could be used safely to predict the relative maximum depth of scour for different shape of piers.

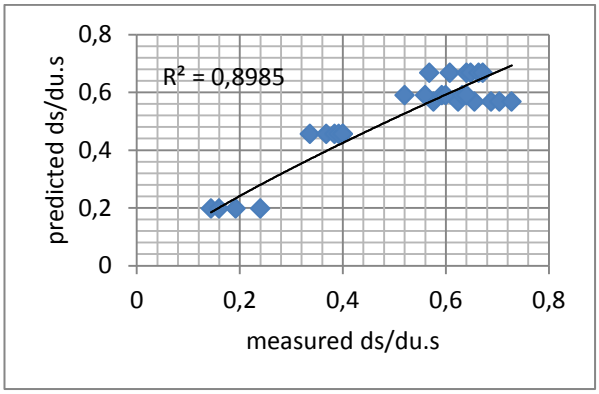

Figure 4.19. Measured $ds/d_{u.s}$ versus predicted $ds/d_{u.s}$

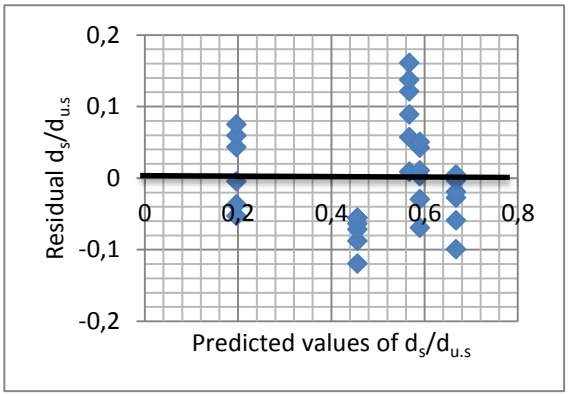

Figure 4.20 Predicted values of $ds/d_{u.s}$ versus residual.

4.6 Use of Downstream-Facing Round Nosed Pier as Countermeasure against Local Scouring

Grimaldi et al. (2009) investigated the behavior of a slot as countermeasure against local scouring through a circular bridge pier. The results showed that the slot reduces the local scour at pier. The maximum reduction of the scour depth was about 30% in the best configurations.

Using downstream-facing round nosed pier (4-10 cm) as countermeasure against local scouring plays the same role as a slot, the DS-FRNP acts by reducing the strength of the downflow and, consequently, of the horseshoe vortex.

The results showed that the downstream facing round nosed pier reduces local scour. The reduction of maximum scour depth was 54% when compared to the circular pier and 40% compared with upstream facing round nosed pier. However, the DS-FRNP does not need any alteration or modification to reduce scour and the maximum reduction was higher than a slot. Changing the orientation of bridge pier (as is located downstream facing to the flow) is an effective countermeasure for reducing local scour depth.

4.7 Scour Pattern around Circular, RNP, US-FRNP and DS-FRNP

Computer software called Surfer version (11) was used to sketch the scour pattern around bridge piers for Series (1-6).

Figures (4.21- 4.32) show the scour pattern around the circular, round nosed (RNP), upstream facing round nosed (US-FRNP) and downstream facing round nosed (DS-FRNP) piers. The downstream facing round nosed pier minimizes the scour depth, producing a little scour in the front and on the sides of the pier, but the scour in the pier's rear was more than that of upstream facing round nosed pier due to the separation

of flow occurred with a small amount at the beginning and then increased gradually according to the shape of downstream facing round nosed pier .In contrast for upstream facing round nosed pier the separation increased and then decreased, producing a little scour at the wake region.

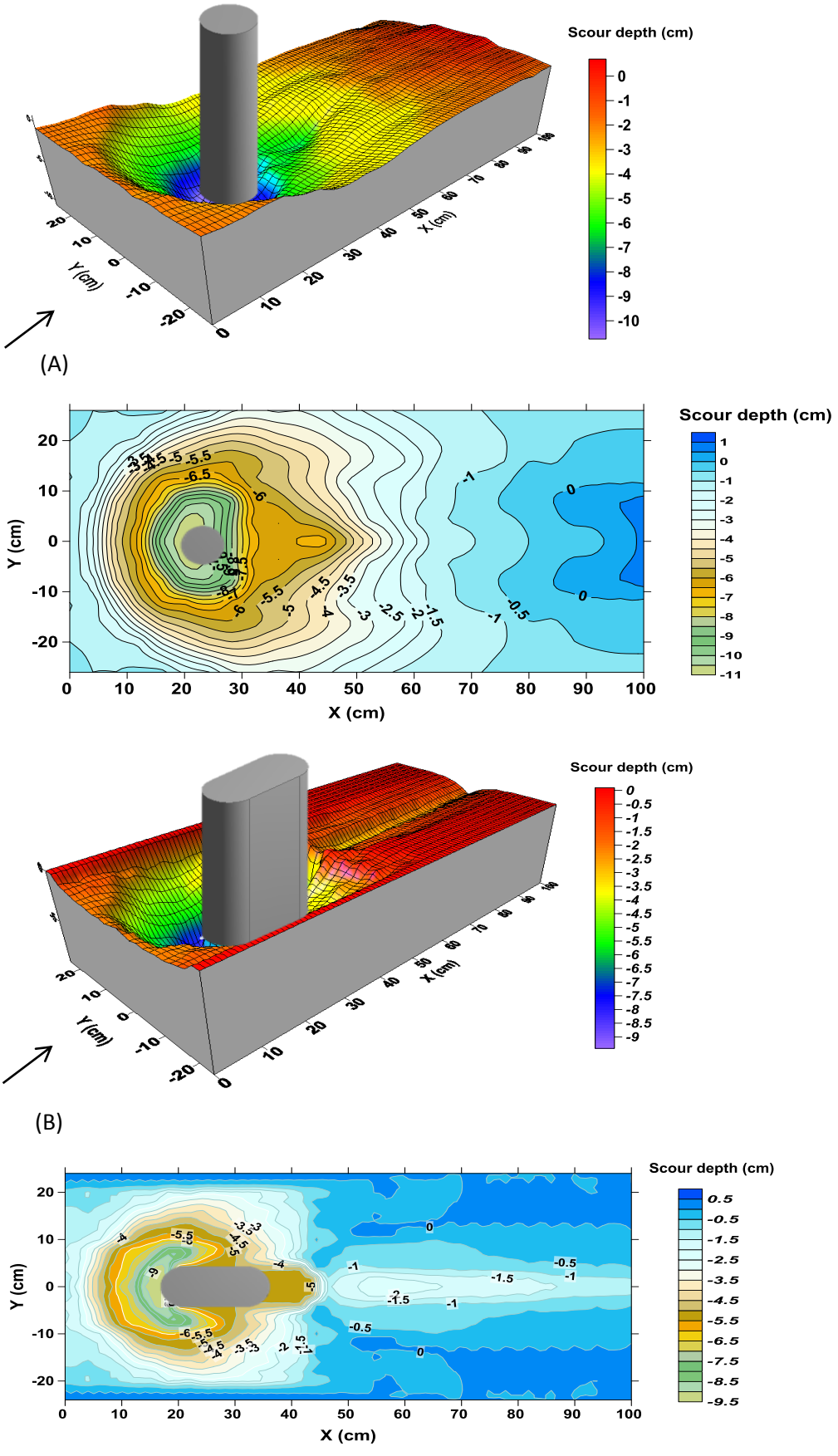

Figure 4.21 Scour pattern around A) Circular pier and B) RNP, Q=58 L/s

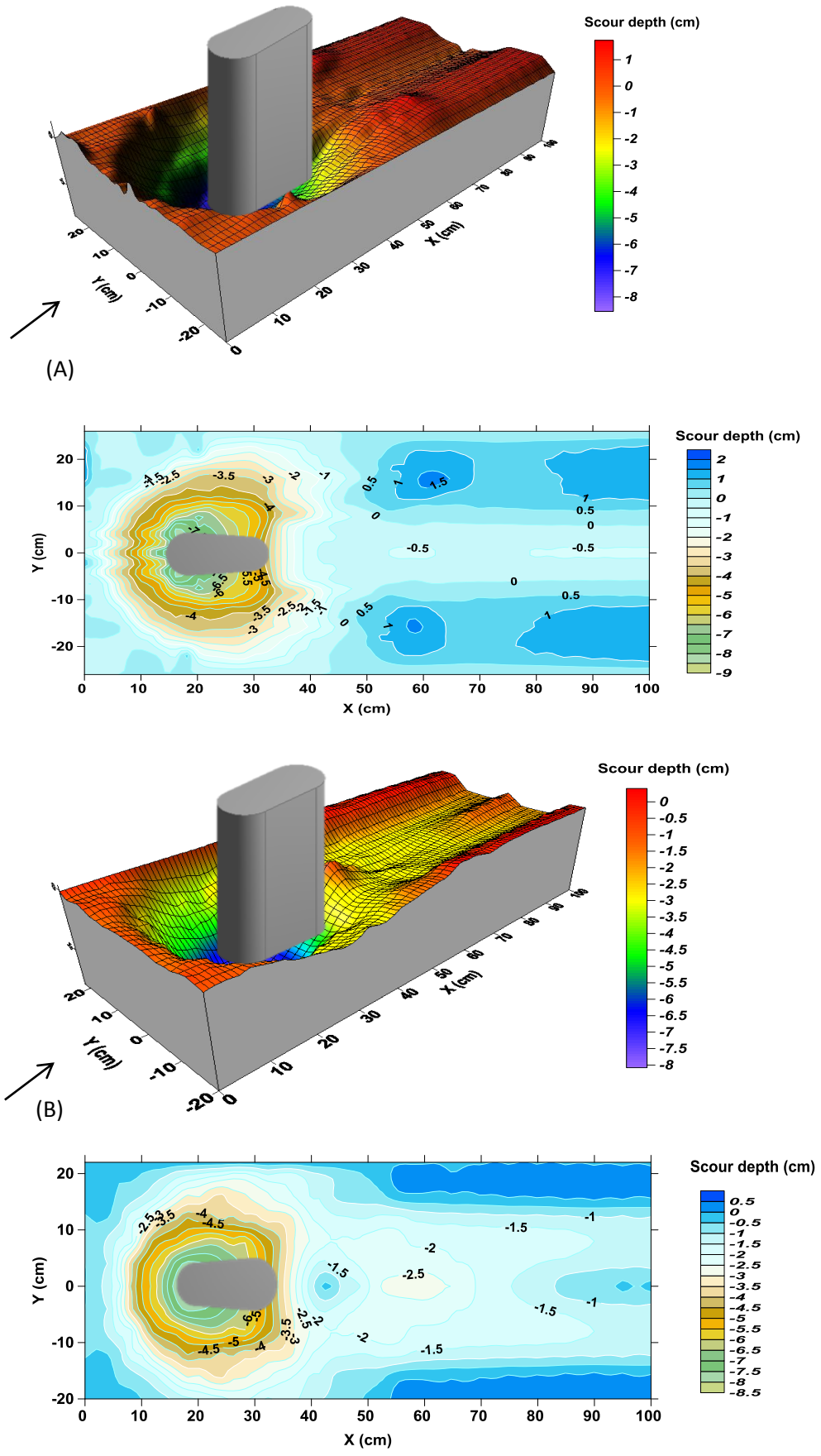

Figure 4.22 Scour pattern around A) US-FRNP 10-8 cm and B) DS-FRNP 8-10 cm, Q= 58 L/s

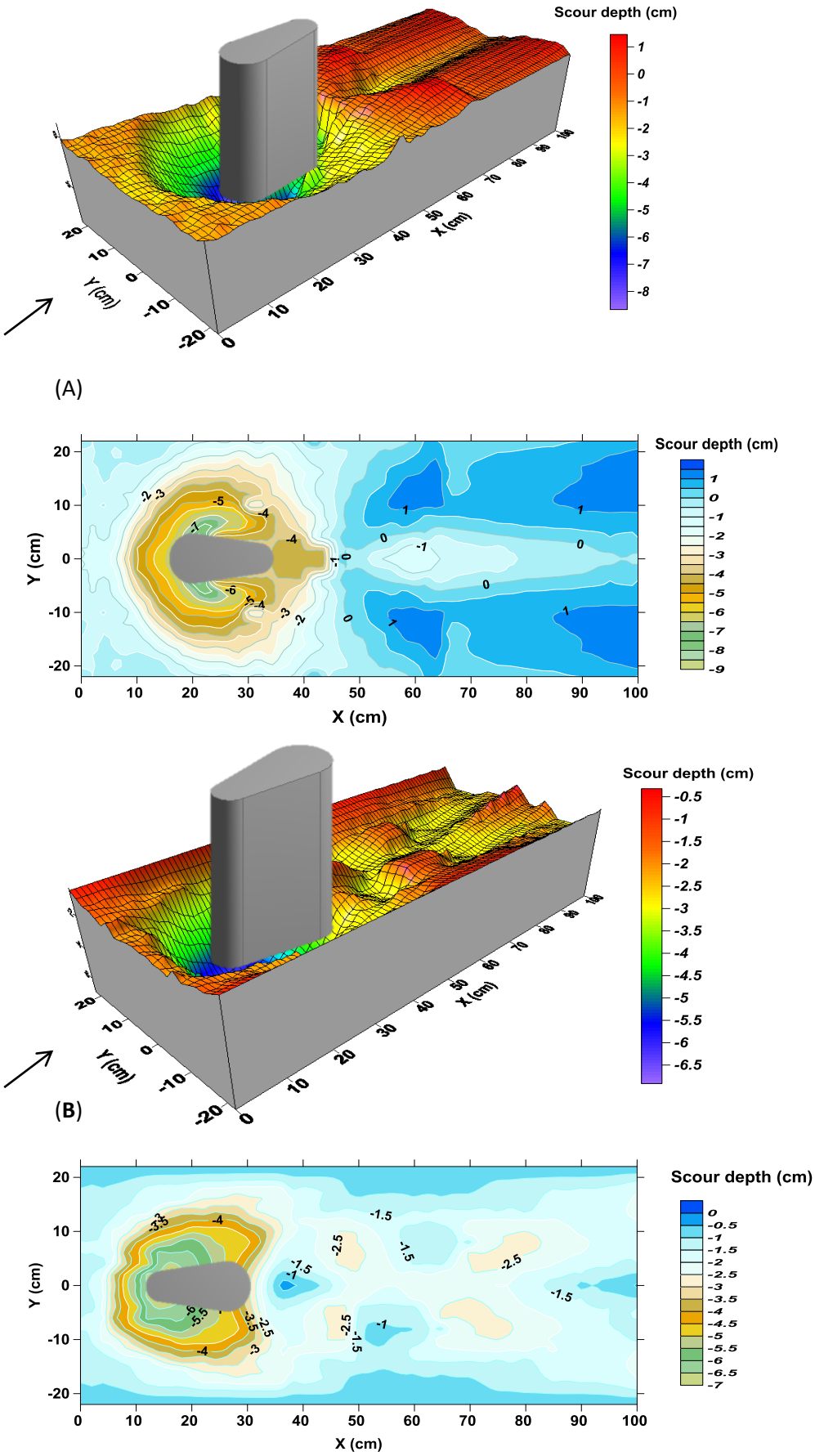

Figure 4.23 Scour pattern around A) US-FRNP 10-6 cm and B) DS-FRNP 6-10 cm Q=58 L/s

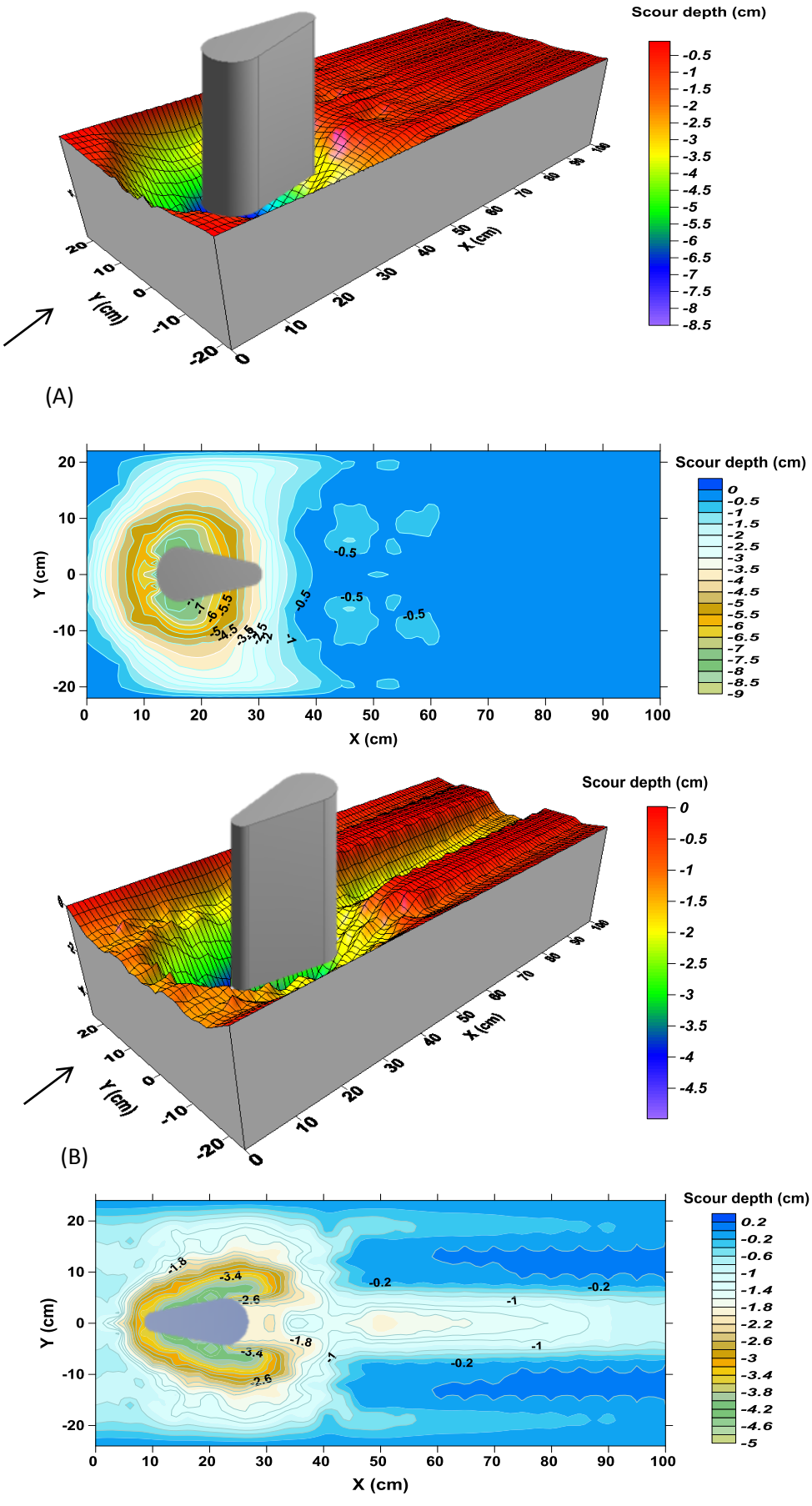

Figure 4.24 Scour pattern around A) US-FRNP 10-4 cm and B) DS-FRNP 4-10 cm Q=58 L/s

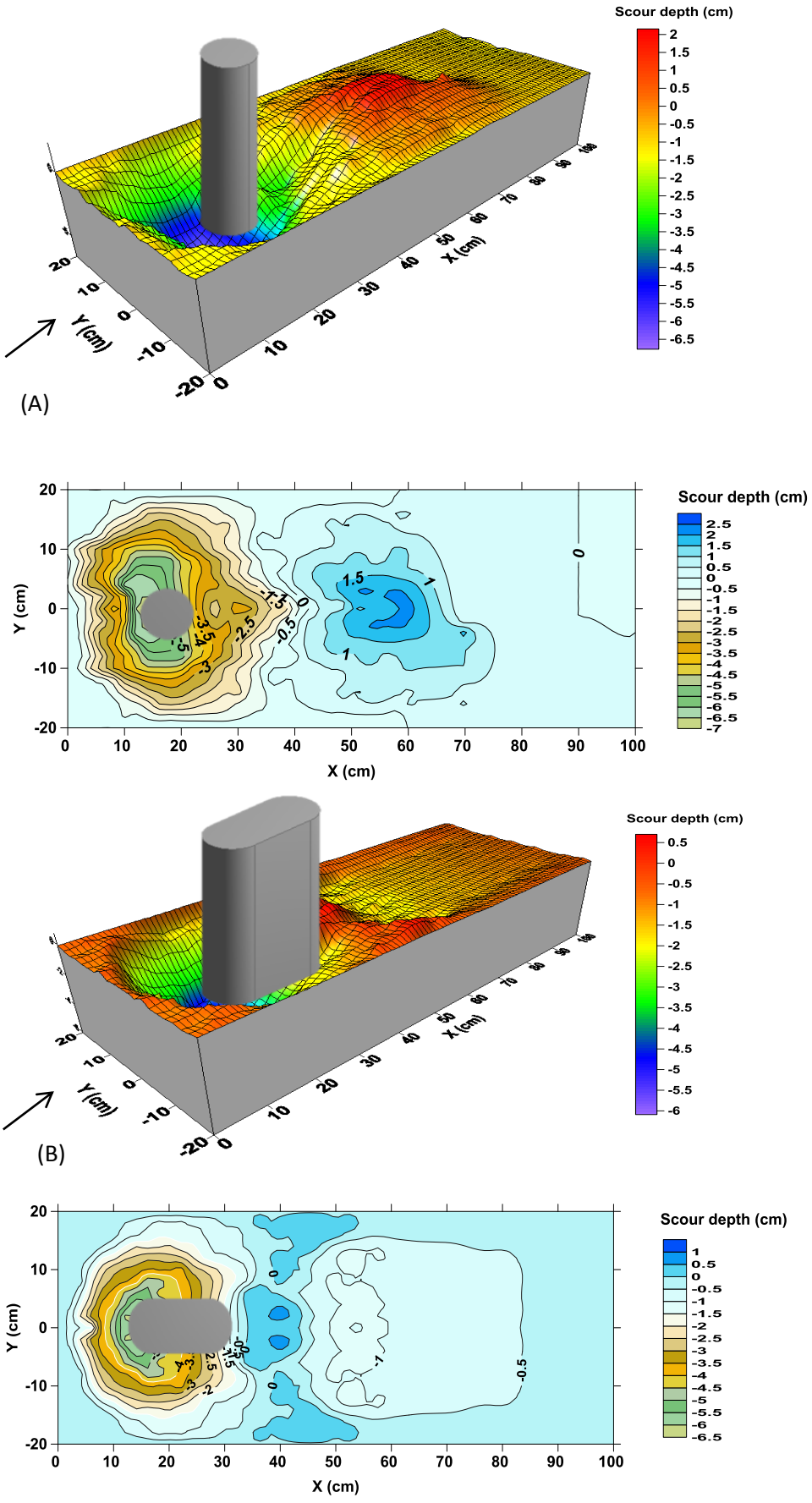

Figure 4.25 Scour pattern around A) Circular pier and B) RNP, Q=48 L/s

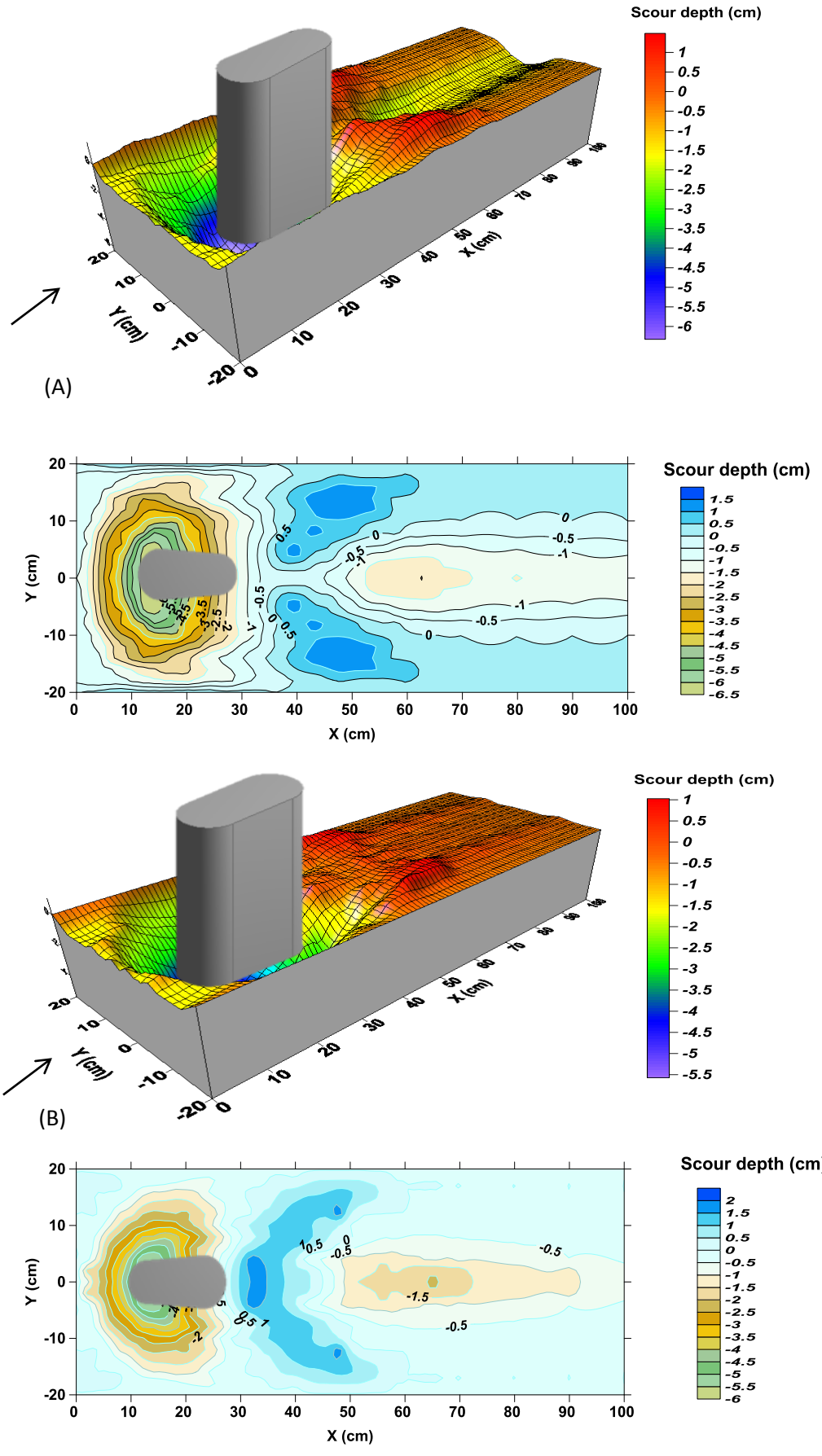

Figure 4.26 Scour pattern around A) US-FRNP 10-8 cm and B) DS-FRNP 8-10 cm, Q= 48 L/s

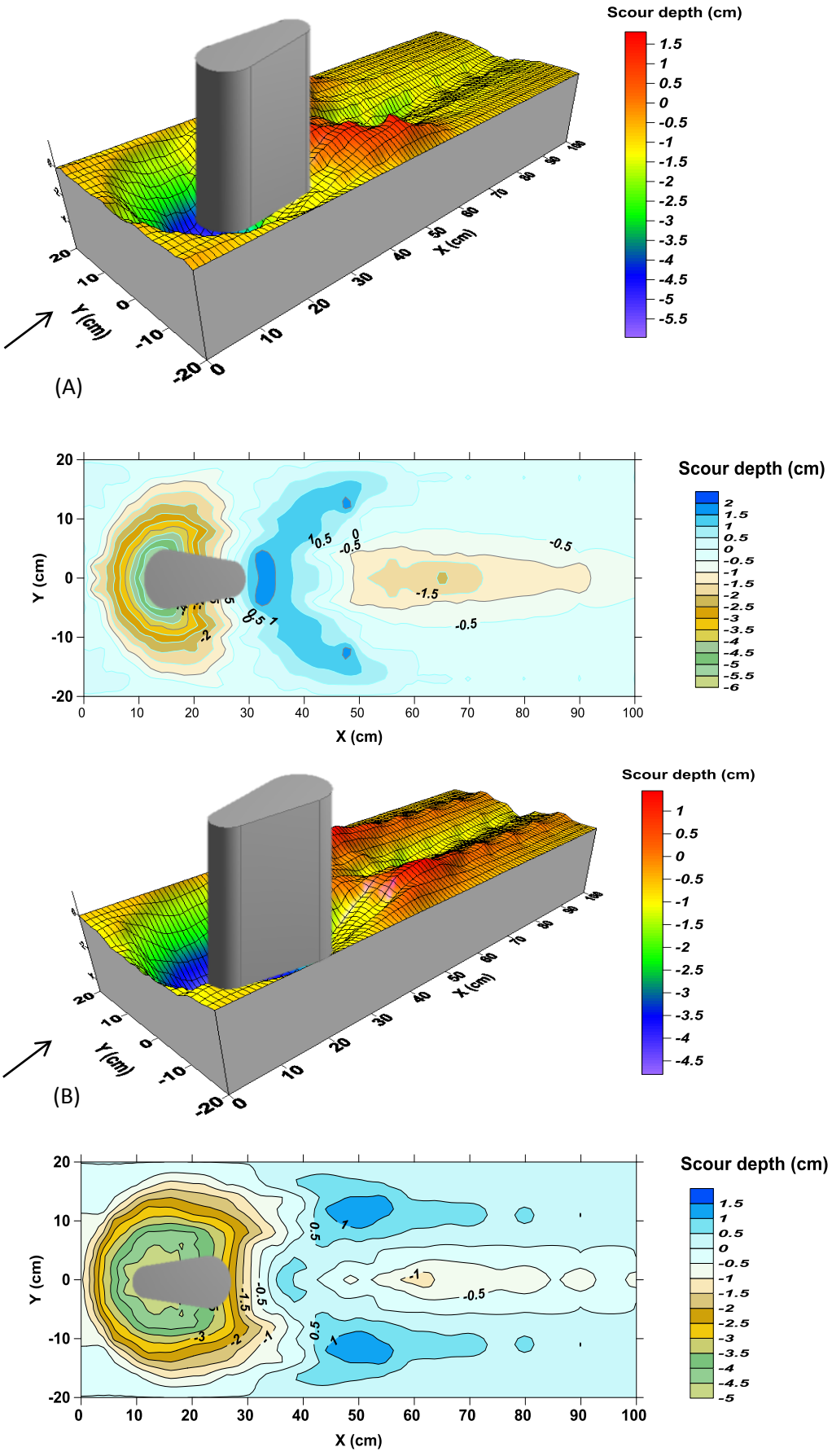

Figure 4.27 Scour pattern around A) US-FRNP 10-6 cm and B) DS-FRNP 6-10 cm Q=48 L/s

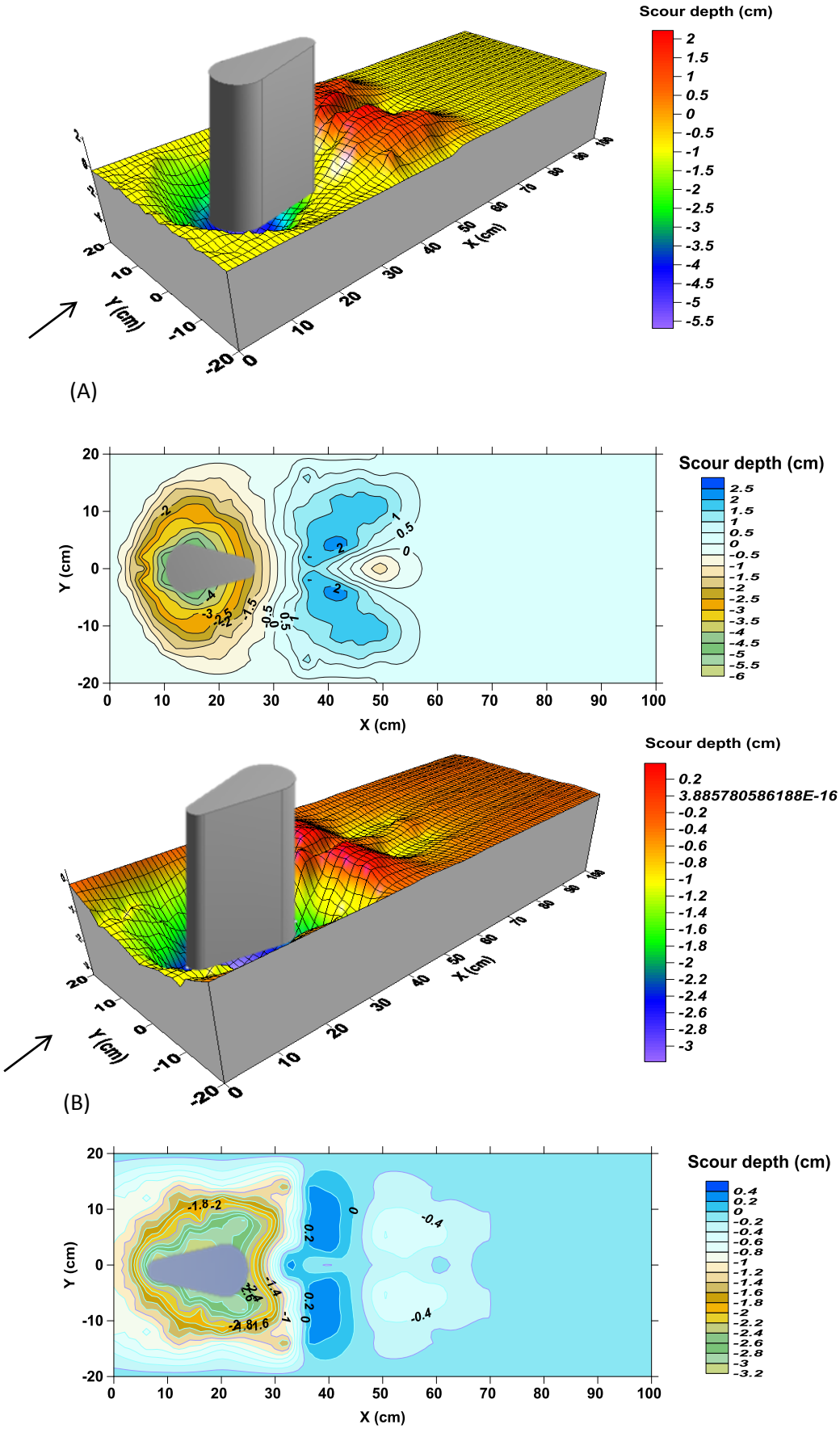

Figure 4.28 Scour pattern around A) US-FRNP 10-4 cm and B) DS-FRNP 4-10 cm Q=48 L/s

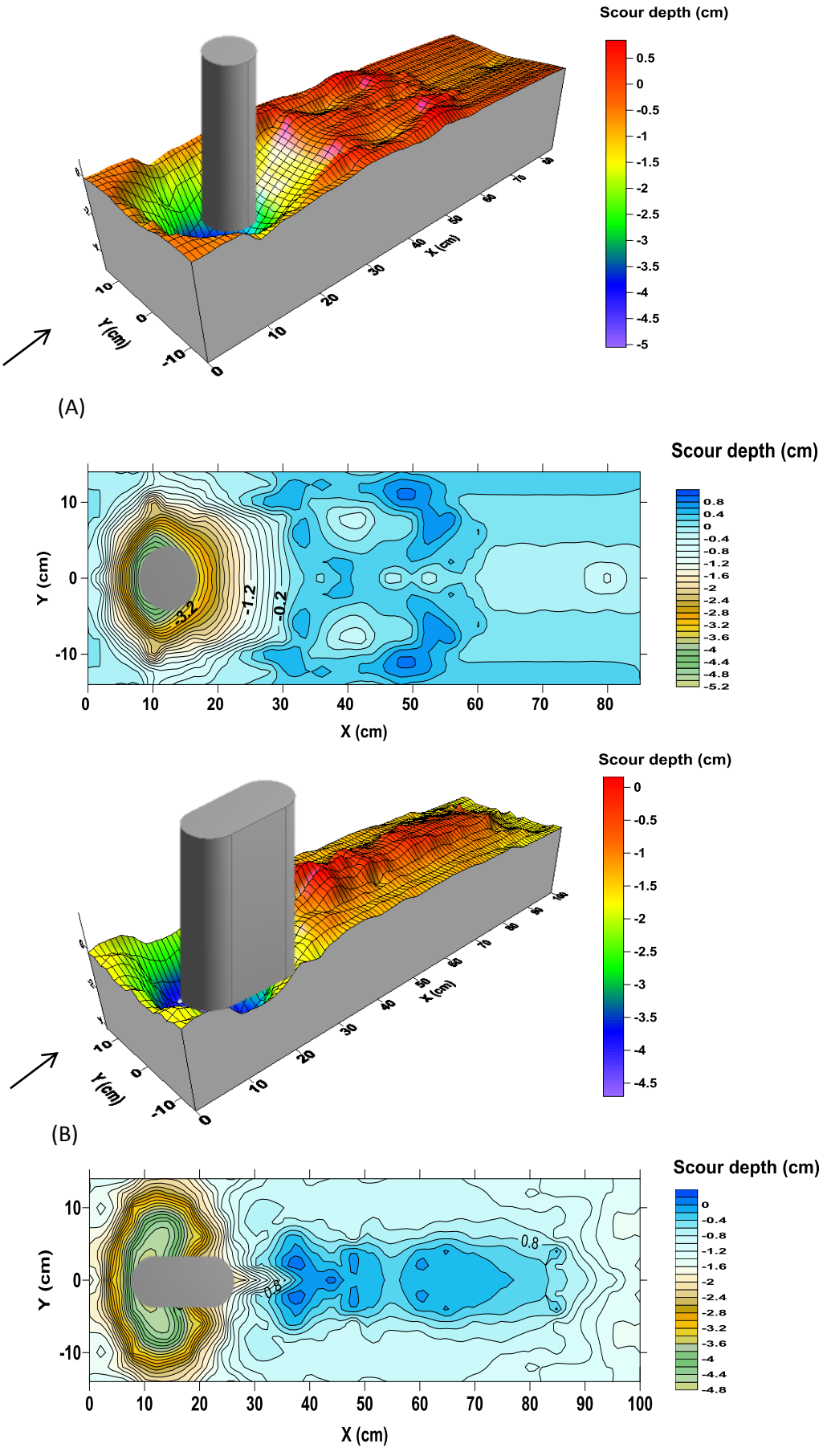

Figure 4.29 Scour pattern around A) Circular pier and B) RNP, Q=38 L/s

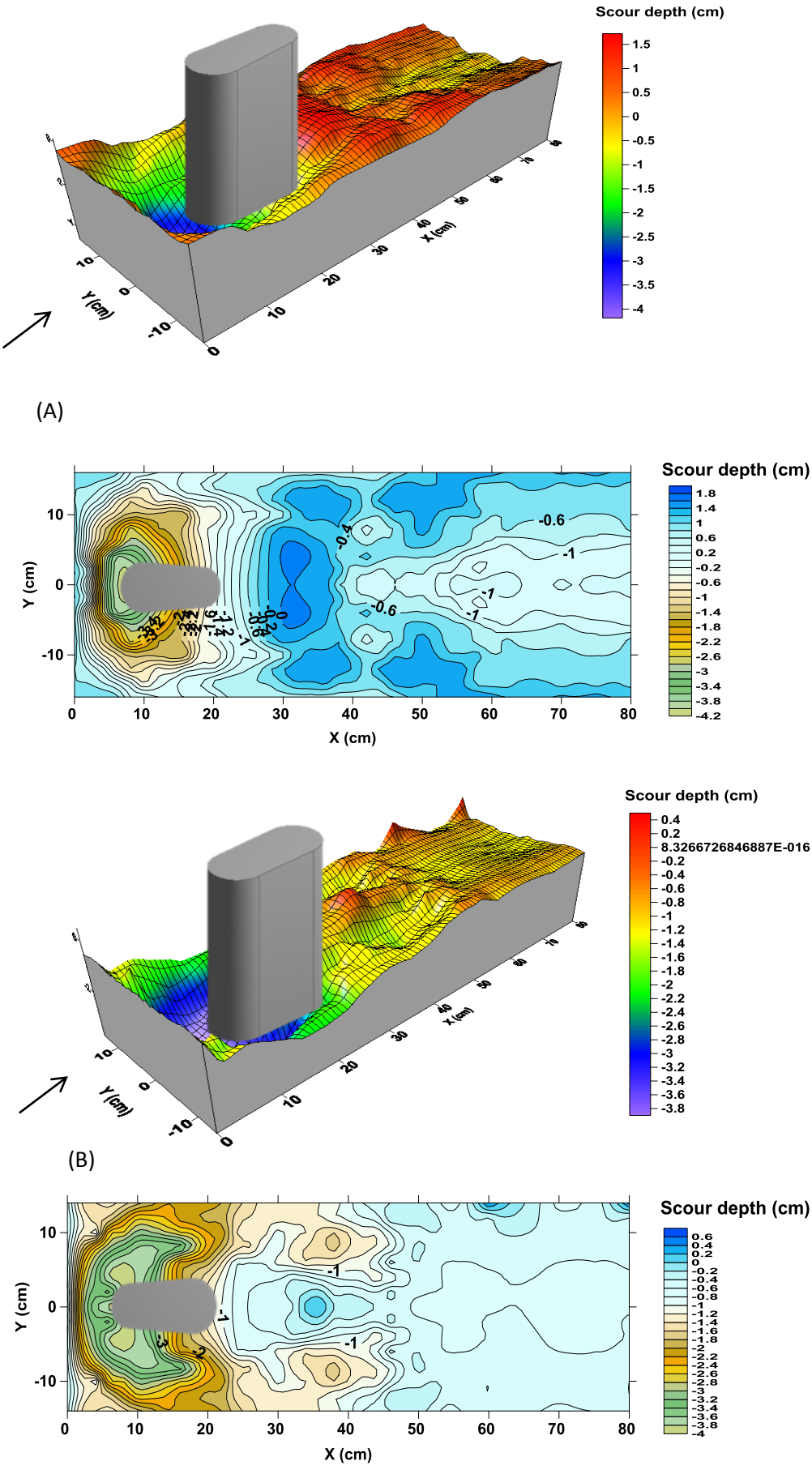

Figure 4.30 Scour pattern around A) US-FRNP 10-8 cm and B) DS-FRNP 8-10 cm, Q= 38 L/s

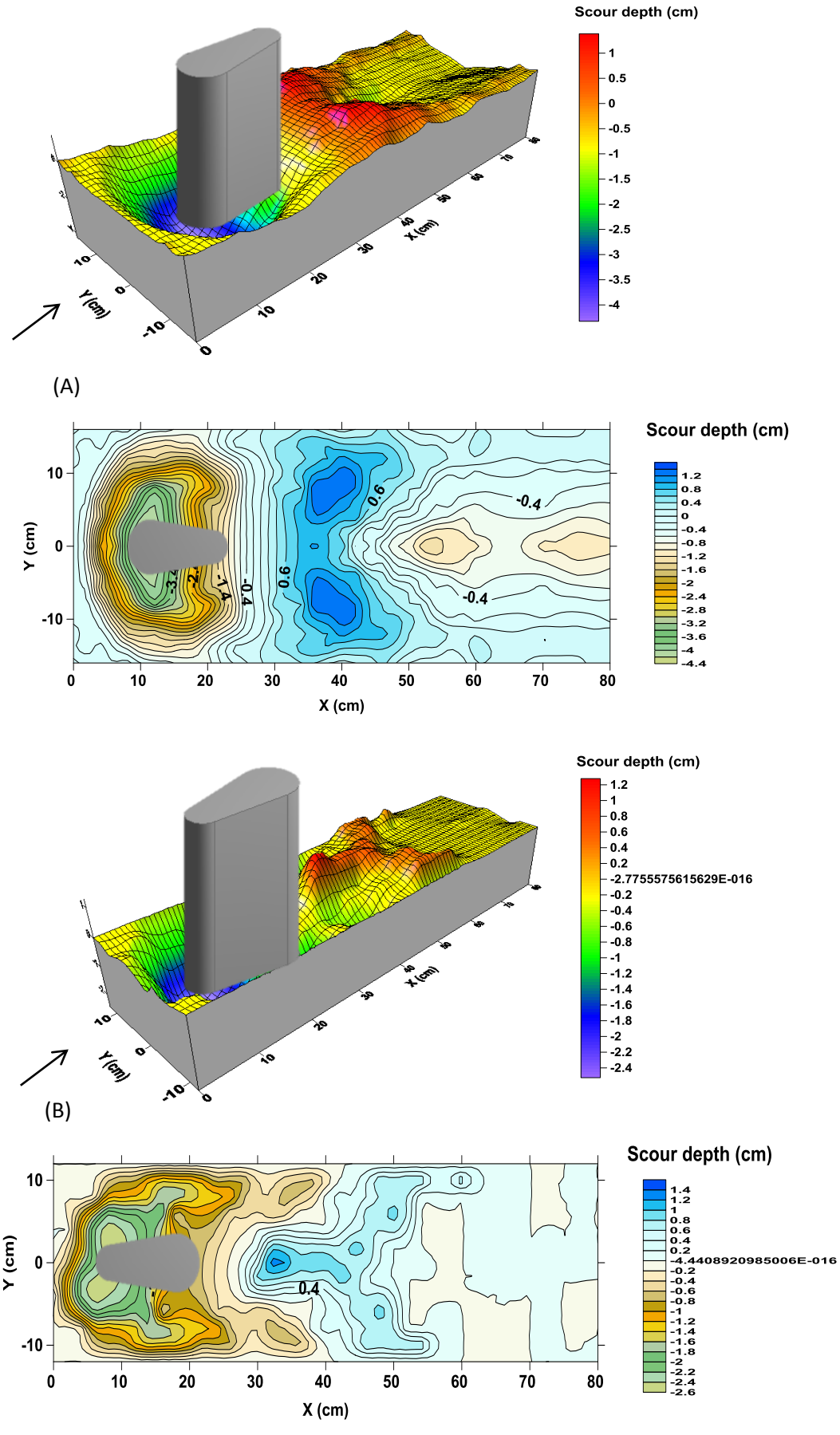

Figure 4.31 Scour pattern around A) US-FRNP 10-6 cm and B) DS-FRNP 6-10 cm Q=38 L/s

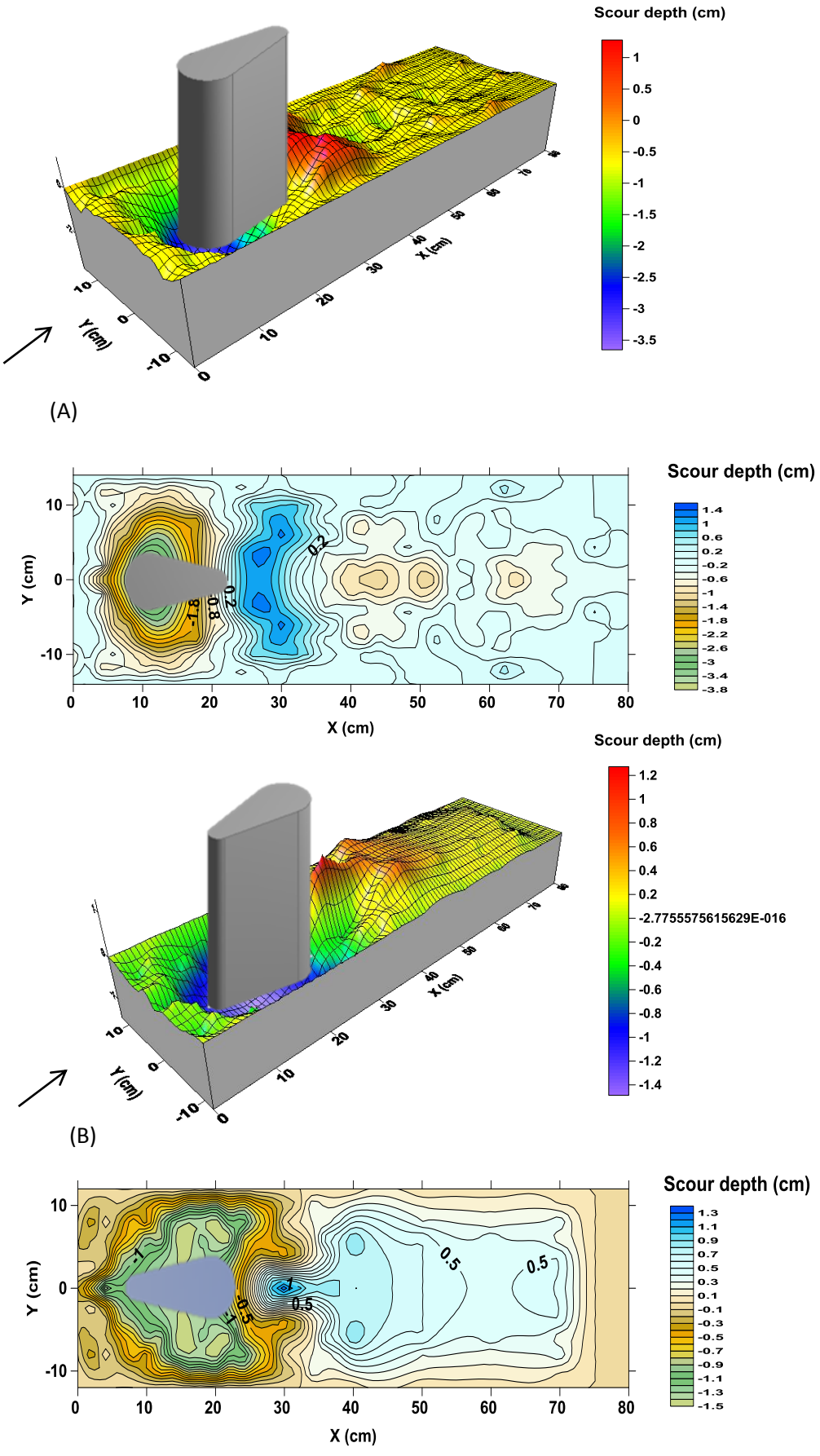

Figure 4.32 Scour pattern around A) US-FRNP 10-4 cm and B) DS-FRNP 4-10 cm Q=38 L/s

4.8 Use of Downstream-Facing Aerofoil-Shaped Bridge Piers to Reduce Local Scour

The current study is to provide a new method to reduce scour depth in front of bridge pier. The idea of this method is dependent on the change the orientation of an aerofoil pier so that it faces downstream rather than upstream according to the direction of flow (named after here as downstream-facing aerofoil-shaped pier). The downflow deflected away from the front of the downstream-facing aerofoil-shaped pier and the vortex becomes small and does not affect the pier. In this study three piers (upstream-facing aerofoil, downstream-facing aerofoil and circular) were tested under live-bed condition with flow intensity of 0.058 m^3/s for duration 5 hours. The velocity field measurements were obtained using an Acoustic Doppler Velocimeter (ADV). The results showed that, the downstream-facing aerofoil-shaped pier reduces local scour around the pier. The reduction of the scour hole volume was about 87% compared with circular pier and the maximum depth of scour reduced 59% compared with upstream-facing aerofoil and 68% compared with circular pier. The present experimental study shows that downstream-facing aerofoil design can reduce scour depth, thereby reduces the potential need for countermeasures.

4.8.1 Maximum Scour depth around piers for Series 7

Experimental results of the Series 7 (G1 and G2) within cohesion less bedding material have been compared and discussed in this section. Time evolution in scour depth measured at the upstream face of (A1, G1 and G2). The results are a comparison of scour and sediment scour hole depths for the circular (A1) and upstream-facing aerofoil (G1) piers were quite similar which was expected due to the identical shape on the upstream side of the pier as illustrated in Figure 4.33. A 68 % reduction in scour hole depth of the downstream-facing aerofoil pier was observed as compared to the circular

pier and 59% reduction as compared to the upstream-facing aerofoil pier. The effect of the horseshoe vortex was reduced due to the down flow being deflected away from the base of downstream aerofoil pier. The development of the scour hole around the pier perimeter is therefore strongly influenced by this down flow.

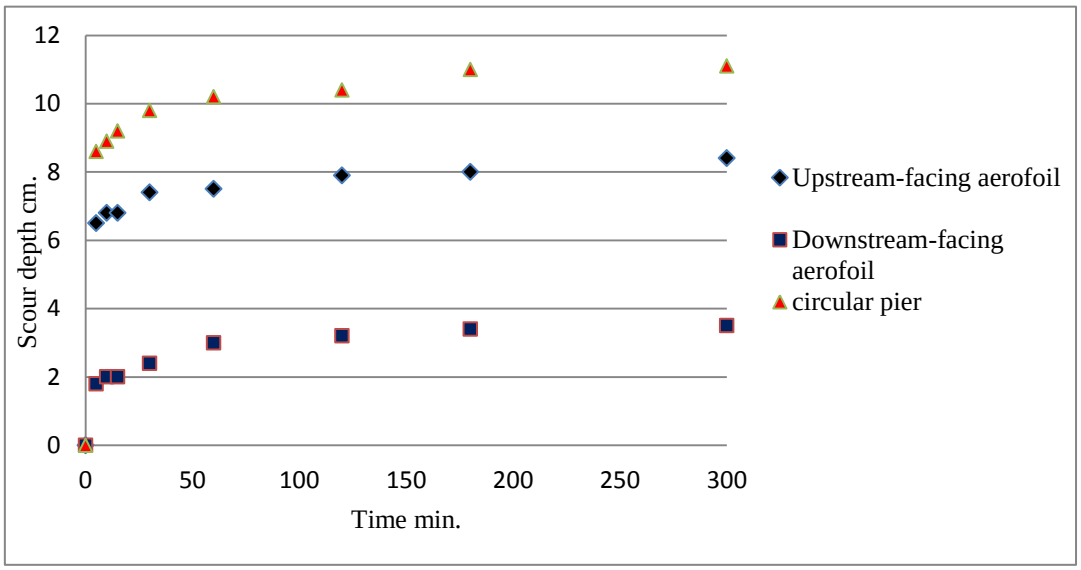

Figure 4.33 Time evolution in scour depth measured at the upstream face of the piers

4.8.2 Scour Hole Dimensions

Dimensions of the scour holes for each run of experiments were measured. The top width of scour in the transverse direction, distance from upstream face to front outer edge of hole, and depth at upstream face were compared for each of the three bridge piers as shown Table 4.4.

Table 4.4 Scour hole dimensions from physical modeling

Dimensions of scour hole	Downstream-facing aerofoil-shaped pier	Upstream-facing aerofoil-shaped pier	Circular pier
Top Scour Hole Width (m).	0.24	0.44	0.50
Distance from Upstream face to front outer edge of hole (m).	0.04	0.14	0.18
Depths at Upstream face (m).	0.035	0.085	0.11

4.8.2.1 Longitudinal and Transvers Sections around the piers for series A1, G1 and G2

The longitudinal distance from the pier to the outer edge of scour hole and top width of scour hole were measured.

The percentage reduction in distance from the upstream face of the pier to the upstream front outer edge of the hole as compared to the circular pier was 22% for the upstream-facing aerofoil pier and 78% for the downstream-facing aerofoil pier as in Figure 4.34 and Figure 4.35 demonstrate the top scour holes of three piers. The top scour hole width of downstream-facing aerofoil shaped pier was 52 % less than the circular pier and 12 % less than the upstream-facing aerofoil pier because the effect of the horseshoe vortex was reduced due to the down flow being deflected away from the base of downstream-facing aerofoil pier.

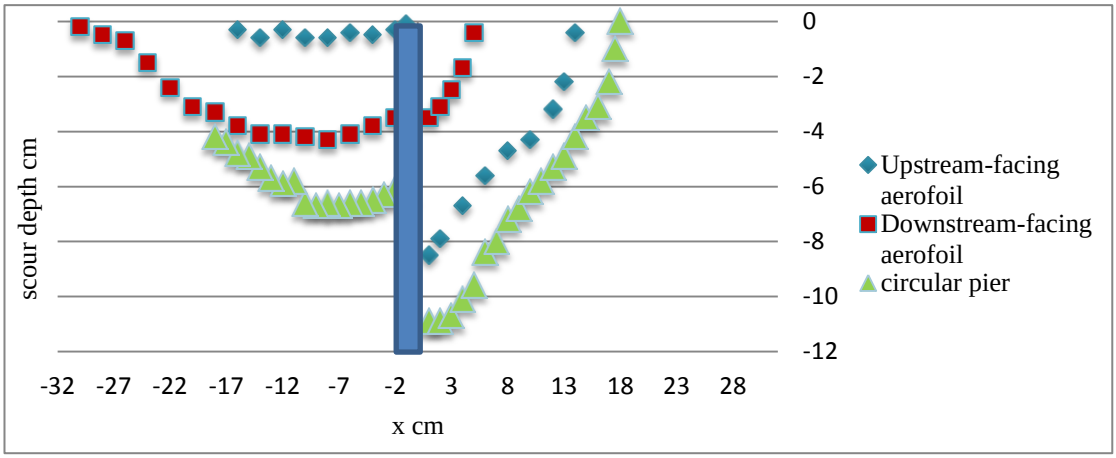

Figure 4.34 Longitudinal scours holes of series A1, G1 and G2

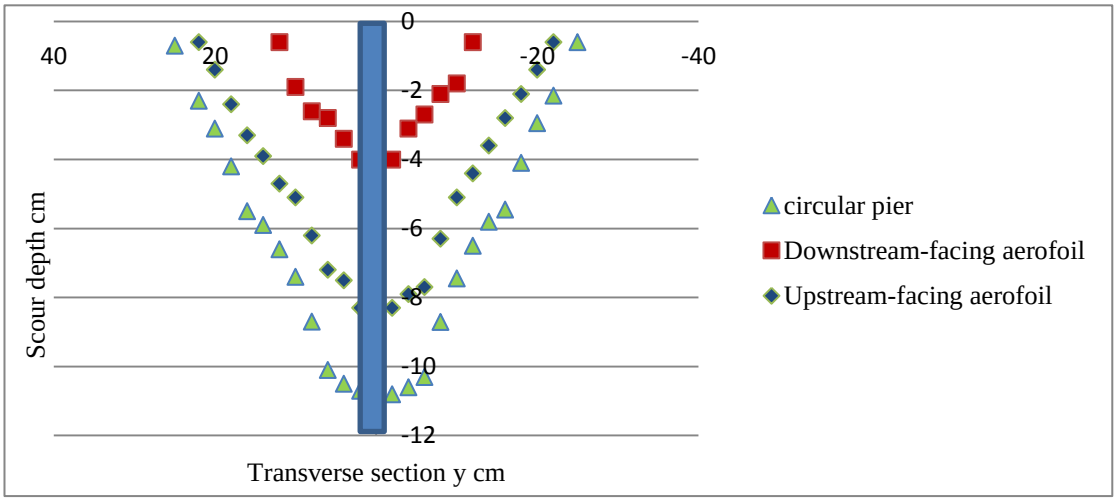

Figure 4.35 Transverse scour holes of series A1, G1 and G2

4.8.3 Scour Pattern around the piers for series A1, G1 and G2

Figure 4.36 shows the scour pattern around the circular, upstream–facing aerofoil shaped (US-FASP) and downstream-facing aerofoil shaped (DS-FASP) piers. At the upstream face of circular and US-FASP geometry shape of scour hole were quite similar due to the identical shape on the upstream side of the pier. The DS-FASP minimizes the scour depth, producing a little scour in the front, but deep scour at the sides and pier's rear because the effect of the horseshoe vortex was reduced due to the down flow being

deflected away from the base of downstream-facing aerofoil shaped bridge pier and it shedding sides and goes downstream.

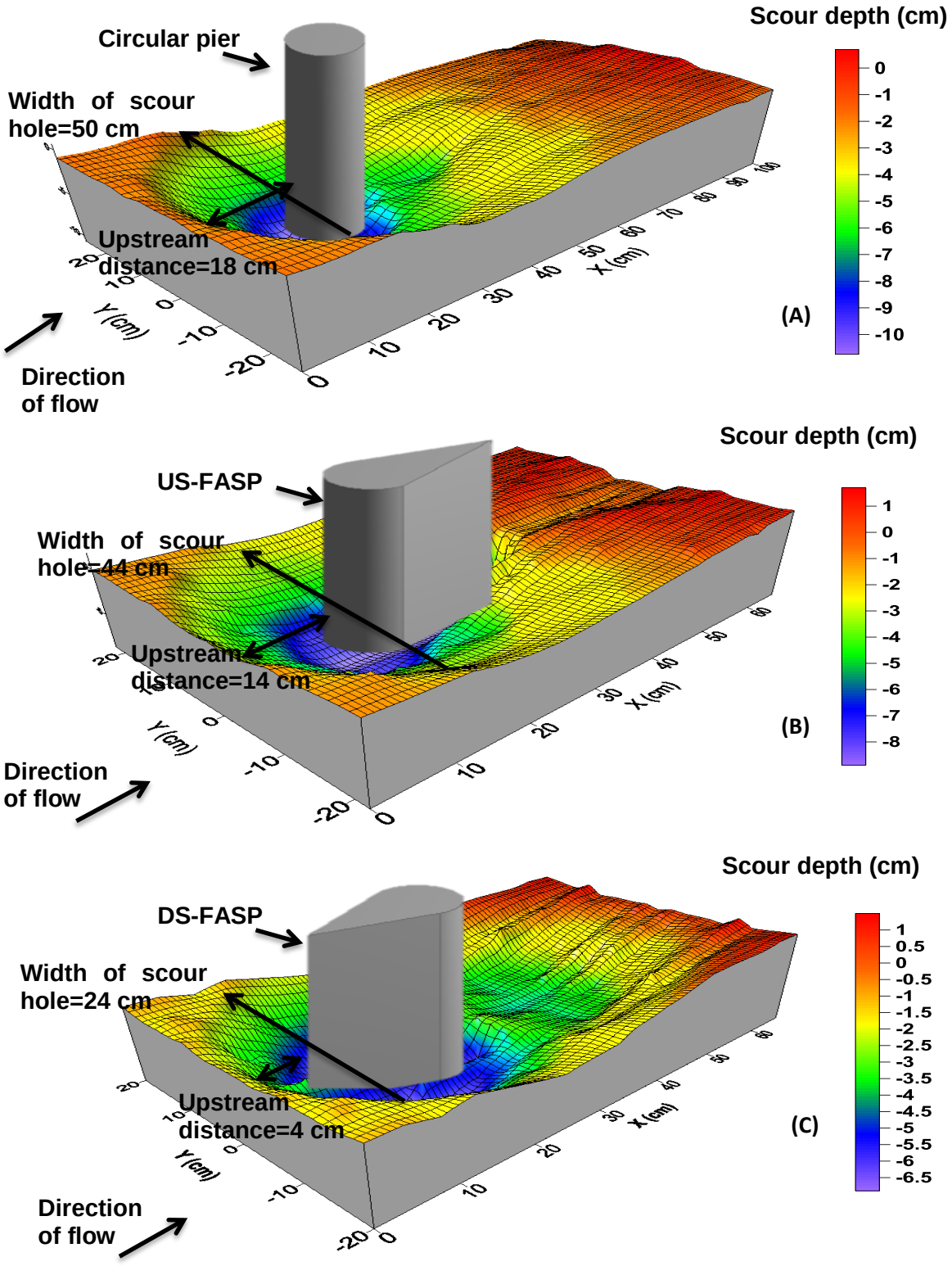

Figure 4.36 Scour pattern around A) Circular pier B) Upstream-facing aerofoil C) Downstream-facing aero foil

4.8.4 Flow velocity vector around piers for series A1, G1 and G2

Figure 4.37 shows flow velocity vector around piers for series A1, G1 and G2, a strong horseshoe vortex was detected in the upstream reach of circular and upstream-facing aerofoil shaped piers positioned at the base of piers, but the effect of horseshoe vortex reduced (not so visible) due to the down flow being deflected away from the base of downstream-facing aerofoil pier. It is seen from Figure 4.37 that, a strong wake vortex was visible and leading into scour hole in the downstream reach of circular and downstream-facing aerofoil piers.

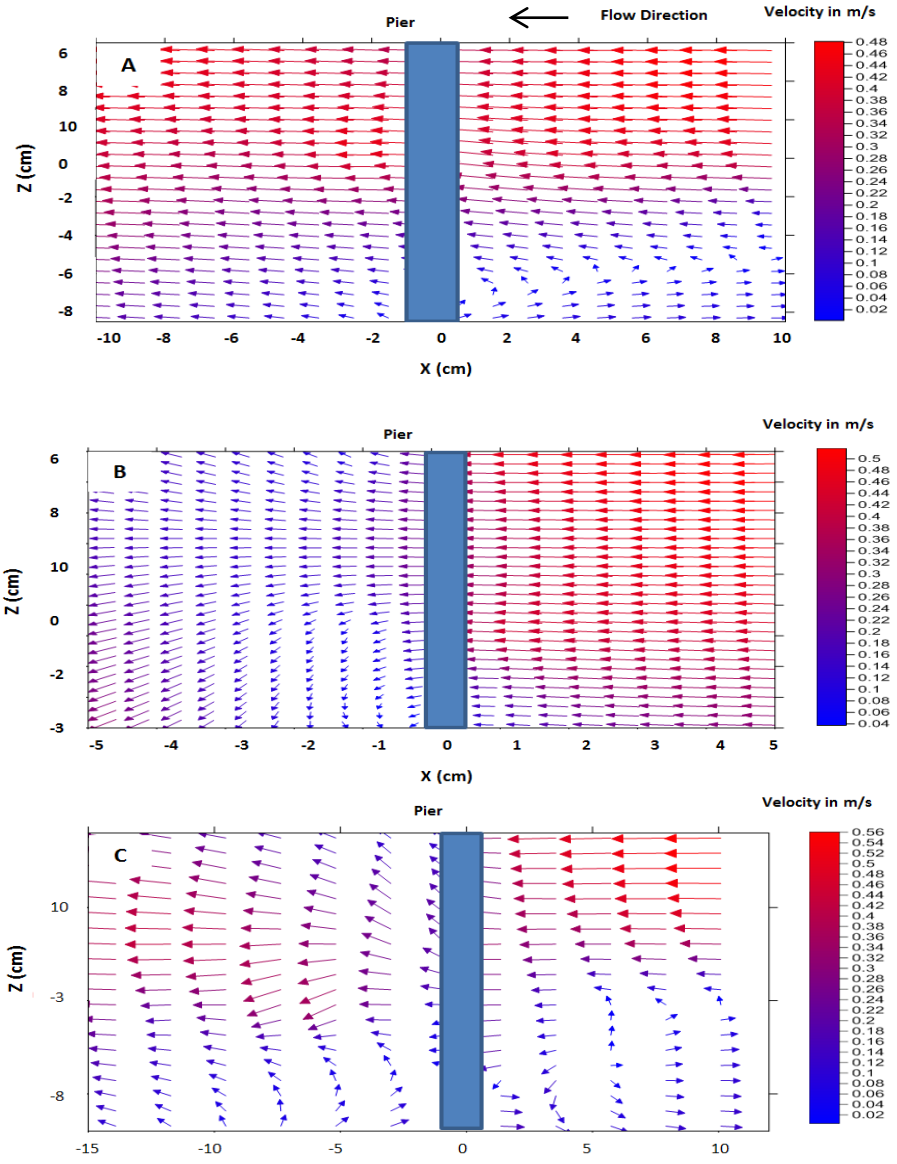

Figure 4.37 Time average velocity vectors of A) Upstream-facing aerofoil B) Downstream-facing aero foil C) Circular pier

4.9 Flow Field Measurements around pier for Series 1-7

The three-dimensional flow field in scour hole for duration 3 hours is experimentally investigated. An Acoustic-Doppler Velocimeter (ADV) was used to measure instantaneously the three components of the velocities in the vertical symmetry plane of the flow before and after the bridge piers. The measured velocity vector (u, w) distributions in the upstream and downstream planes are shown in Figures 4.38, 4.39 and 4.40.

In the Series (1,2 and 3), flow approaching the bridge piers (circular, RNP and US-FRNP) the longitudinal velocity component decreases to 0 m/s at the upstream of the bridge piers. The longitudinal velocity component u beginning to show negative values, meaning that flow reversal occur in the scour hole due to the separation of flow as shown in Figure 4.38 (A,B,C,D and G), producing a downward flow and subsequently vortex formed at the foot of the pier named horseshoe vortex. The same trend is observed in Figures (4.39 and 4.40).

The region close to the bridge pier, the vertical velocity component w grows considerably and reaches negative (downward) values -0.256 m/s upstream run A3, notably in the scour hole, $z \leq 0$ and approach the US-FRNP strong downward flow grows immediately upstream of the piers.

While the transversal velocity component v remains practically negligible, but shows close the bridge piers small values as in run A3 ranges from -0.04 m/s to 0.01 m/s. Downstream of the bridge piers, close and behind the piers the *u*-components are small and show clearly flow reversal towards the water surface and the bed indicating the formation of wake vortex as in Figures (4.38-4.40).

The Series (4, 5 and 6) after changing the orientation of bridge pier to flow direction, as the flow approaches the DS-FRNP the longitudinal velocity component u increases and passes the pier as shown in Figure 4.38 (H), that it is mean a little flow or no sign of reversal flow appear producing little downward flow occur at the base of the pier, beside the effect of horseshoe vortex decreased and decreased the potential for scouring the bed locally.

In the wake region of the pier increases the activity of wake vortex more than the US-FRNP does. Because of the separation of flow occurred in small area and then increased at the end of DS-FRNP produces a strong wake vortex as illustrated in Figures (4.38-4.40).

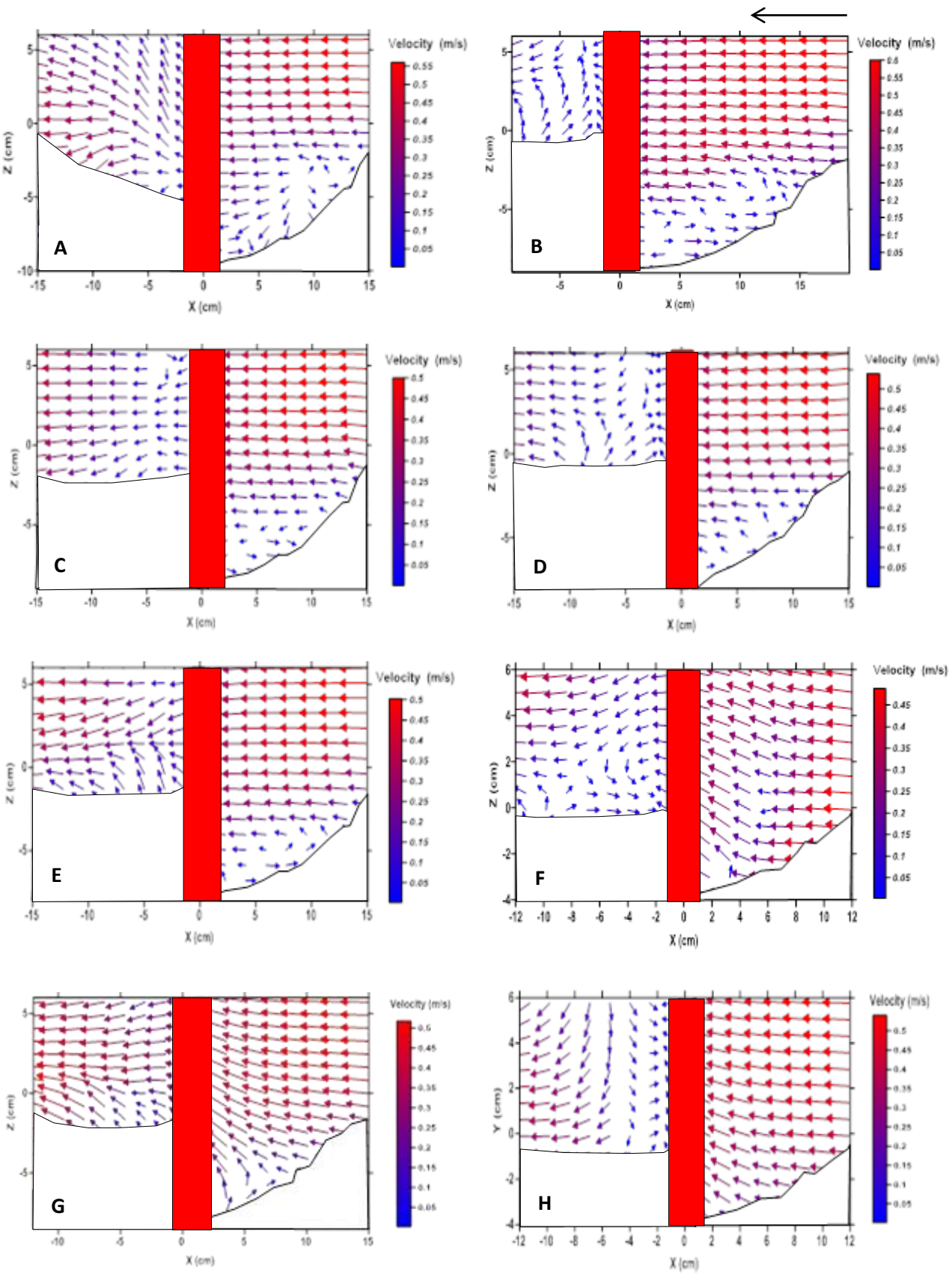

Figure 4.38 Time-averaged velocity vectors along the vertical plane of symmetry of the pier (D, F, H) DS-FRNP 8-10, 6-10 and 4-10 respectively), (A) circular pier (C, E, G) US-FRNP 10-8, 10-6, 10-4 and (B) 10-10 with Q= 58 L /s

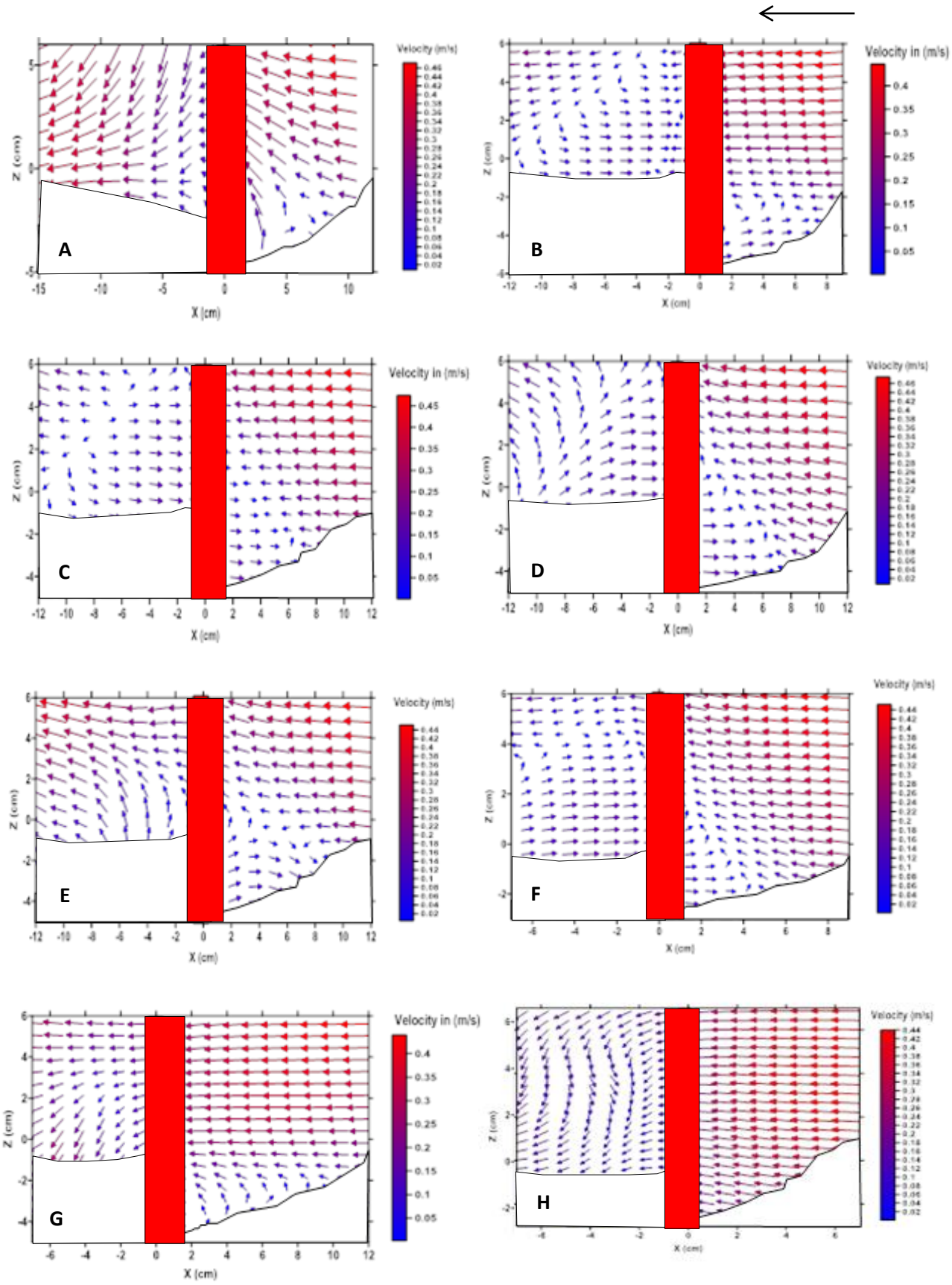

Figure 4.39 Time-averaged velocity vectors along the vertical plane of symmetry of the pier (D, F, H) DS-FRNP 8-10, 6-10 and 4-10 respectively), (A) circular pier (C, E, G) US-FRNP 10-8, 10-6, 10-4 and (B) 10-10 with Q 48 L /s

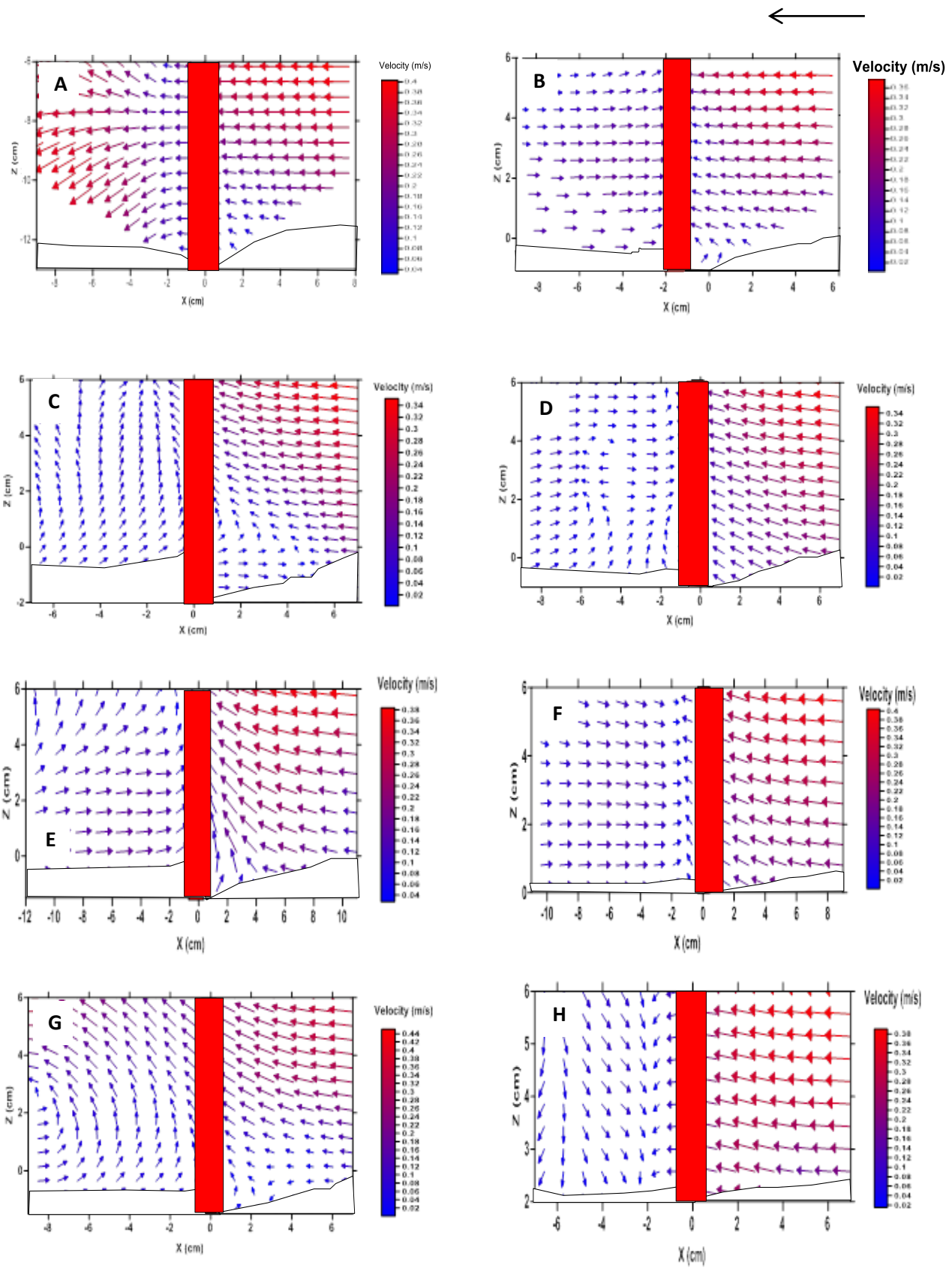

Figure 4.40 Time-averaged velocity vectors along the vertical plane of symmetry of the pier (D, F, H) 0DS-FRNP 8-10, 6-10 and 4-10 respectively), (A) circular pier (C, E, G) US-FRNP 10-8, 10-6, 10-4 and (B) 10-10 with Q= 38 L /s

4.9.1 Flow Field Measurements around Bridge Piers for Series 1 (A3, A4, A5), Series 4 (D1, D2, D3) and Series 7 (G1, G2)

4.9.1.1 Time-averaged longitudinal velocity (u)

The contours (plotted by Surfer 11) of time-averaged longitudinal velocity u for Series 1, 4 and 7 (A3, A4, A5, D1, D2, D3, G1, G2) at upstream planes are shown in Figures (4.41, 4.42) which represent the characteristic of the passage of the flow in the center line of the channel upstream of the piers. At $\theta = 0^0$ the magnitude of longitudinal velocity u passing around piers is higher in runs (D1, D2, D3, and G2) than (A3, A4, A5, G1) near the pier as shown in Figures (4.41, 4.42) respectively. Therefore, for (A3, A4, A5, and G1) the separation of the approaching flow is evident just beneath the edge of the scour hole forming a reversal flow inside the scour hole ($z \leq 0$). The decrease in streamwise velocity was met with an increase in magnitude of the vertical velocity. This can be explained by the fact that when the water hit the pier, it flowed downward as found by (Dey et al 2007).

As the water approach the US-FRNP as in Figure 4.42, the longitudinal velocity decreases with decreasing the distance to the pier. This result in water flow separating and passing around the pier, while the downward flow moved in the opposite direction of approaching flow (reversal flow). The downward flow has a great potential of scouring the bed locally and causing bridge failure.

Change the orientation of bridge pier (DS-FRNP) was minimized the effect of downward flow, as the flow approach the pier most of flow moving around the pier potential of downflow for scouring the bed as in Figure 4.41.

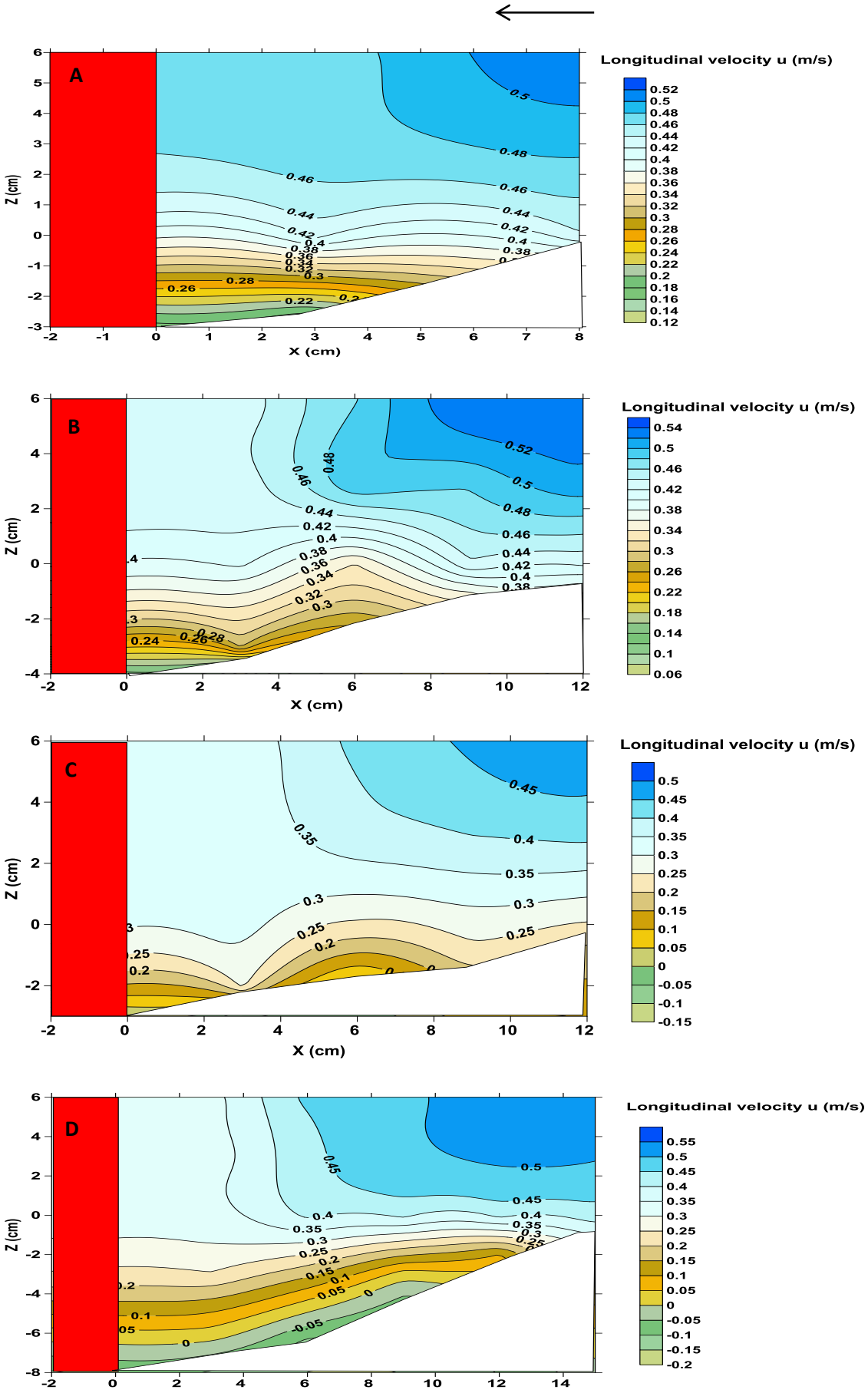

Figure 4.41 Contours of time-averaged longitudinal velocity at upstream plane of the piers A) DS-FAFP B) DS-FRNP 4 -10 ,C) DS-FRNP 6-10 and D) DS-FRNP 8-10

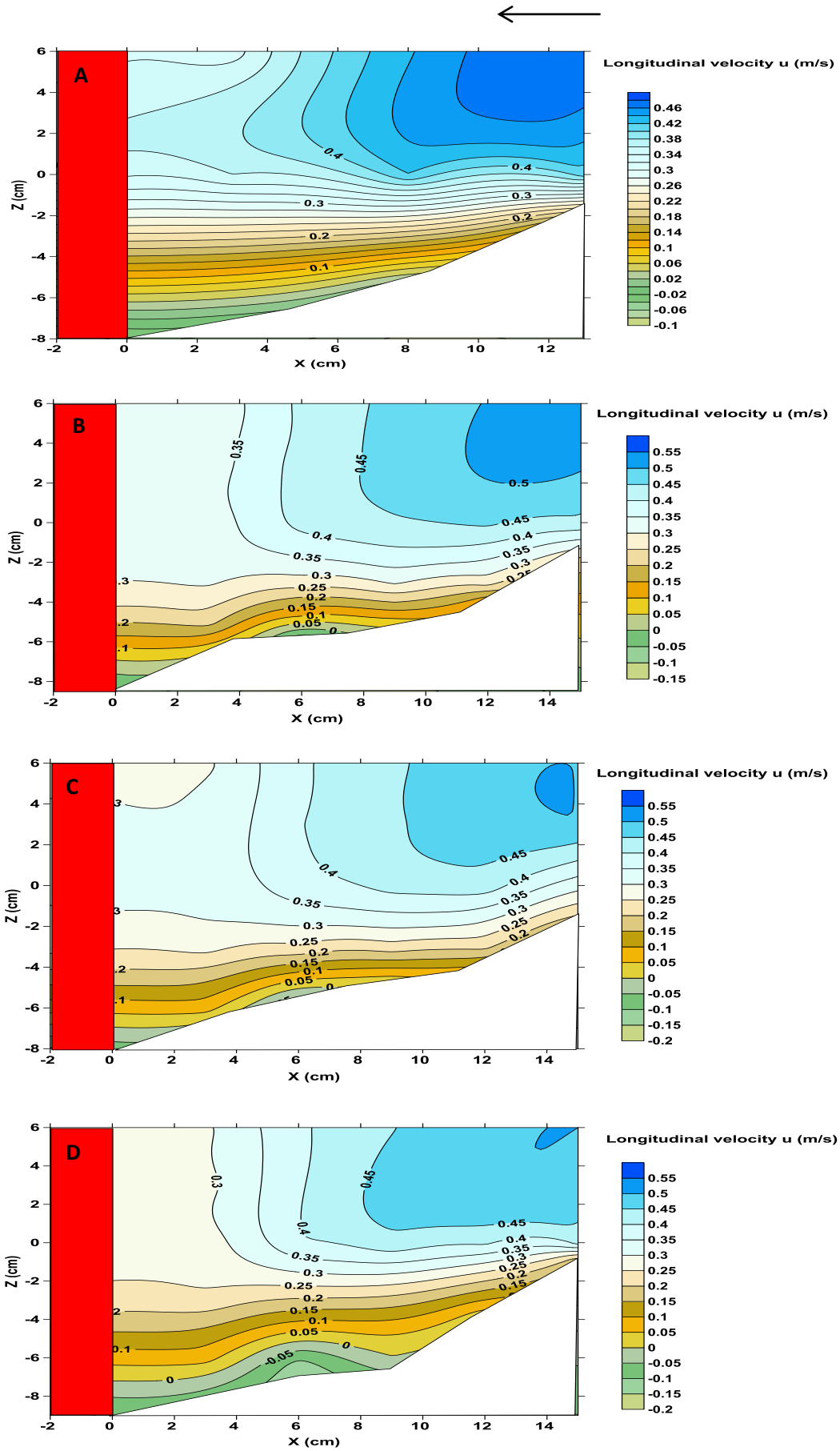

Figure 4.42 Contours of time-averaged longitudinal velocity at upstream plane of the piers A) DS-FAFP B) US-FRNP 10-4 ,C) US-FRNP 10-6 and D) US-FRNP 10-8

4.9.1.2 Time-averaged transvers velocity (v)

The contours of time -averaged transvers velocity (v) are shown in Figures (4.43 and 4.44) at the plane upstream the bridge piers for DS-FRNP (D1, D2, D3, and G2) and US-FRNP (A3, A4, A5, and G1). The small value of (v) remains practically negligible, but the small value were showed in scour hole and close the bridge piers, small values of $v \approx -0.05$ m/s, indicating that the flow becomes three dimensions Graf and Istiarto (2002).

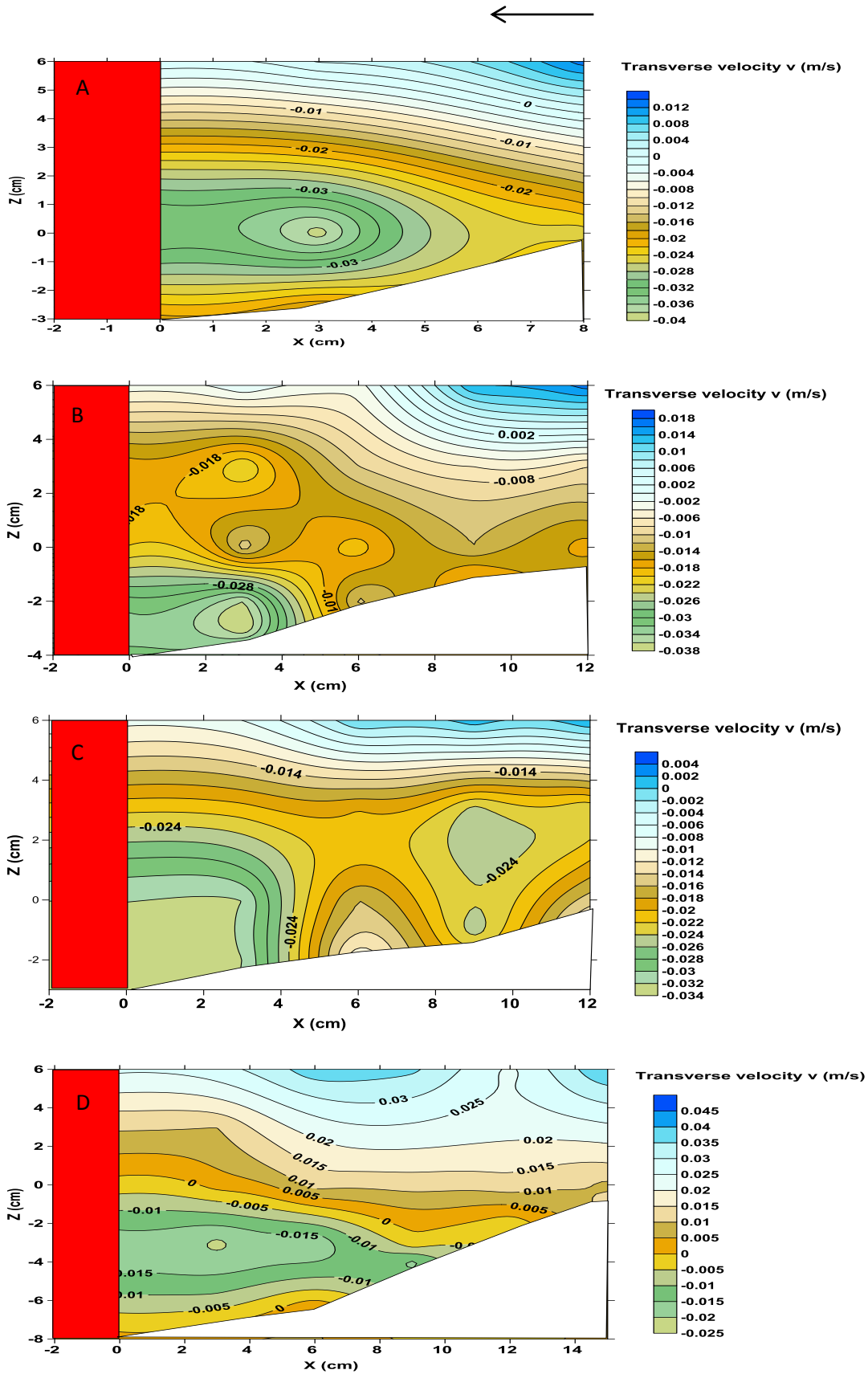

Figure 4.43 Contours of time-averaged transvers velocity at upstreamplane of the piers A) DS-FAFP B) DS-FRNP 4-10,C) DS-FRNP 6-10 and D) DS-FRNP 8-10

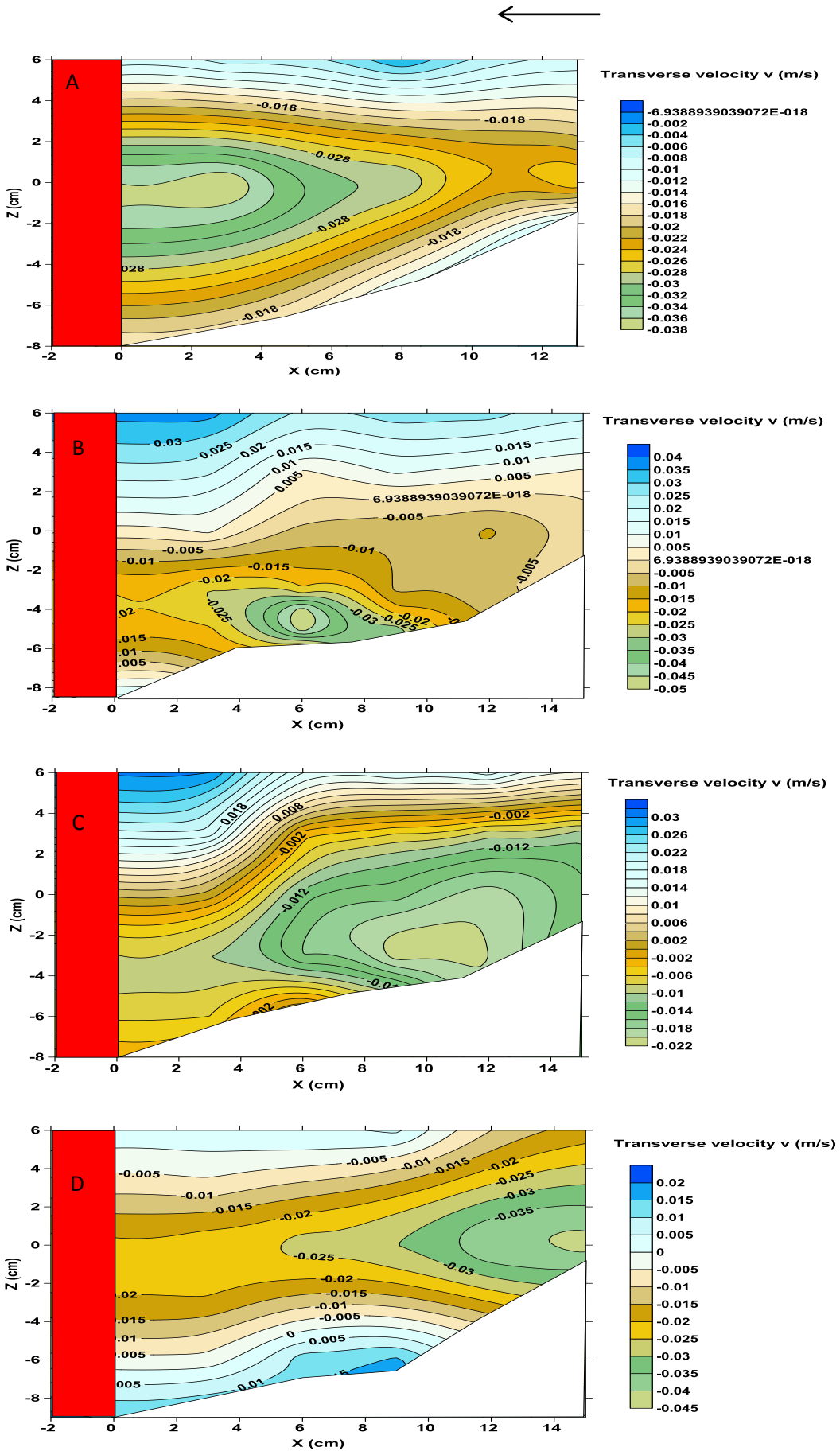

Figure 4.44 Contours of time-averaged transvers velocity at upstreamplane of the piers A) US-FAFP B) US-FRNP 10-4,C) US-FRNP10-6 and D) US-FRNP 10-8

4.9.1.3 Time-averaged vertical velocity (w)

Figures (4.45 and 4.46) represent the contours of the time-averaged vertical velocity w at the upstream plane for scour hole at bridge piers (D1, D2, D3, and G2) and (A3, A4, A5 and G1). The magnitude of w increases in the downward direction from the free surface indicating that there exists a downward negative pressure gradient (Dey et al. 2007). The core of maximum w that occurs near the piers. For upstream of the pier, reversed velocity occurs near the base. Thus, it verifies that a strong horseshoe vortex exists upstream of the pier inside the scour hole.

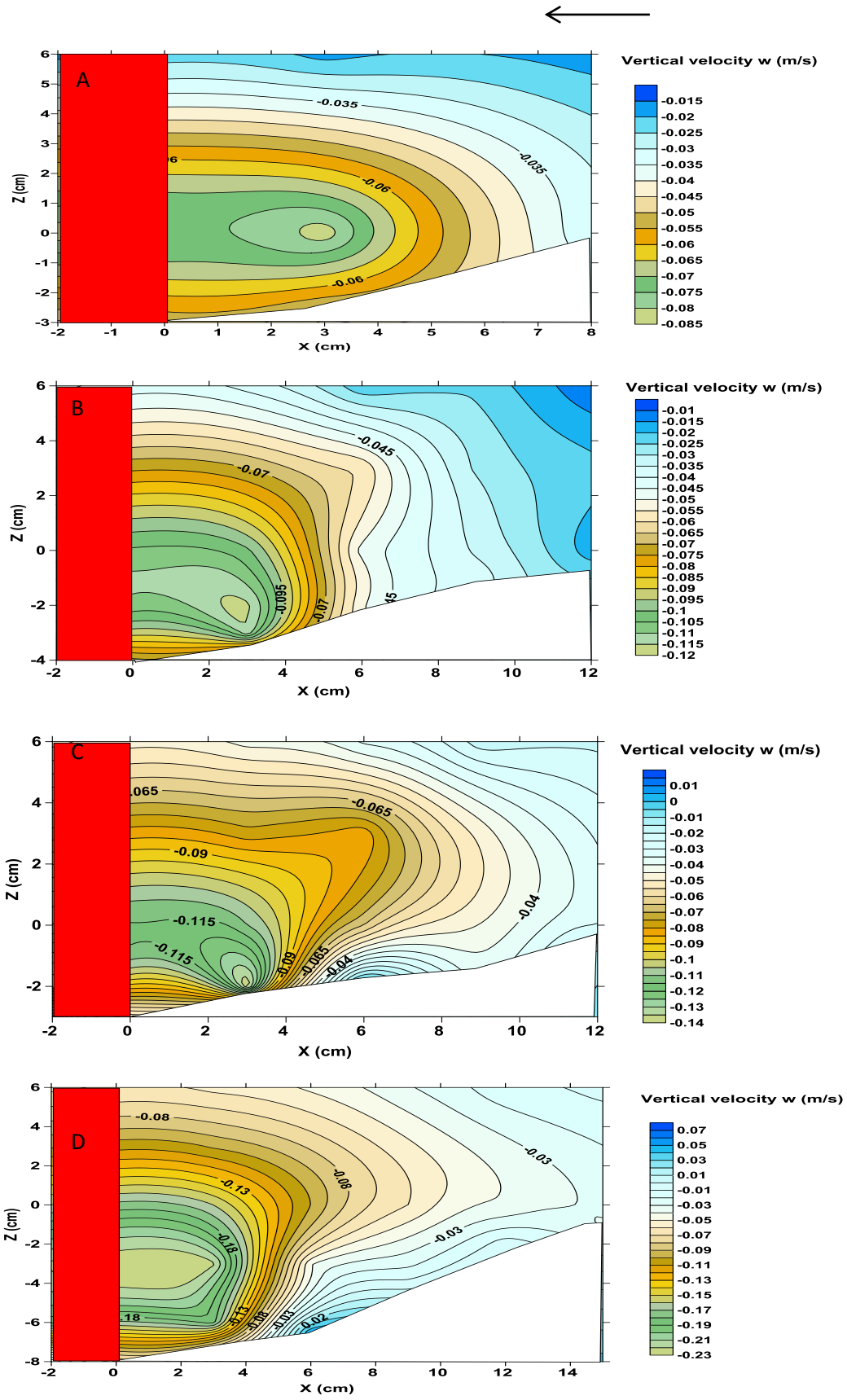

Figure 4.45 Contours of time-averaged vertical velocity at upstreamplane of the piers A) DS-FAFP B) DS-FRNP 4-10 ,C) DS-FRNP 6- 10 and D) DS-FRNP 8 -10

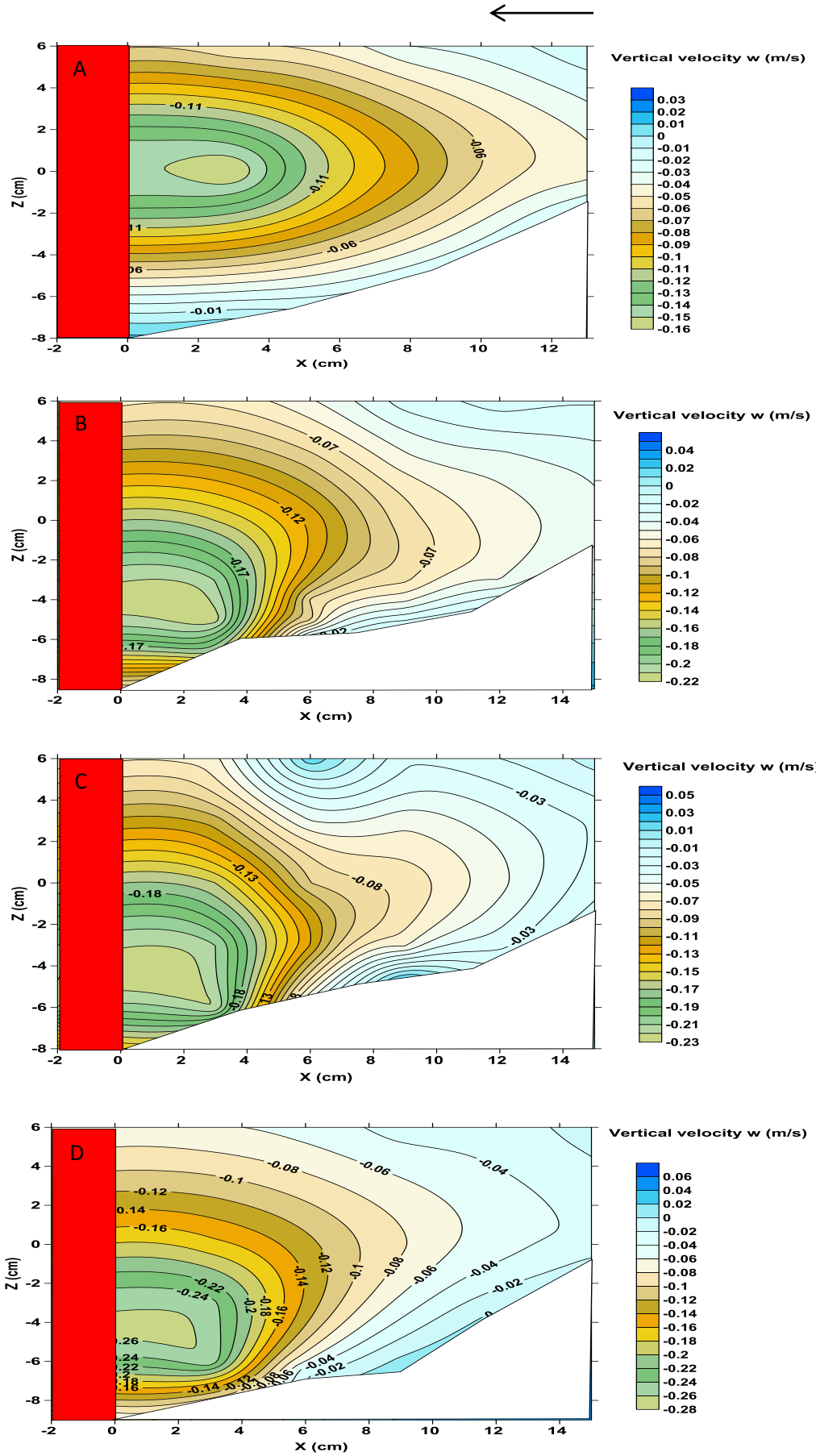

Figure 4.46 Contours of time-averaged vertical velocity at upstreamplane of the piers A) US-FAFP B) US-FRNP 10-4 ,C) US-FRNP 10-6 and D) US-FRNP 10-8

4.9.2 Turbulent Field

4.9.2.1Turbulent intensities for runs A3, A4 and A5

The pattern of turbulent intensities $\overline{u'u'}$, $\overline{v'v'}$ and $\overline{w'\,w'}$ in (m/s) at the upstream plane for scoured bed for runs A3, A4 and A5 (US-FRNP) are shown in Figures (4.47, 4.48 and 4.49). The longitudinal and transverse intensities were larger than the vertical one. The turbulence intensities are in fact the root-mean-square values of the velocity fluctuations. At the pier front the magnitudes $\overline{u'u'}$, $\overline{v'v'}$ and $\overline{w'\,w'}$ increased toward the scoured bed, besides the turbulence intensities increased with decreasing distance to the pier (x=3 cm) due to the downflow and flow separation. Figures (4.47, 4.48 and 4.49) reveal that the distributions of, $\overline{u'u'}$, $\overline{v'v'}$ and $\overline{w'\,w'}$ are almost similar. In general, there is a core of high turbulence intensity on the scoured bed as a result of flow separation.

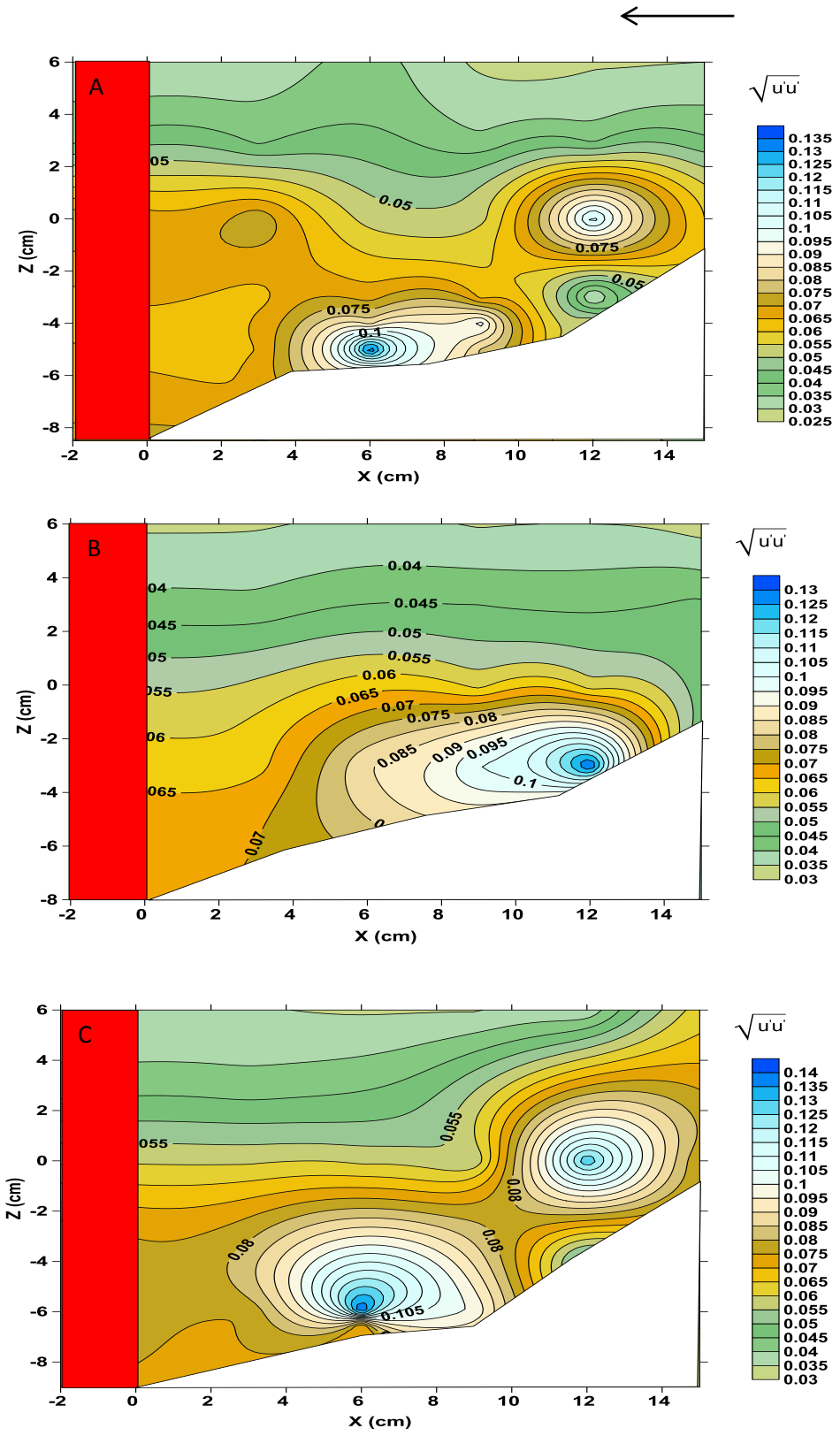

Figure 4.47 Contour of longitudinal intensity $\overline{}$ in (m/s) at upstream plane A) US-FRNP 10-4 cm, B) US-FRNP 10-6 cm and C) US-FRNP 10-8 cm

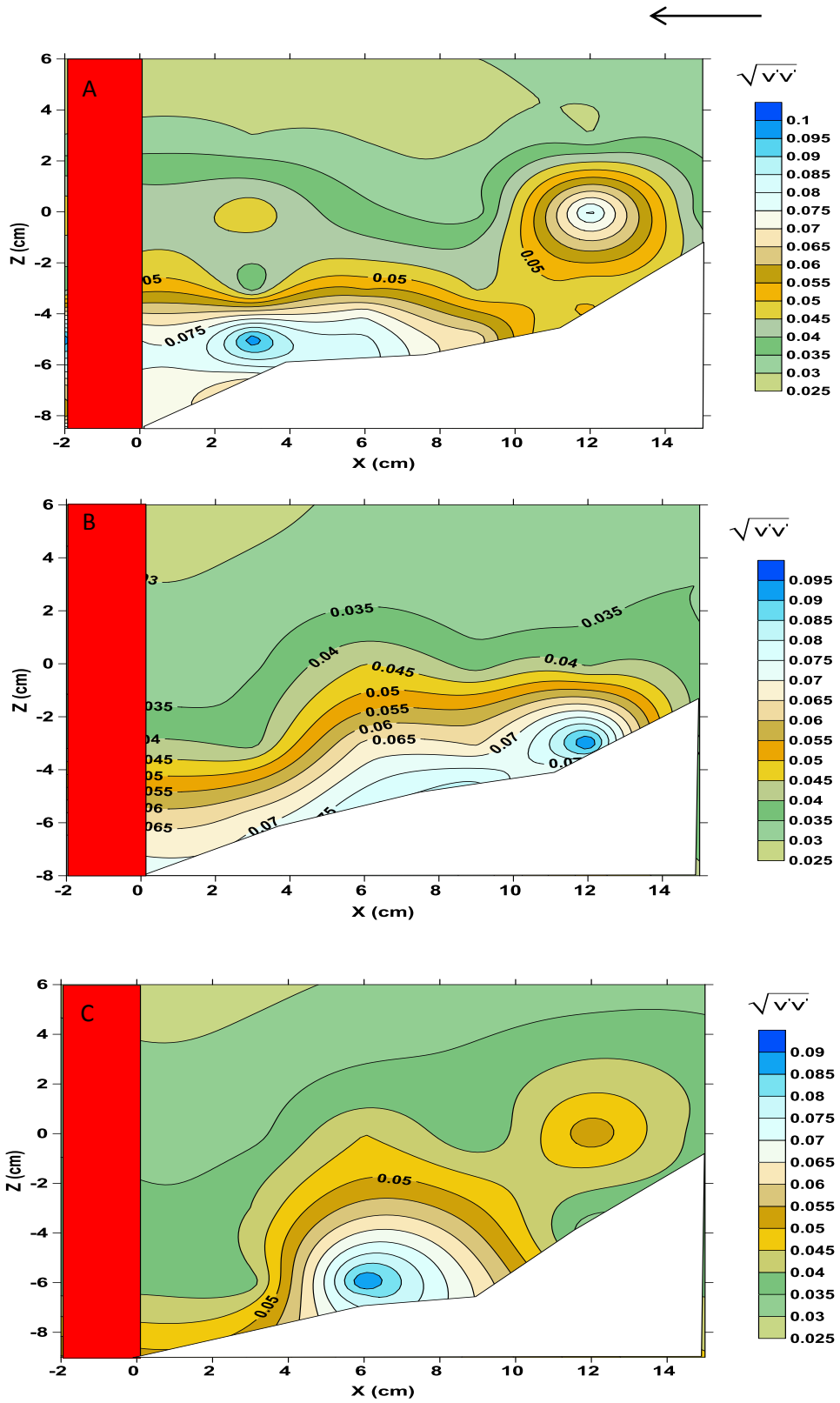

Figure 4.48 Contour of transverse intensity $\overline{v'v'}$ in (m/s) at upstream plane A) US-FRNP 10-4 cm, B) US-FRNP 10-6 cm and C) US-FRNP 10-8

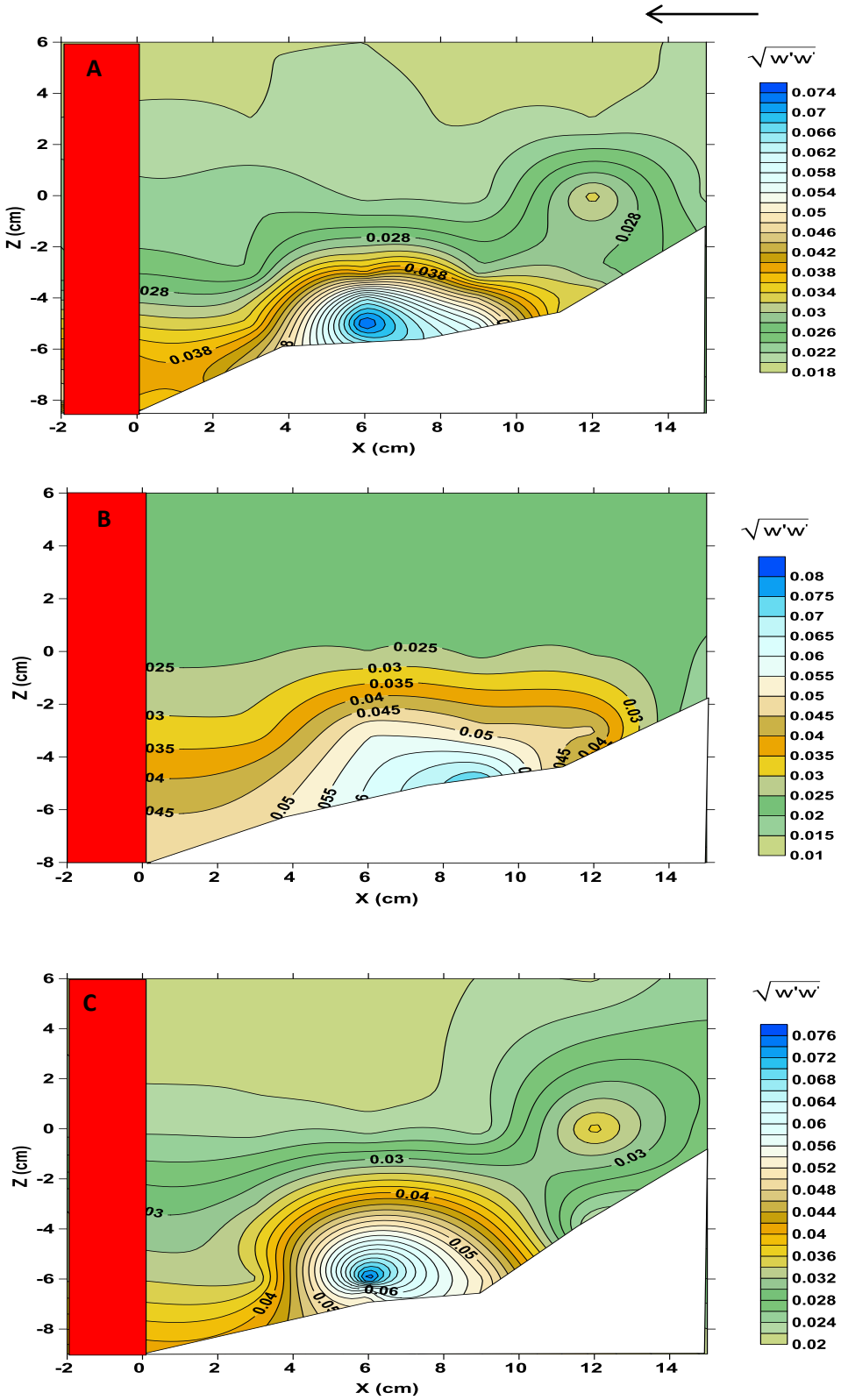

Figure 4.49 Contour of vertical intensity $\overline{}$ in (m/s) at upstream plane A) US-FRNP 10-4 cm, B) US-FRNP 10-6 cm and C) US-FRNP 10-8 cm

4.9.2.2 Turbulent intensities for runs D1, D2 and D3

The pattern of turbulent intensities $\overline{u'u'}$, $\overline{v'v'}$ and $\overline{w'\,w'}$ in (m/s) at the upstream plane for scoured bed for runs D1, D2 and D3 DS-FRNP are shown in Figures(4.50, 4.51 and 4.52).As it observed in US-FRNP the longitudinal and transverse intensities were larger than the vertical one. At the pier front, the magnitudes $\overline{u'u'}$, $\overline{v'v'}$ and $\overline{w'\,w'}$ increased toward the scoured bed, besides the turbulence intensities increased with decreasing distance to the pier (x=3 cm) due to the downflow and flow separation. In general, most of a core of high turbulence intensity at the upstream pier side and on the scoured bed as a result of flow separation.

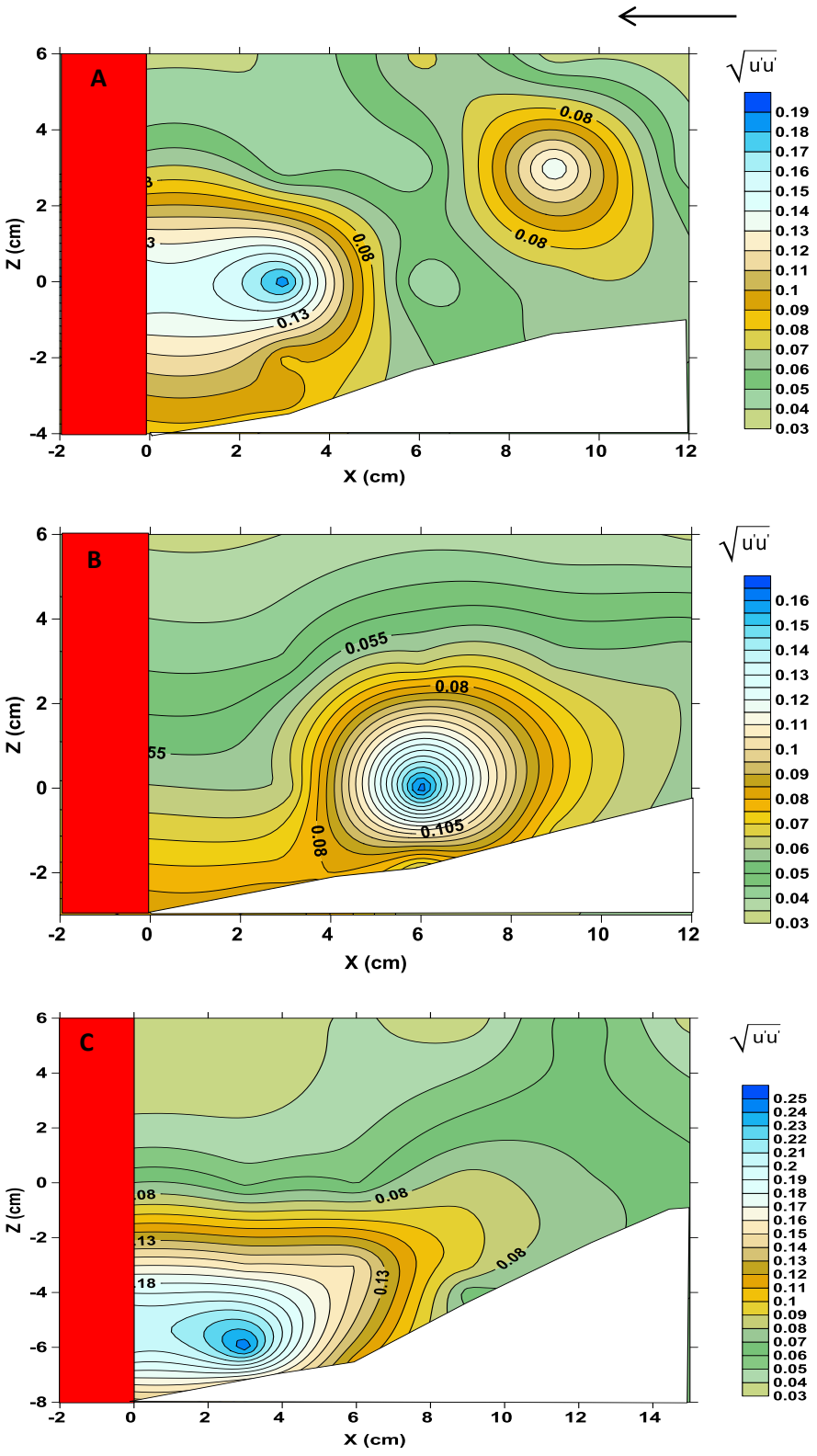

Figure 4.50 Contour of longitudinal intensity $\overline{u'u'}$ in (m/s) at upstream plane A) DS-FRNP 4-10 cm, B) DS-FRNP 6-10 cm and C) DS-FRNP 8-10 cm

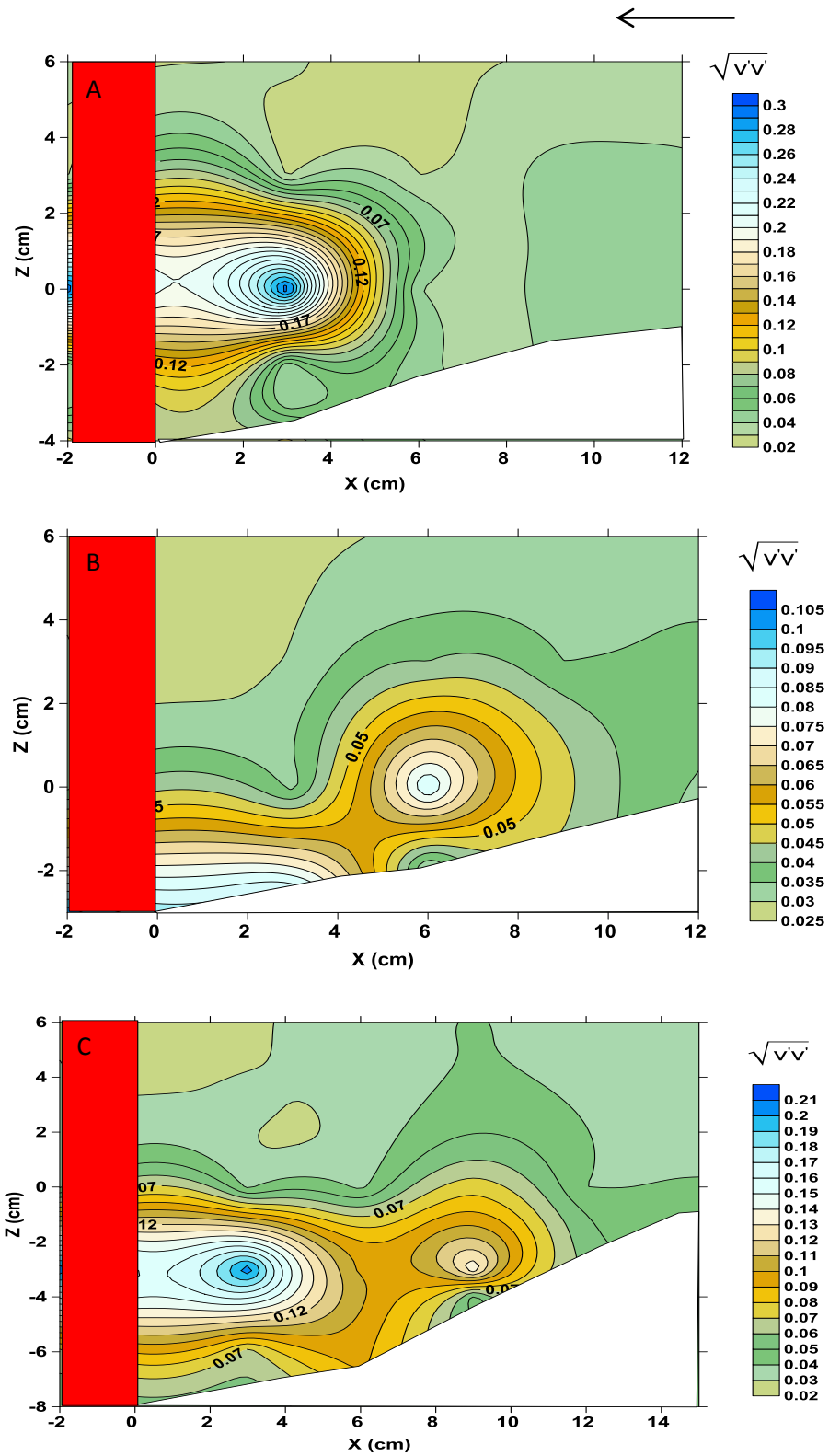

Figure 4.51 Contour of transverse intensity $\overline{v'v'}$ in (m/s) at upstream plane A) DS-FRNP 4-10 cm, B) DS-FRNP 6-10 cm and C) DS-FRNP 8-10 cm

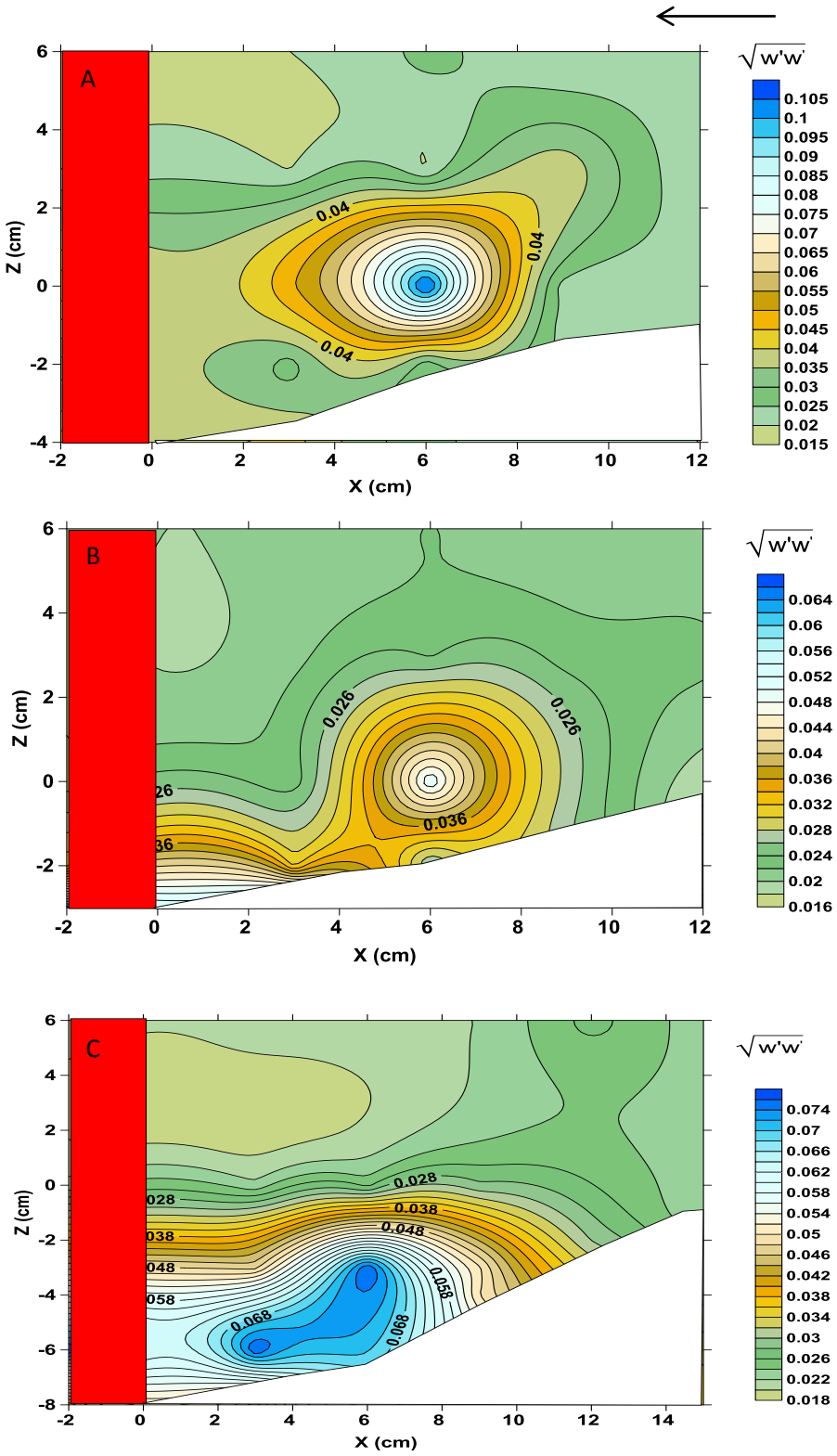

Figure 4.52 Contour of vertical intensity $\overline{w'\,w'}$ in (m/s) at upstream plane A) DS-FRNP 4-10 cm, B) DS-FRNP 6-10 cm and C) DS-FRNP 8-10

4.9.2.3 Turbulent kinetic energy TKE

The TKE is the sum of the mean of the product and square of each of the fluctuating components of the velocity fluctuations Jamieson, (2013). This is mathematically represented by the following equation: $TKE = 0.5\ u'u' + v'v' + w'\,w'$ …….. (4.5)

Where u', v', and w', are respectively the fluctuating components of velocity in the x, y and z.

The distributions of turbulent kinetic energy, whose contours are shown in Figures 4.53 and 4.54, are similar to those of turbulence intensities. From Figure 4.53, it is clear that the area of highest turbulent kinetic energy (TKE) were observed near and under the water surface for DS-FRNP (D1, D2 and D3), while for US-FRNP (A3, A4 and A5) as in Figure 4.54, the highest turbulent kinetic energy were observed above the scoured bed. This may be due to the change of orientation of bridge piers and the effect of the upstream side on the incoming flow.

The results of velocity vectors, turbulent intensities components and turbulent kinetic energy obtained by using ADV are useful for validation of CFD that can be used to simulate scouring around bridge elements to improving their design (Diab et al. 2010).

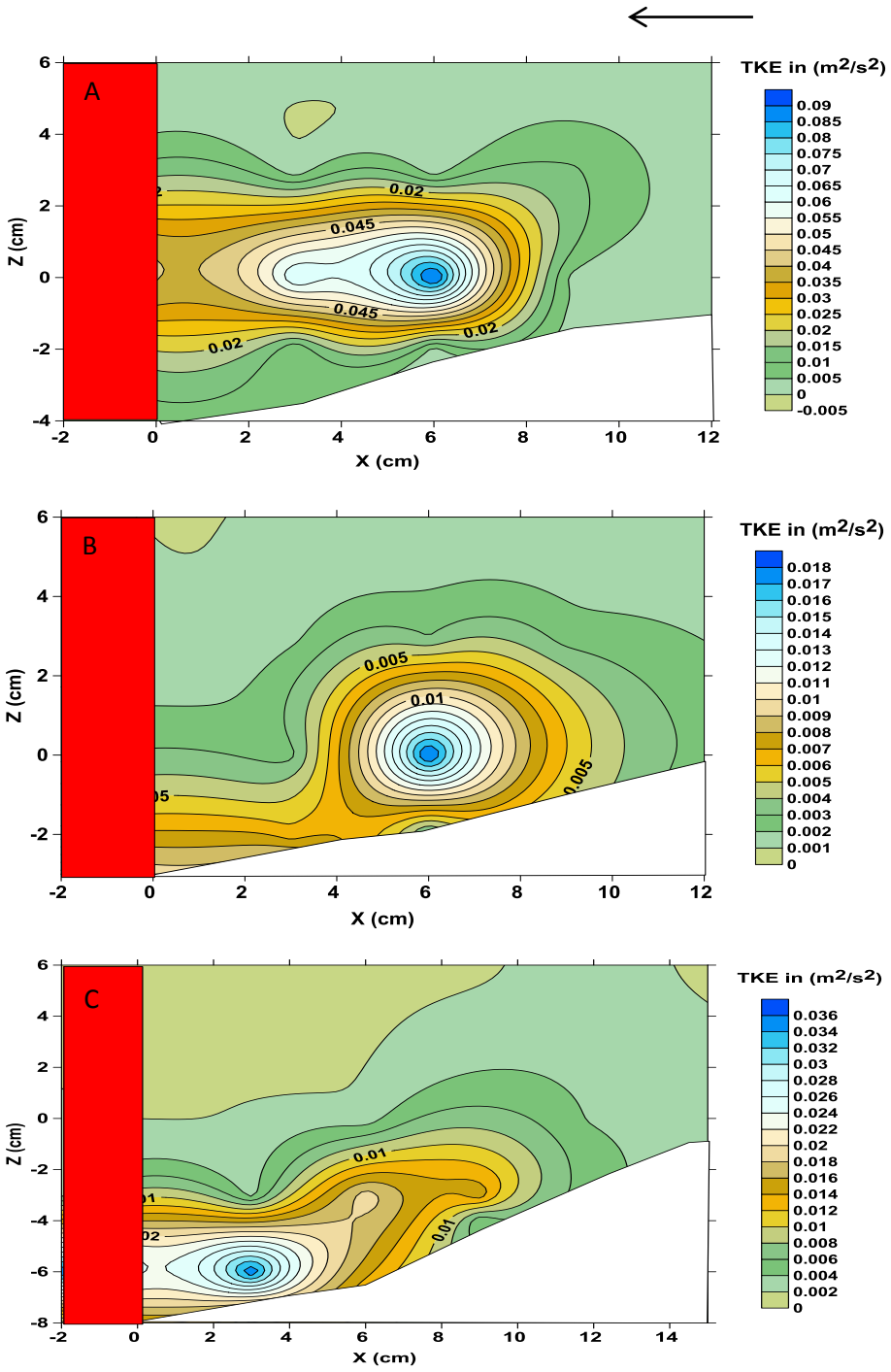

Figure 4.53 Contour of turbulent kinetic energy, TKE in (m^2/s^2) at upstream plan A) DS-FRNP 4-10 cm, B) DS-FRNP 6-10 cm and C) DS-FRNP 8-10

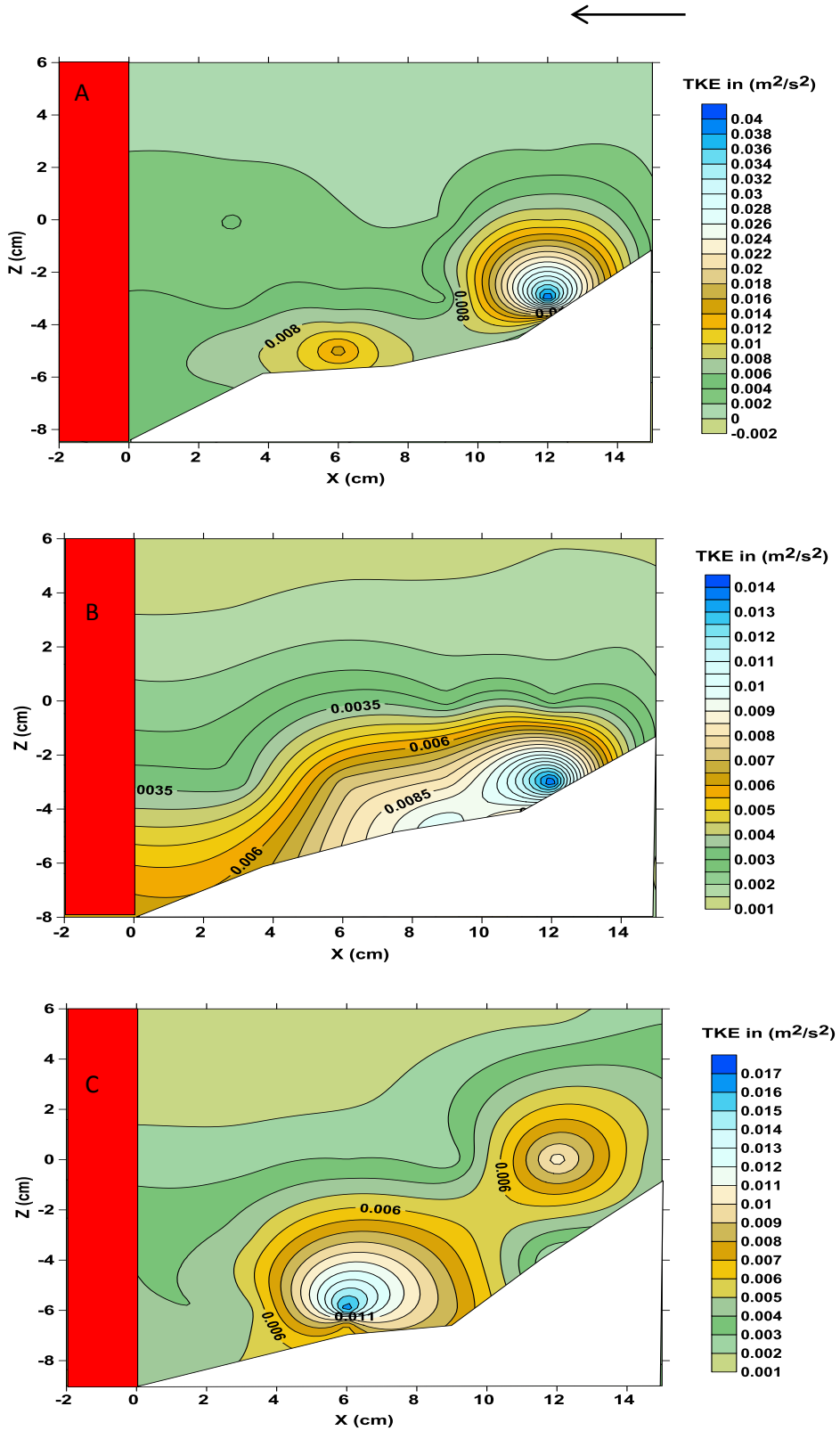

Figure 4.54 Contour of turbulent kinetic energy, TKE in (m^2/s^2 at upstream plane A) US-FRNP 10-4 cm, B) US-FRNP 10-6 cm and C) US-FRNP 10-8 cm

4.9.2.4 Bed Shear Stresses

For non-uniform and unsteady flows in open channels or natural rivers, bed shear stress is important for estimating sediment transport rate. Therefore, many methods to calculate bed shear stresses are available in the literature. Among them, civil engineers (Beheshti and Ataie-Ashtiani 2010) often adopt the Reynolds stresses method in Dey and Barbhuiya (2005). If using the near-bed Reynolds stresses to approximate bed shear stress the mathematical equation is:

$\tau = \rho \sqrt{(u'v' + u'w')2 + (v'w' + u'v')2}$. Figure 4.55 (A and B) shows the shear stress above the scoured bed, 3 cm away from the pier the magnitude of shear is high and then decrease downstream.

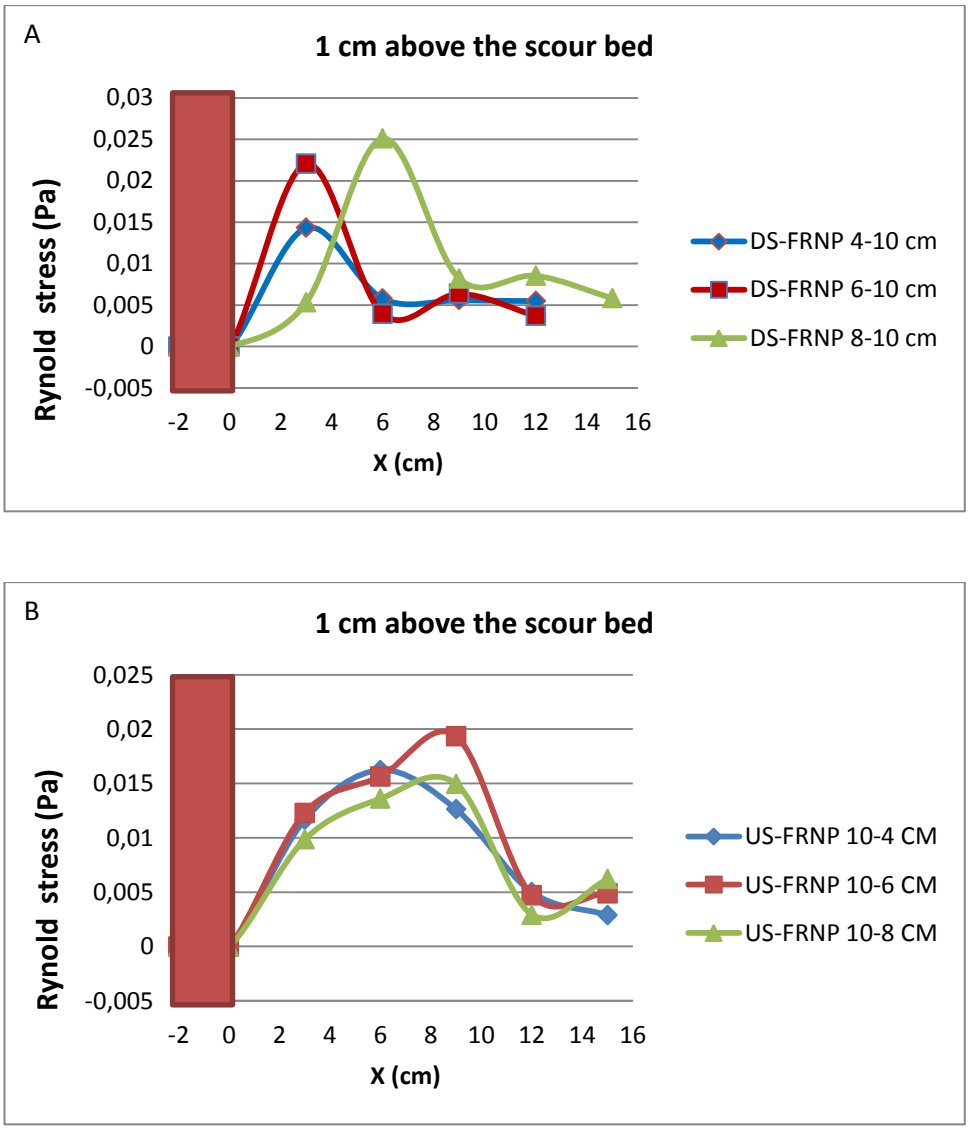

Figure 4.55 shows the bed shear stress above the scour bed of A) DS-FRNP (D1, D2 and D3) and B) US-FRNP (A3, A4 and A5), using Dey method

Another common method of calculating the bed shear stress involves the turbulent kinetic energy (TKE). This method uses the turbulent fluctuations in the three spatial directions u', $v'$and w'. In this case $\tau_b = C_1 \frac{1}{2}\rho(u'u' + v'v' + w'w')$, where C_1 is a proportionality constant equal to 0.19 (Kim, *et al.*, 2000, Pope, *et al.*, 2006). Figure 4.56 (A and B) shows the bed shear stress above the scour bed, 3 cm away from the pier the magnitude of shear is high and then decrease downstream.

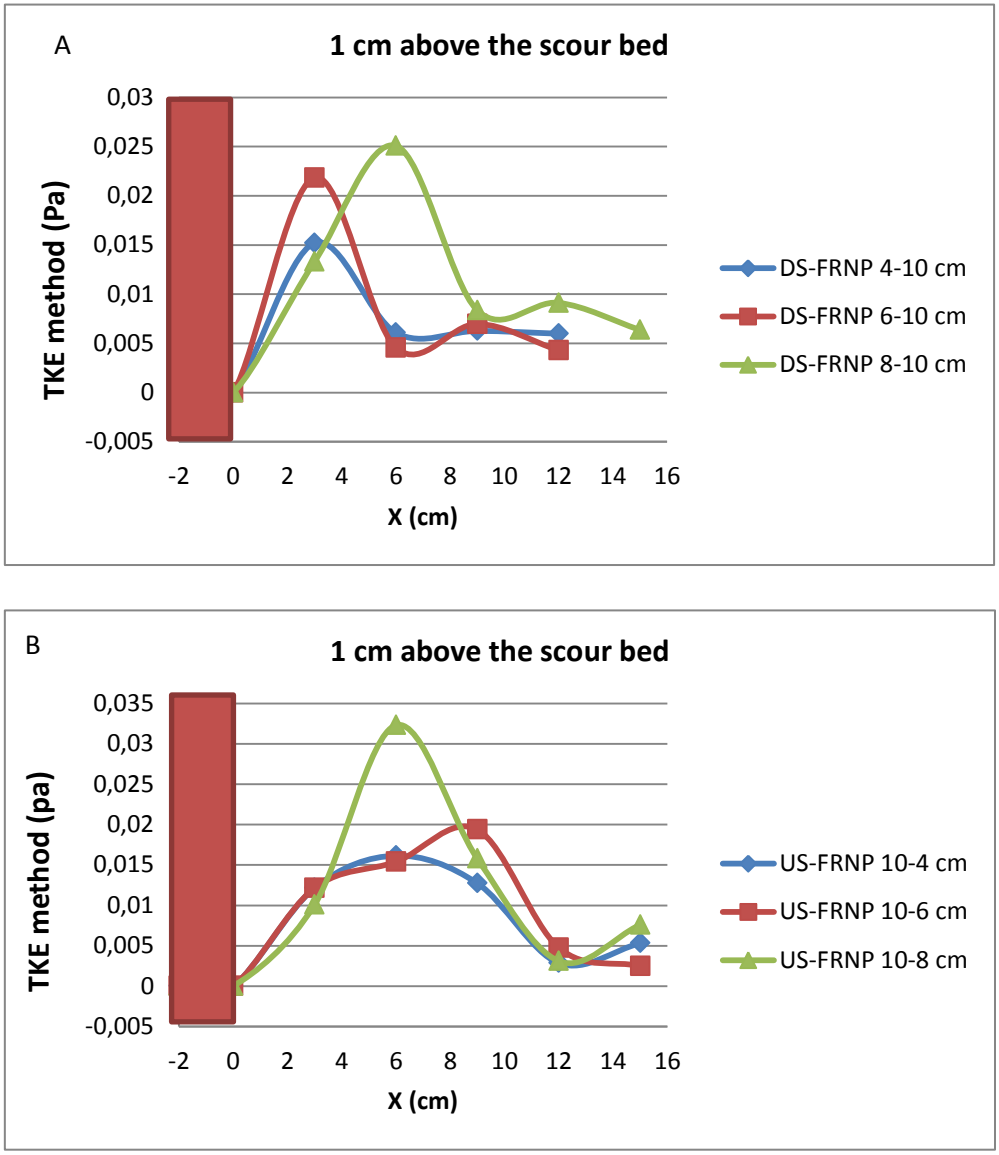

Figure 4.56 shows the bed shear stress above the scour bed of and A) DS-FRNP (D1, D2 and D3) and B) US-FRNP (A3, A4 and A5), using TKE method

From Figures 4.55 and 4.56 two methods (Dey and TKE) were used to calculate the bed shear stress, the two methods yielded same results of shear stress for DS-FRNP. However, the results of shear stress for US-FRNP are the same by using the two methods expect the pier 10-8 cm produces smaller shear stress in Dey method and bigger value by using TKE method. The same results indicate that both methods maybe valid for calculating bed shear stresses since they yielded consistent results.

CHAPTER 5

CONCLUSION AND RECOMMENDATION

5.1 Conclusion

The shape of bridge piers has important effect on the local scour. The research experimentally examined the effect of different shapes of bridge piers to find a reliable efficiency before field application, especially under live-bed scour conditions. The current study also provides a new method to reduce scour depth, the idea of this method is dependent on the change of the orientation of upstream-facing round-nosed pier so that it faces downstream rather than upstream according to the direction of flow (named after here as downstream-facing round nosed pier).

Changing the orientation of bridge pier is not only effective for reducing scour but it is also much more economic when it is compared with countermeasure techniques like riprap and slot. This experimental study was conducted in order to assess the reduction of local scour around (upstream facing round- nosed, downstream facing round-nosed and circular bridge piers). The results of comparison between the performances of bridge piers under different conditions reveal that downstream facing round-nosed bridge pier is an effective countermeasure to reduce the depth of scour. Downstream-facing round-nosed pier reduces scour depth, length of scour hole and scour hole width more than upstream-facing round-nosed, round-nosed and circular bridge piers. The writer hopes that the results of the present study will be benefitted by the designers and engineers. From the research and results, the following conclusions can be obtained:

1. Maximum scour depth was observed to occur at the upstream face of the bridge piers in all experiments for upstream-facing round nosed pier and upstream-facing aero foil shaped pier due to significant effect of downflow which produces horse shoe vortex.
2. The maximum reduction of scour depth for downstream-facing round nosed pier 4-10 cm was 54% when compared to the circular pier and 40% compared with upstream facing round nosed pier 10-4 cm.
3. The downstream-facing round nosed pier 4-10 cm and downstream-facing aerofoil shaped pier had a reduction in the scour hole volume of 83% and 87% respectively when compared to the circular pier.
4. Changing the orientation of bridge pier DS-FRNP caused delay in scouring mechanism and rate of scouring.
5. The performance of aerofoil and upstream-facing round nosed pier improved by locating it as downstream-facing aerofoil and downstream-facing round nosed piers to the flow.
6. The armor layer formed on the channel bed and scour hole around the piers, increases the effective critical bed shear stress, which prevents the further growth of scour hole.
7. Changing the orientation of bridge pier DS-FRNP design can reduce scour depth, thereby reducing the potential need for countermeasures.
8. Increasing the flow intensity and pier size leads to increase in scour depth surface area of scour hole and volume.
9. The effect of horse shoe vortex upstream the downstream-facing round nosed pier was reduced due to the down flow being deflected away from the base of the bridge pier.
10. The effect of the wake vortex at the downstream-facing round nosed pier was found to have a more significant effect for initiating scour than upstream-facing round nosed pier.

11. As the flow approaches the bridge piers, the longitudinal velocity component decreases at the upstream of the bridge piers, the longitudinal velocity component u begins to show negative values, and this indicates that the flow reversal occurs in the scour hole due to the separation of flow, producing a downward flow, and subsequently, a vortex is formed at the foot of the pier named horseshoe vortex.
12. Downstream-facing round nosed bridge pier has a significant effect in reducing downflow and subsequently horseshoe vortex.
13. The distribution of turbulent kinetic energy TKE was similar to that of the turbulent intensity components. The area of highest turbulent kinetic energy (TKE) was observed near and under the water surface for DS-FRNP, while for US-FRNP the highest turbulent kinetic energy was observed above the scoured bed. The effect of turbulence leads to intensive scouring in front of the US-FRNP.
14. The maximum bed shear stress was observed in US-FRNP 10-8 cm and in DS-FRNP 8-10 cm rather than the others.
15. In spite of the considerable effort attained in this experimental work achievement, the complete knowledge of mechanism that rule changing the orientation of bridge pier is still far to be reached.

5.2 Recommendations

1. It would be useful to test the downstream-facing round nosed bridge pier in the field and compare it with the laboratory result.
2. The performance of change the orientation of bridge pier to reduce scour depth under clear- water condition should be tested.
3. More investigation should be done with different pier length and alignment according to flow direction for local scour under clear-water and live-bed condition.

4. Measurement of local scour around two or group of downstream-facing round nosed pier in clear-water and live bed condition.
5. This study could be supplemented with (CFD) analysis to get more results to compare with the obtained scour depths from the experiments.
6. The turbulent flow field study has given a good idea about the mechanism of local scour at US-FRNP and DS-FRNP. Additional measurements of the flow velocities and turbulence around two or group of upstream and downstream-facing round nosed pier should be investigated.

REFERENCES

Abed, L. and Gasser, M. M. (1993). Model study of local scour downstream bridge piers, Proceedings National Conf. on Hydraulic Engineering, San Francisco, 1738–1743.

Afzal M, S. (2013). 3D Numerical Modeling of Sediment Transport under Current and Waves, Thesis presented to the Norwegian University of Science and Technology, in partial fulfillment of the requirements for the degree of Master of Engineering.

Ahmed, F., and Rajaratnam, N. (1998). Flow around bridge piers. *J. Hydraul. Eng.*, **124** (3), 288–300.

Akib S, Jahangirzadeh A, Basser H (2014). Local scour around complex pier groups and combined piles at semi-integral bridge. *J Hydrol Hydromech* **62**, 108–116.

Ali, K.H.M., and Lim, S.Y. (1986). Local Scour Caused by Submerged Wall-Jets, Proceedings of the Institution of Civil Engineers, London, England, **Vol. 81**, No. 2, 607-645.

Ali, K., and Karim, O. (2002). Simulation of flow around piers. *Journal of Hydraulic Research, IAHR*, **40** (2), 161-174.

Ataie-Ashtiani, B. and Aslani-Kordkandi, A. (2012). Flow field side-by-side piers with and without scour hole, *European Journal of Mechanics B/Fluids*, **36**, 152-166.

Baker, C. J. (1980). The Turbulent Horseshoe Vortex, *Journal of Wind Engineering and Industrial Aerodynamics*, **Vol. 6,** No. 1-2, 9-23.

Barbhuiya, A. K. and Dey, S. (2004). Local scour at abutments: a review, Sad Hana, Proc. Indian Acad. Sci., **29**, 449-476.

Beheshti, A. A., and Ataie-Ashtiani, B. (2010). Experimental Study of Three Dimensional Flow Field around a Complex Bridge Pier. *ASCE Journal of Engineering Mechanic*, **Vol. 136**, No. 2, Pages 143-154.

Bozkus, Z., Osman, Y. (2004). Effects of Inclination of Bridge Piers on Scouring Depth, *ASCE Journal of Hydraulic Engineering*, **Vol.130**, No. 8, 827-832.

Breusers, H. N. C. (1965). Scour around drilling platforms. International Association of Hydraulic Research.

Breusers, H. N. C. and Raudkivi, A. J. (1991). Scouring. IAHR hydraulic structures design manual, Rotterdam, The Netherlands, 2.

Breusers, H. N. C., Nicollet, G. and Shen, H. W. (1977). Local scour around cylindrical piers, *Journal of Hydraulic Research*, **15** (3), 211-252.

Bonasoundas, M. (1973). Non-Stationary Hydro- morphological Phenomena and Modeling of Scour, Processes. Congress of the International Association of Hydraulic Research, **2**, 9-16. Sao Paulo, Brazil.

Chabert, J. A. (1956). Etude des affonillements author des, Laboratoire National Hydraulique, Chatou, France.

Chen, S.C., Chan H.C., Wu, T.Y. (2012). Experimental investigation of the Flow Field around a Bridge Pier with Hooked collar. ICSE6 Paris, August, 27–31.

Chiew, Y. M. (1984). Local scour at bridge piers, *Rep*. No**. 355**, University of Auckland, School of Eng., Auckland, New Zealand.

Chiew, Y.M. (1992). Scour Protection at Bridge Piers, *J. Hydraulic. Eng*, *ASCE*, 118 (9), 1260-1269.

Eckerle, W. A., and Awad, J. K. (1991). Effect of Free stream Velocity on the Three-Dimensional Separated Flow Region in Front of a Cylinder, *ASME Journal of Fluids Engineering*, **Vol. 113**, 37-44.

Dargahi, B. (1987). Flow field and local scouring around a cylinder. Bulletin Nr. TRITAVBI- **137**, The Royal Institute of Technology, Stockholm, Sweden.

Dargahi, B. (1990). Controlling Mechanism of Local Scouring, *Journal of Hydraulic. Engineering, ASCE,* **Vol. 116**, No.10, 1197-1214.

Das, S., Ghosh, S. and Mazumdar, A. (2012). Flow field past a Triangular Pier due to Sediment Transportation at Clear Water Equilibrium Scour Hole. Int. *J. Emerg. Trends Eng. Dev.*, **7(2)**, 380-388.

Das, S., Das, R., Mazumdar, A. (2013). Comparison of Characteristics of Horseshoe Vortex at Circular and Square Piers. *Research Journal of Applied Sciences, Engineering and Technology* **5**(17), 4373-4387.

Dey, S. (1995). Three-dimensional vortex flow field around a circular cylinder in quasi-equilibrium scour Hole, Acad. Sci., 20 December, 871–885.

Dey, S., Bose, S. K., and Sastry, G. L. N. (1995). Clear Water Scour at Circular Piers, *Journal of Hydraulic Engineering, ASCE*, **121**(12), pp. 869-876.

Dey, S., and Raikar, R. (2007). Characteristics of Horseshoe Vortex in Developing Scour Holes at Piers, *Journal of Hydraulic Engineering*, 399-413.

Dr Les Hamill , (1999). Bridge Hydraulic Theory and Practice, first published, by E and *FN* spon, pp. 347-348.

Ettema, R. (1980). Scour at Bridge Piers. University of Auckland, School of Engineering, Auckland, New Zealand, Rep. No. **216**.

Ettema, R., Mostafa, E., Melville, B., and Yassin, A. (1998). Local scour at skewed piers, *Journal of Hydraulic Engineering, ASCE*, **124** (7), 756-459.

Federal Highway Administration. (2001). Evaluating Scour at Bridge – Fourth Edition, Report No. FHWA-01-001, U.S. Department of Transportation, Washington, D.C.

Franzetti, S., Larcan, E., and Mignosa, P. (1981). Erosione localizzata alla base delle pile dei ponti: considerazioni su risultati di un'indagine sperimentale su modello, Local scour at cylindercal piers, considerations on a laboratori model results). Memorie e Studi dell'Istituto di Idraulica e Costruzioni idrauliche del Politecnico di Milano, **296** (in Italian).

Franzetti, S., Larcan, E., and Mignosa, P. (1982). Influence of tests duration on the evaluation of ultimate scour around circular piers, International Conference on the

Hydraulic Modelling of Civil Engineering Structures, organized by *BHRA Fluid*

Engineering, University of Warwick, Coventry, England, 22-24.

Grimaldi, C., Gaudio, R., Calomino, F.; Cardoso, A.H. (2009). Control of scour at bridge piers by a downstream bed sill. *J. Hydraulic. Eng.* **135** (1), 13–21.

Ghiassi, R. and Abbasnia, A. (2013). Investigation of Vorticity Effects on Local Scouring, *The Arabian Journal for Science and Engineering, AJSE*, **38**, 537-548.

Graf, W.H, and Istiarto, I, (2001). Flow Pattern in the Scour Hole around a Cylinder. *Journal of Hydraulic Research*, **Vol. 40**, No. 1, pp. 13-20.

Graf, W.H., and Istiarto, I. (2002). Flow pattern in a scour hole around a cylinder. *Journal of Hydraulic Research, IAHR*, **40** (1), 13-20.

Greco, J. J. (1990). The flow structure in the vicinity of a cylinder-flat plate juncture: flow regimes, periodicity and vortex interactions. M.S. Thesis, Department of Mechanical Engineering and Mechanics, Lehigh University.

Gobert, C., Link, O., Manhart, M., and Zanke, U. (2010). Discussion of Coherent Structures in the Flow Field around a Circular Cylinder with Scour Hole by G. Kirkil, S. Constaninescu and R. Ettema. *J. of Hydr. Eng., ASCE*, **136** (1), 82-84.

Guemou, (2013). Numerical investigations of the bridge pier shape influence on the bed shear. Academic Center of Ain Temouchent, Algeria, **vol. 18**, Bund. Y. 5686.

Gupta, A.K. and Gangadharaiah, T. (1992). Local scour reduction by a delta wing-lick passive device, Proc., 8th Congr. of Asia and Pacific Reg. Div., 2, CWPRS, Pune, India, B471-B481.

Heidarpour, M., Khodarahmi, Z. and Mousavi, S.F. (2003). Control and reduction of

local scour at bridge pier groups using slot. Proceedings, IAHR Congress, Thessaloniki, Greece, August 24 - 29, 7 p.

Hoffmans, G.J.C.M., and Verheij, H.J. (1997). Scour Manual, A.A. Balkema, Rotterdam, Netherlands.

Hosny M., M. (1995). Experimental Study of Local Scour around Circular Bridge Piers in Cohesive Soils. Ph.D. Dissertation, Civil Engineering Department, Colorado State University, *Fort Collins, Colorado, USA.*

Jamieson, E. C. (2013). Turbulence and Vorticity in a Laboratory Channel Bend at Equilibrium Clear-Water Scour with and with Stream Barbs, *Journal of Hydraulic Engineering*, 259-268.

Jau-Yau Lu, M. Asce, Zhong-Zhi Shi, Jian-Hao Hong, Jun-Ji Lee, and Rajkumar V. Raikar. (2011).Temporal Variation of Scour Depth at Non-uniform Cylindrical Piers, *Journal of Hydraulic Engineering*.

Jones, J.S., Sheppard, D.M. (2000). Scour at Wide Bridge Piers, 2000 Joint Conference on Water Resource Engineering and Water Resources Planning and Management,

ASCE, US Department of Transportation, Federal Highway Administration, Turner-Fairbank Highway Research Centre.

Johnson, P.A., Hey, R.D., Tessier, M. and Rosgen, D.L. (2001). Use of vanes for control of scour at vertical wall abutments. *Journal of Hydraulic Engineering, ASCE*, **127**(9), 772-778.

Karim, O.A., and Ali, K.H.M. (2000). Prediction of Flow Patterns in Local Scour Holes Caused by Turbulent Water Jets, *Journal of Hydraulic Research*, **Vol. 38**, No. 4, 279-288.

Kirkil, G., Contastantinescu, G., and Ettema, R. (2008). Coherent structures in the flow field around a circular cylinder with scour hole. *Journal of Hydraulic Engineering, ASCE*, **134** (5), 572-587.

Kuila. A. (2013). Analysis of Clear Water Scour and Horseshoe Vortex Flow Field around Eccentric Circular Piers Arranged in Tandem, Thesis presented to the, Jadavpur University, in partial fulfillment of the requirements for the degree of Master of Engineering.

Kumar, V, Ranga Raju, K.G. and Vittal, N. (1999). Reduction of Local Scour around Bridge Piers Using Slot and Collar, Technical Note, *J. Hydr. Eng, ASCE*, **125** (12), 1302-1305.

Lagasse, P.,F, Richardson, E.,V. (2001). ASCE Compendium of Stream Stability and Bridge Scour papers, *Journal of Hydraulic Engineering, ASCE*, **Vol. 127**, Issue 7, 531-533.

Larras, J. (1963), Profondeurs Maximales D'Erosion des Fond Mobiles Autour des Piles en Riviere, Ann. Ponts et Chassees, **133** (4), 411-424.

Lauchlan, C.S. (1999). Piers scour countermeasures. PhD Thesis, Department of Civil and Resources Engineering, University of Auckland, Auckland, New Zealand.

Laursen, E., and Toch, A. (1956). Scour around bridge piers and abutments, Bulletin No. 4, Iowa Highway Research Board.

Laursen, E. M. (1963). An Analysis of Relief Bridge Scour, *Journal of Hydraulics Division, ASCE*, **89** (3), 93–118.

Lee, S. O., and Sturm, T. W. (2009). Effect of sediment size on physical modeling of bridge pier scour, *Journal of Hydraulic Engineering, ASCE*, **135** (10), 793-802.

Link, O., Gobert, Ch., Manhart, M. y and Zanke, U.(2008a). Effect of the horseshoe vortex system on the geometry of a developing scour hole at a cylinder. Proceedings of the Fourth International Conference for Scour and erosion ICSE-**4**, Tokyo, Japan, 5-7 November, Chuo University, 162-168.

McIntosh, J.L., (1989). Use of scour prediction formulae, Proceedings of the Bridge Scour Symposium: McLean, VA, Federal Highway Administration Research Report FHWA-RD-90-035 LLC, (2000) Colorado, U.S.A., 550 p.

Melville, B. W. (1975). Local scour at bridge sites, Rep. No. **117**, School of Engineering, University of Auckland, Auckland, New Zealand.

Melville, B. W., and Raudkivi, R. J. (1977). Flow characteristics in local scour at bridge piers, *Journal of Hydraul. Res.*, **15**(4), 373–380.

Melville, B. W., and Sutherland, A. J. (1988). Design Method for Local Scour at Bridge

Piers, *Journal of Hydraulic Engineering, ASCE*, **114** (10), 1210-1226.

Melville, B. W., and Chiew, Y. M. (1999). Time Scale for Local Scour at Bridge Piers,

Journal of Hydraulic Engineering, ASCE, **125** (1), 125-136.

Melville, B. W. and Coleman, S. E. (2000). Bridge scour, Water Resources Publications, Fort Collins, Colorado, USA.

Mendoza-Cabrales, C. (1993). Computation of flow past a cylinder mounted on a flat Plate, Proceedings - National Conference on Hydraulic Engineering, Venice, Italy, 899-904.

Mia, M.,F., and Nago, H. (2003). Design method of time-dependent local scour at circular bridge pier, *Journal of Hydraulic Engineering, ASCE*, **129** (6), 420-427.

Ming Zhao, and Liang Cheng. (2010). Experimental and numerical investigation of local scour around a submerged vertical circular cylinder in steady currents, *Journal of Since Direct, Coastal Engineering,* **Vol. l57**, 709–721.

Mohammad, E., M. (2005). A conceptual model for flow and sediment routing for a watershed northern Iraq , Ph.D Thesis , Water resources Dep., College of engineering, Mosul University , Mosul ,Iraq.

Molinas, A. (2003). Bridge Scour in Non-uniform Sediment Mixtures and in Cohesive Materials, Synthesis Report. Report Nr. FHWA-RD-03-083.

Mostafa, E. A. (1994). Scour around skewed bridge piers, PhD thesis. Alexandria

University, Alexandria, Egypt.

Mubeen Beg, M., and Beg, S. (2013). Scour Reduction around Bridge Piers: A Review, *International Journal of Engineering Inventions*, **Vol. 2**, Issue 7**,** 07-15.

Muzzammil, M. and Gangadhariah, T. (2003). The Mean Characteristics of Horseshoe Vortex at Cylindrical Pier, *Journal of Hydraulic Research*, **41**(3), 285-297.

Muzzammil, M., Gangadhariaiah, T., and Gupta, A.K. (2004). An experimental investigation of a horseshoe vortex induced by a bridge pier, Water Management Journal, Proceeding of the Institution of Civil Engineers, Thomas Telford Journals, London, **157** (2), 109-119.

Nagata, N., Hosoda, T., Nakato, T., and Muramoto, Y. (2005). Three-dimensional numerical model for flow and bed deformation around river hydraulic structures, *Journal of Hydraulic Engineering, ASCE,* **Vol. 131**, No. 12, 1074-1087.

Oliveto, G., and Hager, W. (2002). Temporal evolution of clear-water pier and abutment scour, *Journal of Hydraulic Engineering*, *ASCE,* **128** (9), 811-820.

Oliveto, G., and Hager, W. (2005). Further results to time-dependent local scour at bridge elements, *Journal of Hydraulic Engineering, ASCE*, **131** (2), 97-105.

Olsen, N., and Melaaen, M. (1993). 3D calculations of scour around cylinders, *Journal of Hydraulic Engineering, ASCE*, **119** (9), 1048-1054.

Olsen, N., and Kjellesvic, H. (1998). 3D numerical flow modeling for estimation of maximum local scour depth, *Journal of Hydraulic Research, IAHR*, **36** (4), 579-590.

Onen, F. (2014). Prediction of scour at a side-weir with GEP, ANN and regression models, *Arab. J. Sci. Eng*. **39**, 6031–6041.

Othman, K., Bilal, A., and Suleiman, I. (2012). Morphologic Characteristics of Tigris River with at Mosul City, *Tikrit engineering journal*, **vol.19** No. 3.

ÖZALP, C., M. (2013). Experimental Investigation of Local Scour around Bridge Pier Groups, Thesis presented to the, Middle East Technical University, in partial fulfillment of the requirements for the degree of Master of Civil Engineering.

Raudkivi, A.J. and Ettema, R. (1977a). Effect of sediment gradation on clear-water scour and measurement of scour depth, Proc.17th Congress IAHR, Baden-Baden, **4**, 512 – 527.

Raudkivi, A.J. and Ettema, R., (1977b). Effects of sediment gradation on clear water scour, *Journal of Hydraulic Engineering, ASCE*; **103** (10), 1209-1212.

Raudkivi, A.J., and Ettema, R. (1983). Clear-water scour at cylindrical piers, *Journal of Hydraulic Engineering, ASCE,* **109** (3), 338-350.

Raudkivi, A.J. (1986). Functional trends of local scour at bridge piers, *Journal of the Hydraulics Division, ASCE,* **112** (1), 1-13.

Richardson, J., E. and Panchang, V., G. (1998). Three-dimensional simulation of scour-inducing flow at bridge piers. *J. of Hydraulic Engineering*, ASCE, **124**, 530-540.

Roads, D. O., (2013). Bridge Scour Manual, Queensland, State of Australia.

Roulund, A., Sumer, B. M, Fredsoe, J. and Michelsen, J. (2005). Numerical and experimental investigation of flow and scour around a circular pile, *Journal of Fluid Mechanics,* **Vol. 534**, 351–401.

Said, N., Mhiri, H., Bournot, H., and Le Palec, G. (2008). Experimental and numerical modelling of the three-dimensional incompressible flow behavior in the near wake of circular cylinders, *Journal of Wind Engineering and Industrial Aerodynamics*, **Vol. 96**, No. 5, 471–502.

Shen, H.W., Schneider, V.R., and Karaki, S.S. (1966). Mechanics of Local Scour, Colorado State University, Civil Engineering Dept., Fort Collins, Colorado, Pub. No. CER66-HWS22.

Shen, H. W., Schneider, V. R., and Karaki, S. (1969). Local scour around bridge piers, *Journal of Hydraulic Division, ASCE*, **95** (6), HY6, 1919–1940.

Sheppard, D. M., Ontowirjo, B., and Zhao, G. (1995). Local scour near single piles in steady currents. Proceeding of the first Hydraulics Engineering Conference, San Antonio.

Sheppard, D.M., Odeh, M., and Glasser, T. (2004). Large scale clear-water local pier scour experiments. *Journal of Hydraulic Engineering, ASCE,* **130** (10), 957-963.

SonTek (2001). Acoustic Doppler Velocimeter (ADV) principles of operation. SonTek ADV Technical Manual, SonTek, San Diego.

Sumer, B. M., and Fredsøe, J.(1992). The mechanics of scour in the marine environment, World Scientific, Singapore.

Tafarojnoruz, A., Gaudio, R., Dey, S. (2010a). Flow-altering countermeasures against scour at bridge piers: review. *J. Hydraul. Res.* **48** (4), 441–452.

Tafarojnoruz, A., Gaudio, R., Calomino, F. (2012). Evaluation of flow altering countermeasures against bridge pier scour. *J. Hydraul. Eng*. **138**, 297–305.

Tseng, M. H., Yen, C., L. and Song, C. S. (2000), Computation of Three-Dimensional Flow around Square and Circular Piers, *International Journal for Numerical Methods in Fluids*, **34**, 207-227.

Tuna, C. and Emiroglu, E. (2013). Effect of Step Geometry on Local Scour Downstream of Stepped Chutes, *The Arabian Journal for Science and Engineering, AJSE*, **38**, 579-588.

Unger, J., and Hager, W. (2007). Down-flow and horseshoe vortex characteristics of sediment embedded bridge piers. Experiments in Fluids, **42**, 1-19.

Vaghefi, M. Ahmadi, A. Faraji, B. (2015). The Effect of Support Structure on Flow Patterns around T-Shape Spur Dike in 90^0 Bend Channel. *The Arabian Journal for Science and Engineering, AJSE*. **doi**: 10.1007/s13369-015-1604-2.

Vautier, E. W. (1972) Flow around a cylindrical pier with scour hole format ion , M.E. Thesis, Civil Eng. Dept. Univ. of Auckland, New Zealand.

Vittal, N., Kothyari, U.C. and Haghighat, M. 1994. Clear-water scour around bridge pier group. *Journal of Hydraulic Engineering, ASCE*, 120 (11): 1309-1318.

Wen, F. M., et al. (1993). The Separated Flow Around a Circular Bridge Pier, ASCE Hydraulic Engineering, Proc. National Conference, 905-910.

Wu, S, and Rajaratnam, N. (1995). Free jumps, submerged jumps, and wall jets. *J. Hydraul. Res.*, **33** (2), 197-212.

Yanmaz, A.M., Altinbilek, H.D. (1991), Study of Time-Dependent Local Scour around Bridge Piers, *J. Hydraulic Engineering*. **Vol. 117,** No.10,1247-1268

Zanke, U. (1982a). Kolke am Pfeiler in richtungskonstanter Strömung und unter Welleneinfluß. Mitteilungen des Franzius-Instituts, TU Hannover. Heft **54**, 381- 416 (in German).

Zarrati, A., M., Gholami, H., and Mashahir, M.B. (2004). Application of collar to control scouring around rectangular bridge piers. *Journal of Hydraulic Research, IAHR*, **42** (1), 97-103.

Zarrati, A.M., Nazariah, M. and Mashahir, M.B (2006). Reduction of local scour in the vicinity of bridge pier group using collars and riprap, *Journal of Hydraulic Engineering, ASCE*, **132**(2), 154-162.